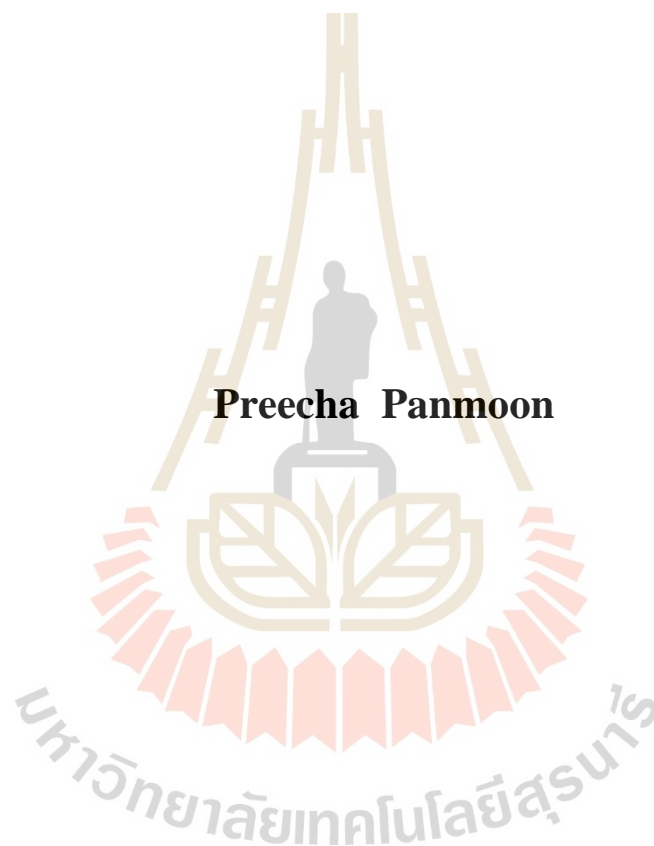


**SEASONAL METHANE FLUXES FROM A NATURAL  
WETLAND IN NAKHON RATCHASIMA**



**Preecha Panmoon**

**A Thesis Submitted in Partial Fulfillment of the Requirements for the**

**Degree of Master of Science in Environmental Pollution and Safety**

**Suranaree University of Technology**

**Academic Year 2020**

การปล่อยแก๊สมีเทนฟลักซ์ตามฤดูกาลจากพื้นที่ชุ่มน้ำธรรมชาติ  
ในจังหวัดนครราชสีมา



วิทยานิพนธ์นี้เป็นส่วนหนึ่งของการศึกษาตามหลักสูตรปริญญาวิทยาศาสตรมหาบัณฑิต

สาขาวิชามลพิษสิ่งแวดล้อมและความปลอดภัย

มหาวิทยาลัยเทคโนโลยีสุรนารี

ปีการศึกษา 2563

**SEASONAL METHANE FLUXES FROM A NATURAL WETLAND  
IN NAKHON RATCHASIMA**

Suranaree University of Technology has approved this thesis submitted in partial fulfillment of the requirements for a Master's Degree.

Thesis Examining Committee

Patchara Suwanathada

(Dr. Patcharawadee Suwanathada)

Chairperson

Paweena Panichayapichet

(Dr. Paweena Panichayapichet)

Member

Amornpon Changsuphan

(Dr. Amornpon Changsuphan)

Member

Nares Chuersuwan

(Assoc. Prof. Dr. Nares Chuersuwan)

Member (Thesis Advisor)

Chatchai Jothityangkoon

Chalalai Hanchenlaksh

(Assoc. Prof. Dr. Chatchai Jothityangkoon) (Asst. Prof. Dr. Chalalai Hanchenlaksh)

Vice Rector for Academic Affairs and Dean of Institute of Public Health

Quality Assurance

ปรีชา พันธุ์มูล : การปล่อยแก๊สมีเทนฟลักซ์ตามฤดูกาลจากพื้นที่ชุ่มน้ำธรรมชาติในจังหวัดนครราชสีมา (SEASONAL METHANE FLUXES FROM A NATURAL WETLAND IN NAKHON RACHASSIMA). อาจารย์ที่ปรึกษา : รองศาสตราจารย์ ดร.นเรศ เชื้อสุวรรณ, 161 หน้า.

การศึกษานี้มีวัตถุประสงค์เพื่อประเมินปริมาณการปล่อยแก๊สมีเทนจากพื้นที่ชุ่มน้ำธรรมชาติตามฤดูกาลในจังหวัดนครราชสีมาและศึกษาปัจจัยที่มีอิทธิพลต่อค่าแก๊สมีเทนฟลักซ์ คือ อุณหภูมิของดิน ค่าพีเอชของดิน ค่าสภาพรีดิวซ์ของดิน ชนิดของเนื้อดิน และปริมาณคาร์บอนในดิน ดำเนินการเก็บตัวอย่างแก๊สมีเทนรายเดือน ด้วยเทคนิคชุดครอบปิดแบบอยู่กับที่ และวิเคราะห์หาความเข้มข้นด้วยเทคนิคแก๊สโครมาโทกราฟีที่ใช้เฟลม ไอออไนเซชัน โดยดำเนินการระหว่างเดือนธันวาคม พ.ศ. 2561 ถึงเดือนพฤศจิกายน พ.ศ. 2562

การตรวจวัดชนิดของเนื้อดินในห้องปฏิบัติการพบว่า พื้นที่ชุ่มน้ำเป็นดินทราย มีค่าแก๊สมีเทนฟลักซ์ในช่วง 1.9 - 22.7 มก./ม.<sup>2</sup>/วัน โดยมีค่ากลาง  $10.1 \pm 5.4$  มก./ม.<sup>2</sup>/วัน (ค่ามัธยฐาน  $\pm$  ค่าเบี่ยงเบนมาตรฐาน) ค่ามัธยฐานของแก๊สมีเทนฟลักซ์ในฤดูฝนคือ  $14.1 \pm 5.0$  มก./ม.<sup>2</sup>/วัน ส่วนในช่วงฤดูแล้งมีค่ามัธยฐาน  $8.8 \pm 5.2$  มก./ม.<sup>2</sup>/วัน การทดสอบทางสถิติพบว่า ค่ามัธยฐานของแก๊สมีเทนฟลักซ์ระหว่างฤดูฝนและฤดูแล้งแตกต่างกันอย่างมีนัยสำคัญ ( $p < 0.05$ ) ปริมาณการปล่อยแก๊สมีเทนฟลักซ์ของพื้นที่ชุ่มน้ำในฤดูฝนและฤดูแล้งอยู่ในช่วง 1.5-3.1 และ 0.7-2.9 มก./ม.<sup>2</sup> ตามลำดับ ค่าประมาณการปล่อยแก๊สมีเทนต่อปีจากพื้นที่ชุ่มน้ำตามธรรมชาติมีค่าอยู่ในช่วง 1.7-5.7 กก./ม.<sup>2</sup>/ปี

ผลการศึกษาปัจจัยที่มีอิทธิพลต่อค่าแก๊สมีเทนฟลักซ์ในสามช่วงความลึกของดิน พบว่า อุณหภูมิของดินที่ระดับความลึก 2.5 ซม. มีค่าอุณหภูมิสูงกว่าระดับชั้นดินที่ลึกลงไป และผลการทดสอบความสัมพันธ์พบว่า ตัวอย่างดินที่ระดับความลึก 2.5 และ 7.5 ซม. มีความสัมพันธ์ทางบวกอย่างมีนัยสำคัญกับแก๊สมีเทนฟลักซ์ในฤดูฝน ผลของค่าสภาพรีดิวซ์ของดินพบว่า ค่าอยู่ในช่วงระหว่าง 150-326 มิลลิโวลต์ มีความสัมพันธ์ทางลบกับแก๊สมีเทนฟลักซ์ในตัวอย่างดินที่ช่วงความลึก 5-10 ซม. อย่างมีนัยสำคัญเท่านั้น ค่าพีเอชในดินในช่วง 4.5-7.4 และ ไม่มีความสัมพันธ์ทางสถิติกับค่าแก๊สมีเทนฟลักซ์ ส่วนค่าองค์ประกอบทางคาร์บอนในดินพบว่ามีค่าอยู่ระหว่าง 0.04-3.00% และ ไม่มีความสัมพันธ์ทางสถิติกับค่าแก๊สมีเทนฟลักซ์ การศึกษานี้แสดงให้เห็นว่าแก๊ส

มีเทนพลั๊กซ์จากพื้นที่ชุ่มน้ำธรรมชาติมีความผันผวนตามฤดูกาล ในการจัดทำบัญชีการปล่อยแก๊สมีเทนจากพื้นที่ชุ่มน้ำตามธรรมชาติควรพิจารณาถึงความแตกต่างดังกล่าว เพื่อลดความคลาดเคลื่อนจากการประเมิน



สาขาวิชา มลพิษสิ่งแวดล้อมและความปลอดภัย  
ปีการศึกษา 2563

ลายมือชื่อนักศึกษา Peecha PanMoon  
ลายมือชื่ออาจารย์ที่ปรึกษา Nu- Ee

PREECHA PANMOON : SEASONAL METHANE FLUXES FROM A  
NATURAL WETLAND IN NAKHON RATCHASIMA.

THESIS ADVISOR : ASSOC. PROF. NARES CHEURSUWAN, Ph.D. 161  
PP.

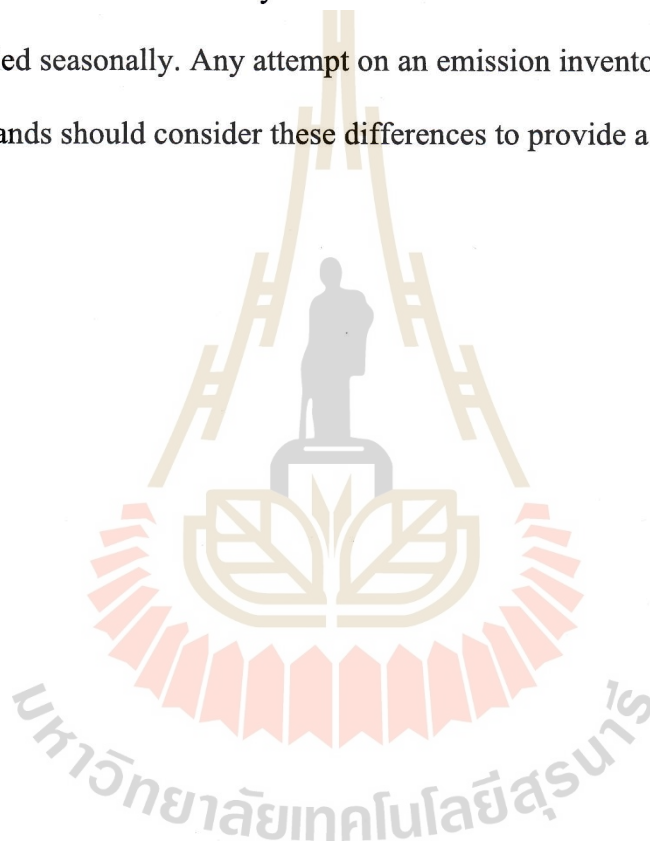
METHANE FLUXES/METHANE EMISSIONS/NATURAL WETLANDS/  
GREENHOUSE GAS

This study investigates seasonal methane fluxes from a natural wetland in Nakhon Ratchasima to estimate an annual methane emission and the effects of influencing factors of soil properties including soil temperature, pH, reducing status (ORP), texture, and carbon contents. Methane gas was measured monthly between December 2018 and November 2019, with the static closed chamber technique and later analyzed by a gas chromatography with a flame ionization detector (FID).

Soil texture analysis indicated the sandy texture of the wetland. The methane fluxes varied from 1.9 to 22.7 mg/m<sup>2</sup>/day with the median  $\pm$  SD of 10.1  $\pm$  5.4 mg/m<sup>2</sup>/day. The methane fluxes during wet season had the median  $\pm$  SD of 14.1  $\pm$  5.0 mg/m<sup>2</sup>/day and 8.8  $\pm$  5.2 mg/m<sup>2</sup>/day in dry season. The median methane fluxes in wet and dry seasons were significantly different with a t-test ( $p < 0.05$ ). The estimates seasonal methane fluxes in wet and dry seasons were 1.5-3.1 and 0.7-2.9 mg/m<sup>2</sup>, respectively. The annual methane emissions from the natural wetland was between 1.7 and 5.7 kg/m<sup>2</sup>/year.

The effects of influencing factors on methane fluxes were investigated at different soil depths. Median soil temperature at a shallow depth of 2.5 cm was warmer than the

deeper soil, varied between 23.0 and 34.5°C. In wet season, soil temperature associated positively and significantly with methane fluxes at 2.5 and 7.5 cm depths. Soil ORP was between 150 and 326 mV, with negatively and significantly related at 5-10 cm depth. Soil pH was in the range of 4.5-7.4 with no relationship with the methane fluxes. Soil carbon ranged from 0.04-3.00%. No relationship between methane fluxes and soil carbon was observed. This study had shown that the methane emission of a natural wetland varied seasonally. Any attempt on an emission inventory of methane from the natural wetlands should consider these differences to provide a better estimation.



School of Environmental Pollution and Safety Student's Signature Preecha PanMoon

Academic Year 2020

Advisor's Signature Nam Cho

## **ACKNOWLEDGEMENTS**

The present study has been successfully done throughout the helping and supporting from important contributors and the scholarships of Master's degree from Suranaree University of Technology.

I would like to express my special thanks to my supportive advisor, Associated Professor Dr. Nares Chuersuwan for his kind-hearted advices and suggestions. I am extremely grateful for his sincere chats in the email and meeting room, his providing some materials in every step of the study, and his personal support in my academic and working endeavours. I would like to express my gratitude and appreciation to my committee members, Dr. Patcharawadee Suwanathada, Dr. Paweena Panichayapichet, and Dr. Amornpon Chansuphan, for their valuable comment, guidance, advice and correction as well as word of encouragement.

I would like to give respectful value to all lecturers and institute staffs for imparting the knowledge and kind support.

Also with many thanks to my friends and seniors for their support, comment, and encouragement as well as their helps on field sampling and laboratory analysis.

Finally, I cannot forget to express the biggest thank and very profound gratitude to parents for all the unconditional support.

Preecha Panmoon



# CONTENTS

	<b>Page</b>
ABSTRACT IN THAI .....	I
ABSTRACT IN ENGLISH. ....	III
ACKNOWLEDGEMENTS .....	V
CONTENTS.....	VI
LIST OF TABLES .....	X
LIST OF FIGURES .....	XIII
SYMBOLS AND ABBREVIATIONS.....	XV
<b>CHAPTER</b>	
<b>I INTRODUCTION.....</b>	<b>1</b>
1.1 Problem statement.....	1
1.2 Research objectives.....	3
1.3 Research scope .....	3
1.4 Expected results .....	4
1.5 Conceptual framework.....	4
<b>II LITERATURE REVIEWS.....</b>	<b>5</b>
2.1 Background .....	5

## CONTENTS (Cont'd)

	<b>Page</b>
2.2 GHGs, sources, and global warming potential.....	7
2.3 Wetlands.....	10
2.4 Methane cycle in wetlands.....	15
2.4.1 Methanogenesis.....	16
2.4.2 Methane reduction.....	20
2.4.3 Pathways of methane transport into the atmosphere.....	23
2.5 Potential factors affecting methanogenesis and methane emission .....	25
2.5.1 Water level .....	25
2.5.2 Oxygen and reducing condition as redox potential.....	26
2.5.3 Soil texture .....	27
2.5.4 Organic matter content as a substrate.....	29
2.5.5 Chemical properties.....	30
2.5.6 Salinity .....	32
2.5.7 pH.....	32
2.5.8 Temperature in methanogenic environments .....	33
2.5.9 Temperature as an influencing factor.....	34
2.5.10 Seasonal variation .....	37
2.6 Quantification of methane emission from wetlands.....	37

## CONTENTS (Cont'd)

		<b>Page</b>
	2.6.1 Chamber techniques .....	38
	2.6.2 Meteorological techniques .....	39
	2.7 Statement of conclusion .....	42
<b>III</b>	<b>METHODS .....</b>	<b>45</b>
	3.1 A study area.....	45
	3.2 Sample collection .....	48
	3.2.1 Air sample collection .....	48
	3.2.2 Soil sample collection .....	49
	3.3 Sample analysis.....	51
	3.3.1 Methane fluxes .....	51
	3.3.2 Soil preparation .....	53
	3.3.3 Analysis of soil carbon.....	53
	3.3.4 Analysis of soil pH.....	54
	3.3.5 Analysis of soil oxidation reduction potential (ORP).....	54
	3.3.6 Analysis of soil texture.....	55
	3.4 Data analysis .....	57
<b>IV</b>	<b>RESULTS AND DISCUSSIONS .....</b>	<b>58</b>

## CONTENTS (Cont'd)

	<b>Page</b>
4.1 Methane concentrations from the natural wetland .....	58
4.1.1 Methane fluxes .....	66
4.1.2 Spatiotemporal dynamics of seasonal methane fluxes .....	70
4.2 Temperature effects on methane fluxes .....	75
4.3 Soil texture effects on methane fluxes .....	82
4.4 Soil pH effects on methane fluxes .....	83
4.5 Soil ORP effects on methane fluxes .....	87
4.6 Soil carbon (%C) effects on methane fluxes .....	91
<b>V CONCLUSIONS AND RECOMMENDATIONS .....</b>	<b>95</b>
REFERENCES .....	98
APPENDICES	
APPENDIX A METHANE CONCENTRATIONS .....	122
APPENDIX B DATA OF INFLUENCING FACTORS .....	148
PUBLICATIONS .....	153
CIRRICULUM VITAE .....	161

## LIST OF TABLES

Table	Page
2.1 The Ramsar Convention's classification for wetlands.....	11
2.2 Example of methanogenic reactions (Zinder, 1993).....	17
2.3 The sequential reactions of organic matter (OM) degradation and redox potential (Faulkner, 2014).....	19
2.4 Anaerobic methane oxidation reactions by archaeas.....	22
2.5 Examples for advantages and limitations of chamber and micrometeorological technique.....	42
3.1 General information of Baan San Kumphaeng Reservoir.....	45
3.2 Considerations for chamber requirement in this study.....	47
3.3 Conditions of GC-FID for methane gas analysis.....	52
3.4 Statistics used in the present study.....	57
3.5 Association level and r value for correlation test.....	57
4.1 Methane concentration, temperature recorded, and graph of methane emissions in February 2019.....	59
4.2 Monthly data on methane flux rate.....	62
4.3 Monthly methane fluxes (n=41) in the wet and the dry season.....	68
4.4 Seasonal estimates of the median methane emissions.....	69
4.5 Examples of methane fluxes from wetlands in Asia.....	71
4.6 Methane flux rate from wetland in different climate zone.....	73

## LIST OF TABLES (Cont'd)

<b>Table</b>	<b>Page</b>
4.7 Soil texture classified by USDA classification.....	82
5.1 Summary of parameter in this study.....	96
A1 Methane concentration, chamber's temperature recorded, and graph for methane emissions in December 2018.....	123
A2 Methane concentration, chamber's temperature recorded, and graph for methane emissions in January 2019.....	124
A3 Methane concentration, chamber's temperature recorded, and graph for methane emissions in February 2019.....	126
A4 Methane concentration, chamber's temperature recorded, and graph for methane emissions in March 2019.....	128
A5 Methane concentration, chamber's temperature recorded, and graph for methane emissions in April 2019.....	130
A6 Methane concentration, chamber's temperature recorded, and graph for methane emissions in May 2019.....	132
A7 Methane concentration, chamber's temperature recorded, and graph for methane emissions in June 2019.....	134
A8 Methane concentration, chamber's temperature recorded, and graph for methane emissions in July 2019.....	136
A9 Methane concentration, chamber's temperature recorded, and graph for methane emissions in August 2019.....	137

## LIST OF TABLES (Cont'd)

<b>Table</b>		<b>Page</b>
A10	Methane concentration, chamber's temperature recorded, and graph for methane emissions in September 2019.....	142
A11	Methane concentration, chamber's temperature recorded, and graph for methane emissions in October 2019.....	142
A12	Methane concentration, chamber's temperature recorded, and graph for methane emissions in November 2019.....	144
A13	Monthly methane flux rates a day.....	146
B1	Air and water temperature during sampling periods.....	148
B2	Soil temperature at each depth during sampling periods.....	149
B3	Soil pH, ORP, and carbon content at each depth during sampling periods.....	151

## LIST OF FIGURES

<b>Figure</b>		<b>Page</b>
1.1	Conceptual frame work .....	4
2.1	Global surface mole fraction of GHGs over the past 2000 years.....	6
2.2	Major transport of methane to the atmosphere (Lai, 2009).....	23
2.3	Methane emissions and water table level (Bubier et al., 1993).....	26
2.4	Methane flux decreased with redox potential increase (Wang et al., 2009).....	27
2.5	Temporal distribution of methane fluxes (Bryeet al., 2013).....	28
2.6	The pH value and methane fluxes (Wang et al., 2009).....	32
2.7	Exponential increase in methane flux with soil temperature from different five observations (Brooks Avery et al., 2003).....	35
2.8	Relative methane flux in a day (Minamikawa et al., 2012).....	37
2.9	The principle of meteorological eddy covariance based on mass balance (Launiainen, 2011).....	40
3.1	An overview of methods.....	44
3.2	Sampling area.....	46
3.3	An acrylic chamber and an aluminum base configuration.....	48
3.4	A set up of five replicated chambers.....	49
3.5	Soil temperature measurement.....	51
4.1	Histogram of methane fluxes (n=52).....	66



## LIST OF FIGURES (Cont'd)

<b>Figure</b>	<b>Page</b>
4.2 Box-Whisker plot between dry and wet season of methane fluxes.....	69
4.3 Observed temperature during sampling periods.....	75
4.4 Soil temperature at each depth.....	76
4.5 Pearson's correlation test of soil temperature and methane fluxes by season.....	78
4.6 Trend of temperature and methane fluxes.....	80
4.7 The appearance of disturbed wetland in October and November 2019.....	81
4.8 Statistics of soil pH at each depth.....	84
4.9 Pearson's correlation test of soil pH and methane fluxes.....	85
4.10 Trend of soil pH and methane fluxes.....	86
4.11 Statistics of soil ORP each depth.....	88
4.12 Trend of soil ORP and methane fluxes.....	88
4.13 Pearson's correlation test of soil ORP and methane fluxes.....	90
4.14 Statistics of soil carbon content at each depth.....	91
4.15 Pearson's correlation test of soil carbon content and methane fluxes.....	92
4.16 Trend of soil carbon content and methane fluxes.....	93
A1 Example of calculating methane fluxes. The data derived from methane concentration of chamber 1 in December 2018.....	146

## SYMBOLS AND ABBREVIATIONS

AD	Anno Domini (in the year of the Lord)
ASTM	American Society for Testing and Materials
CaCl <sub>2</sub>	Calcium chloride
CH <sub>3</sub> CH <sub>2</sub> OH	Ethanol
CH <sub>3</sub> COO <sup>-</sup>	Acetate ion
CH <sub>3</sub> COOH	Acetic acid
(CH <sub>3</sub> ) <sub>2</sub> -S	Dimethyl sulfide
(CH <sub>3</sub> ) <sub>3</sub> -NH <sup>+</sup>	Trimethylammonium ion
CH <sub>3</sub> OH	Methanol
CH <sub>4</sub>	Methane
cm	Centimeter
Co., Ltd.	Company Limited
CO	Carbon monoxide
CO <sub>2</sub>	Carbon dioxide
<i>E<sub>h</sub></i>	Redox potential (hydrogen scale)
ESRL	Earth System Research Laboratories
et al	and others
etc	et cetera
Fe <sup>2+</sup>	Ferrous ion
Fe <sup>3+</sup>	Ferric ion

**SYMBOLS AND ABBREVIATIONS (Cont'd)**

Fe(OH) <sub>3</sub>	Iron (III) hydroxide
g	gram
GC-FID	Gas chromatography with flame ionization detector
GHGs	Greenhouse gases
GWP	Global Warming Potential
H <sub>2</sub>	Hydrogen
H <sub>2</sub> S	Hydrogen sulfide
H <sup>+</sup>	Hydrogen ion
HCO <sub>3</sub> <sup>-</sup>	Bicarbonate ion
HCOOH	Formic acid
H <sub>2</sub> O	Water
hr	hour
i.e.	id est (that is)
IPCC	The Intergovernmental Panel on Climate Change
kJ	kilo joules
m	meters
m <sup>2</sup>	square meters
m <sup>3</sup>	cubic meters
min	minute
ml	milliliter

**SYMBOLS AND ABBREVIATIONS (Cont'd)**

M	molar
Mn <sup>2+</sup>	Manganese (II)
Mn <sup>4+</sup>	Manganese (IV)
MnO <sub>2</sub>	Manganese (IV) oxide
mV	millivolts
n.a.	not analyzed/ unaccountable
N <sub>2</sub>	Nitrogen
NaOH	Sodium hydroxide
NH <sub>3</sub>	Ammonia
NH <sub>4</sub> <sup>+</sup>	Ammonium ion
N <sub>2</sub> O	Nitrous oxide
NO <sub>3</sub> <sup>-</sup>	Nitrate ion
NO <sub>x</sub>	Nitrogen oxide
NOAA	National Oceanic and Atmospheric Administration
O <sub>2</sub>	Oxygen
OH <sup>-</sup>	Hydroxide ion
OM	Organic matter
ORP	Oxidation Reduction Potential
ppb	parts per billion

**SYMBOLS AND ABBREVIATIONS (Cont'd)**

ppmv	parts per million by volume
s	second (time)
S <sup>2-</sup>	Sulfide ion
SO <sub>4</sub> <sup>2-</sup>	Sulfate ion
USA	The United States of America
USDA	The United States Department of Agriculture
USEPA	The United States Environmental Protection Agency
v	Volume
<	less than
>	more than
x	multiply
°C	degree Celsius
%	percent
ΔG	Gibbs free energy
®	registered trademark symbol
kJ	kilojoules
<i>p</i>	probability
&	and

# CHAPTER I

## INTRODUCTION

### 1.1 Problem statement

Greenhouse gases (GHGs) are naturally common constituents in the earth's atmosphere. The majority includes mixed molecules of water (H<sub>2</sub>O), carbon dioxide (CO<sub>2</sub>), methane (CH<sub>4</sub>), and nitrous oxide (N<sub>2</sub>O). These gases absorb heat in the atmosphere and thus influence the Earth's temperature (Fourier, 1824; Stephens and Tjemkes, 1993; Tyndall, 1862). Post-industrial human activities, in the past 200 years, have continuously released more GHGs, annually about 22 x 10<sup>9</sup> tonnes in 1990 to 36.2 x 10<sup>9</sup> tonnes in 2016 (Yue and Gao, 2018). Increased atmospheric GHGs, as a result, enhance greenhouse effect and global warming.

Methane gas has an atmospheric lifetime of about 12.4 years with the global warming potential (GWP) of 87 times relative to that of carbon dioxide and more devastating than carbon dioxide based on a 20-year time horizon (Myhre et al., 2013). This gas is mainly produced by methanogenic bacteria, the process known as methanogenesis. In 2019, atmospheric methane concentrations are 2.6 times higher than pre-industrial levels (Dlugokencky and NOAA/ESRL, 2019). Methane gas is emitted in different proportions from various sources. One significant source is inundated or flooded environments such as wetlands (Laanbroek, 2010).

Quantification of methane emissions from wetlands is important for emission inventory of GHGs emissions. The GHGs inventory in Thailand had been reported in National Communication—a reports submitted to the United Nations Framework Convention on Climate Change (UNFCCC). However, the latest “Thailand’s 2<sup>nd</sup> National Communication” had excluded the GHGs emissions from natural sources, possibly from limited data on methane emissions from the natural wetlands in Thailand. Previous studies on methane emission in Thailand mostly focused on rice cultivation (Khemjaroen, 2001) and constructed wetlands (Chuersuwan et al., 2014; Kaewgamtong, 2002); only two studies focused on natural wetlands but the results were based on one season only (Khemjaroen, 2001). Another study was from mangrove areas (Lekphet et al., 2005). Lack of site-specific methane emission factor is often substitute by the default emission factor from literatures or international organizations, such as Intergovernmental Panel on Climate Change (IPCC) (IPCC, 2013). The locally specific emission factor undoubtedly gives better emission estimation than some value taken from literatures elsewhere.

This research focused on methane gas collection in a natural wetland over one year to provide locally specific methane emission and improved understanding of seasonal methane emission from the natural wetland.

## **1.2 Research objectives**

- 1.2.1 To investigate seasonal methane fluxes from a natural wetland in Nakhon Ratchasima, Thailand.
- 1.2.2 To estimate annual methane emissions from the natural wetland.
- 1.2.3 To evaluate the effects of influencing factors including soil temperature, soil pH, soil reducing status, soil texture, and soil carbon contents on seasonal methane fluxes from the natural wetland.

## **1.3 Scope of the research**

- 1.3.1 Greenhouse gas: methane
- 1.3.2 Natural wetland: Baan San Khampaeng reservoir in Nakhon Ratchasima
- 1.3.3 Observed parameters: ambient temperature, water temperature, and water level fixed at 0 to 5 cm
- 1.3.4 Influencing factors: soil temperature, soil pH, soil reducing status, soil texture and soil carbon content
- 1.3.5 Gas collection technique: static closed chamber
- 1.3.6 Methane analysis: gas chromatography with flame ionization detector
- 1.3.7 Sampling duration: monthly for 12 months
- 1.3.8 Seasons: wet and dry seasons



## 1.4 Expected results

1.4.1 Produce an estimate of the seasonal methane flux from the natural wetland

1.4.2 Provide data for the emission inventory of methane emission as a GHG from natural wetlands.

## 1.5 Conceptual framework

This research involved field sampling of methane gas and measured influencing factors such as temperature, pH, and soil properties, as shown in the conceptual framework (Figure 1.1).

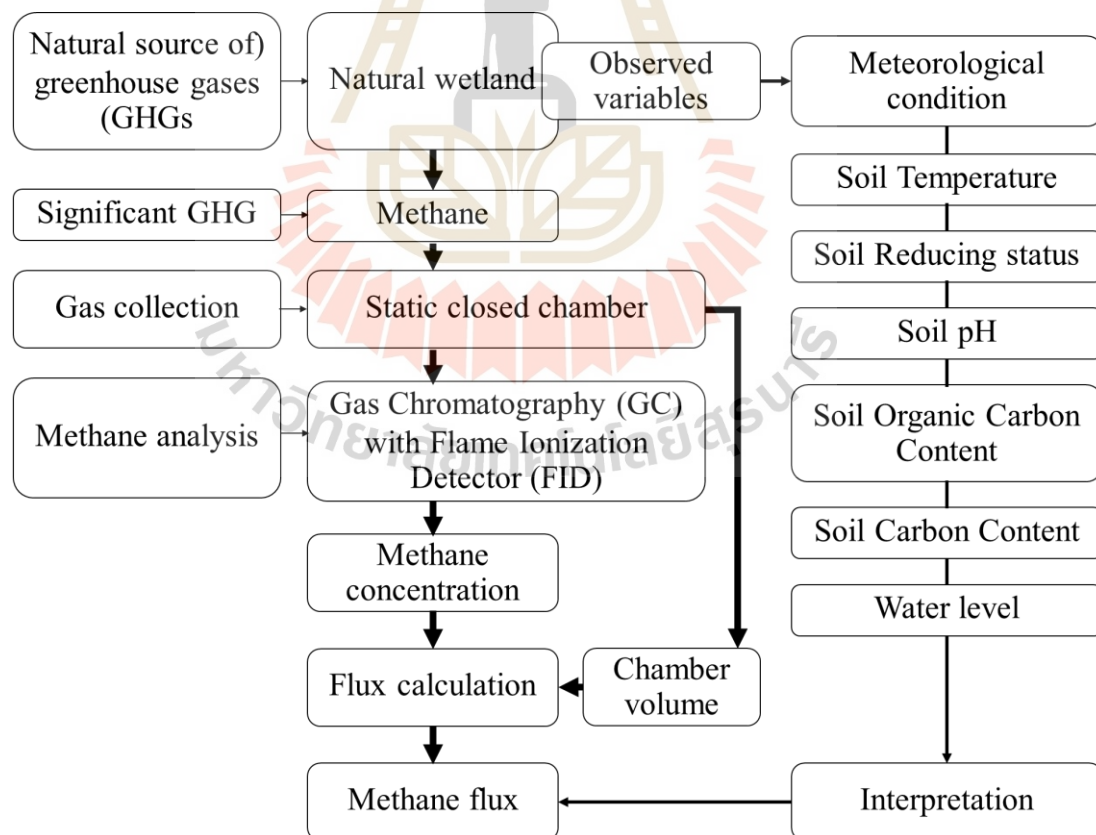


**Figure 1.1** Conceptual framework

## **CHAPTER II**

### **LITERATURE REVIEWS**

#### **2.1 Background**

The greenhouse effect refers to trapping infrared radiation from the earth's surface by greenhouse gases (GHGs). The GHGs naturally regulate the atmospheric temperature of the earth, maintaining the Earth's average temperature to approximately 15°C—the level suitable for life in the biosphere; without them the Earth's average temperature would actually be -18°C (Fourier, 1824). However, the increased anthropogenic greenhouse gas emissions in the atmosphere interfere the balance between incoming and outgoing energy by causing the atmosphere to absorb more heat energy (Atique and Mahmood, 2014).

Before the industrial revolution, atmospheric GHGs were quite steady for thousands of years (Figure 2.1). Natural systems likely remained in balance between GHG emission and sinks. Natural GHG sources and sinks are prevalent on Earth. For example, plants absorb carbon dioxide for photosynthesis during daytime, as a carbon sink. At night plants release carbon by respiring carbon dioxide molecules. Levels of carbon dioxide, methane, and nitrous oxide all have increased from pre-industrial levels by at least double (Figure 2.1). Burning fossil fuel, increasing massive agriculture, the growing human population and demands are the primary sources for rapid increase post-industrial revolution (IPCC, 2014).

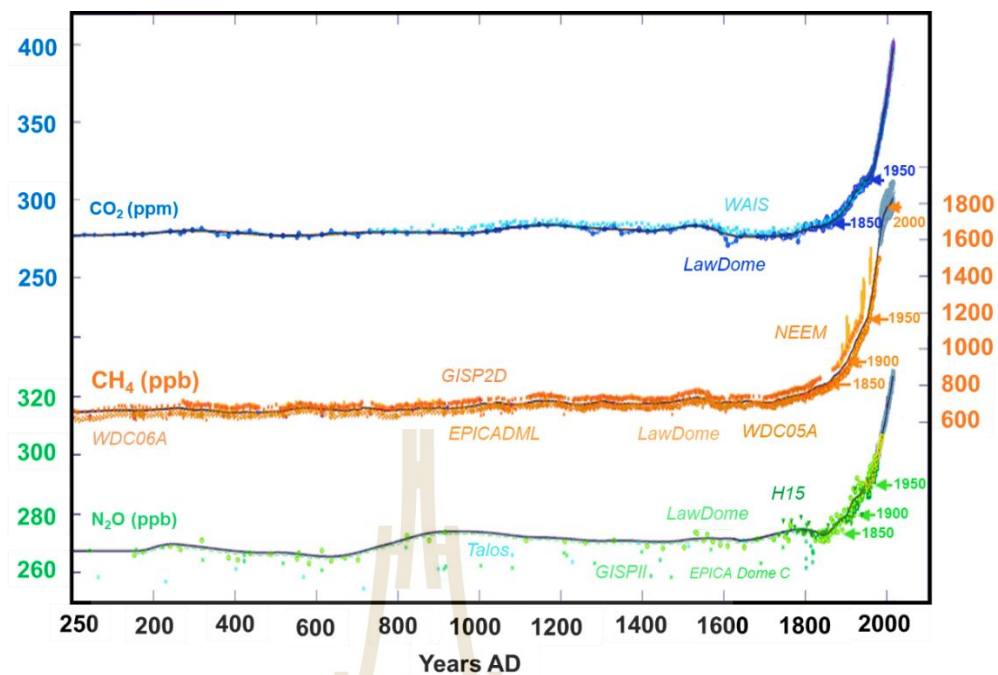


**Figure 2.1** Global surface mole fraction of GHGs over the past 2000 years, derived from modelling with various sources of data, for example, Law Dome, NEEM, and WAIS (Meinshausen et al., 2017).

In 2018, IPCC issues the special report on the impacts of 1.5°C. The report estimates human activities to have caused global temperatures to rise by 1.0°C (between 0.8 and 1.2°C) from pre-industrial levels, Further projections estimate rising 1.5°C between 2030 and 2052, at the current rates of increase. Anthropogenic emissions since pre-industrial period will continue to cause further long-term changes in the climate because some GHG can persist for centuries or even millennia (IPCC, 2018).

## 2.2 GHGs, sources, and global warming potential

Major GHGs influencing Earth's climate system include water vapor, carbon dioxide, nitrous oxide, and methane but water vapor is mostly from natural phenomena. Other gases are emitted differently from various sources. The largest emission is carbon dioxide. Methane ranks second, followed by nitrous oxide (IPCC, 2014).

### 2.2.1 Carbon dioxide

The global carbon cycle is dominated by oceanic and terrestrial respiration. Physical exchange of dissolved carbon dioxide between the air and sea leads atmospheric carbon emission. Carbon dioxide plays a key role in the biological processes such as photosynthesis and respiration in the natural cycle. Many organisms increase respiration with increasing temperature (Pietikäinen et al., 2005). Volcanism and biomass burning are carbon dioxide sources; globally, direct and indirect biomass burning activities in the past have dwarfed other emissions. At present human sources of carbon dioxide are of great importance (Jalota et al., 2018). The main sources include energy-production and transport—the amount of carbon dioxide emitted from electricity generation unit varies greatly depending upon the fuel used and the level of efficiency; rapid increases in worldwide motor vehicle use has increase carbon dioxide emissions in many countries (Miller, 2005). Other sources are land use change, industry, and biomass burning (Pavelka et al., 2018). Atmospheric carbon dioxide increased from about 280 ppm in 1800 to about 400 ppm in 2000 (Figure 2.1). More recent reported the increasing atmospheric carbon dioxide by 40 percent from 278 ppm in 1750 to 414 ppm in 2020 (NOAA/ESRL, 2020).

### 2.2.2 Nitrous oxide

In 1772, Joseph Priestley first described nitrous oxide as relatively inert gas with a slightly sweet odor. Its major sink is by photochemical transformations in the stratosphere decreased the abundance of stratospheric ozone (Pavelka et al., 2018). Nitrous oxide enters the atmosphere naturally and anthropogenically such as during agricultural and industrial activities, combustion of fossil fuels and solid waste, as well as during treatment of wastewater (USEPA, 2020). Atmospheric nitrous oxide concentrations have risen markedly in the past 200 years—increasing from approximate 270 ppb in the pre-industrial era to 315 ppb (Figure 2.1). Current estimates report an ongoing increase of 20 percent from 271 ppb in 1750 to 333 ppb in 2020 (NOAA/ESRL, 2020). Although its concentration is very small compared to carbon dioxide, nitrous oxide is chemically inert and thus can remain in the atmosphere 6 times longer than carbon dioxide (up to 120 years). It also has much greater radiative forcing potential than a molecule of carbon dioxide, or 269 times on a 100-year time horizon.

Microbial activities in oceans and soils known as denitrification produce atmosphere bound nitrous oxides. Temperate and tropical soils dominate natural nitrous oxide emission on the global scale. Natural sources are difficult to distinguish from anthropogenic sources, especially, nitrogen release as fertilizers, ammonia ( $\text{NH}_3$ ) emissions from livestock and nitrogen oxide ( $\text{NO}_x$ ) from fossil fuel combustion (Reay et al., 2007).

Agricultural soils and livestock are the main source of nitrous oxide emissions from humans both directly and indirectly. Agricultural soils are the dominant source, because intensive synthetic-fertilizer use is rising continuously. Widespread (often poorly controlled) use of animal waste as fertilizer leads to substantial nitrous oxide

emissions from agricultural soils. Other important sources include biomass burning as a result of incomplete combustion products, some industries such as nitric acid production and nylon manufacture, burning of coal for electricity generation, livestock farming, and transport also contribute to nitrous oxide emissions (Reay et al., 2007).

### 2.2.3 Methane

In 1776, the Italian physicist named Alessandro Volta first discovered methane. It acts as a strong GHG and plays important roles in oxidizing capacity of the troposphere and depleting ozone in stratosphere (Pavelka et al., 2018). The concentration of methane in the atmosphere has been increasing rapidly since the industrial revolution (Figure 2.1). Levels of methane are more than doubled to the current 1,800 ppb, previously around 700 ppb (Reay et al., 2007). Recent study reported the increasing of methane in the atmosphere by 150 percent from 722 ppb in 1750 to 1,874 ppb in 2020 (NOAA/ESRL, 2020). Methane is more effective at trapping heat from the sun than carbon dioxide, with GWP of 23 times on a mass basis over a 100-year time horizon. Both of natural and anthropogenic activities emit methane into the atmosphere.

Microbial activity is the primary source of methane emission, especially methanogenesis in flooded soils and anaerobic environments. Wetlands are the dominant natural methane sources; the methane production process in wetland soils involves microbial mineralization of organic carbon under anaerobic conditions. Other natural sources include oceans, hydrates, some vegetation, termites and other creatures (Reay et al., 2007).

Ruminants (cattle) are the main anthropogenic sources of methane emission in addition to fossil fuel extraction and transportation. Domestic heating also contributes substantially to atmospheric methane concentration. Rice cultivation is possibly the biggest of all anthropogenic sources because flooded soils of rice paddies provide ideal conditions for generating methane. Agricultural and municipal waste such as livestock and poultry manure are commonly stored in heaps or slurry tanks. Both industrial and domestic wastewater, and sewage produce methane. Other sources include: landfills, wastewater treatment units, livestock, and biomass burning (Reay et al., 2007).

### **2.3 Wetlands**

Wetland definitions and terms are diverse and often confusing or contradictory. Nevertheless, definitions are important both for the scientific understanding and for their related study. In fact, the word “wetland” did not come into common use until at the mid-20<sup>th</sup> century; before then, specialists referred to wetlands by many terms: swamps, marshes, bogs, fens, mires, and moors. The word “wetland” clearly explicitly states land covered or inundated by water, but in science the term depends on point of view and philosophy: hydrography uses water table and inundated period to consider wetlands, agronomy focuses on saturated soil conditions, and botany uses vegetative ability to grow in submerged soil. With diverse definitions wetlands are difficult to define precisely. In addition, wetlands vary in their great geographical extent and the wide variety of hydrologic conditions—wetlands merge the properties between terrestrial and aquatic part around its edge, for instance, rivers, lakes, ocean areas, and small flooding areas—thus, variable conditions lead to difficulty defining “typical”

wetland characteristics. Moreover, the properties in wetlands all vary on a scale: soil, water, soil organic material, and aquatic organic content. (Mitsch and Gosselink, 2015)

We can refer to wetlands as fluctuating areas of interface between aquatic and terrestrial systems, where the water table is usually close or at there to the water surface. In other word, a flooded land with shallow water (Cowardin et al., 1979). Thailand refers wetland to specific definition use in “Ramsar Convention” (Ramsar Convention Secretariat, 2016; Office of Natural Resources and Environmental Policy and Planning, 2013). The Ramsar Convention’s classification is in Table 2.1.

**Table 2.1** The Ramsar Convention’s classification of wetlands

Code	Classification	Example of wetland
<i>Marine/Coastal Wetlands</i>		
A	Permanent shallow marine waters	sea bays and straits
B	Marine subtidal aquatic beds	kelp beds, sea-grass beds, tropical marine meadows
C	Coral reefs	-
D	Rocky marine shores	rocky offshore islands and see cliffs
E	Sand, shingle or pebble shores	sand bars, spits and sandy islets, dune systems and humid dune slack
F	Estuarine waters	permanent water of estuaries and estuarine systems of deltas
G	Intertidal mud, sand or salt flats	-



**Table 2.1** The Ramsar Convention's classification for wetlands (cont'd)

<b>Code</b>	<b>Classification</b>	<b>Example of wetland</b>
H	Intertidal marshes	salt marshes, salt meadows, saltings, raised salt marshes, tidal brackish and freshwater marshes
I	Intertidal forested wetlands	mangrove swamps, nipah swamps and tidal freshwater swam forests
J	Coastal brackish/saline lagoons	brackish to saline lagoons with at least one relatively narrow connection to the sea
K	Coastal freshwater lagoons	freshwater delta lagoons
Zk(a)	Karst and other subterranean hydrological systems	-
<b><i>Inland Wetlands</i></b>		
L	Permanent inland deltas	-
M	Permanent river/ streams/creeks included waterfall	-
N	Seasonal/intermittent/irregular rivers/streams/creeks	-
O	Permanent freshwater lakes (>80,000 m <sup>2</sup> )	large oxbow lakes
P	Seasonal/intermittent freshwater lakes (>80,000 m <sup>2</sup> )	Floodplain lakes

**Table 2.1** The Ramsar Convention's classification for wetlands (cont'd)

<b>Code</b>	<b>Classification</b>	<b>Example of wetland</b>
Q	Permanent saline/brackish/alkaline lakes	-
R	Seasonal/intermittent saline/brackish/alkaline lakes and flats	-
Sp	Permanent saline/brackish/alkaline marshes/pools	-
Ss	Seasonal/intermittent saline/brackish/alkaline marshes/pools	-
Tp	Permanent freshwater marshes/pools on inorganic soils	ponds (<80,000 m <sup>2</sup> ), marshes and swamps with emergent vegetation water- logged for at least most of the growing season
Ts	Seasonal/intermittent freshwater marsh/pools on inorganic soils	sloughs, potholes, seasonally flooded meadows, and sedge marshes
U	Non-forested peatlands	shrub or open bogs, swamps, fens
Va	Alpine wetlands	alpine meadows, temporary from waters snow melt

**Table 2.1** The Ramsar Convention's classification for wetlands (cont'd)

<b>Code</b>	<b>Classification</b>	<b>Example of wetland</b>
Vt	Tundra wetlands	tundra pools, temporary waters from snow melt
W	Shrub-dominated wetlands	shrub swamps, shrub-dominated freshwater marshes, shrub carr, alder thicket on inorganic soils
Xf	Freshwater, tree-dominated wetlands	freshwater swamp forests, seasonally flooded forests, wooded swamps on inorganic soils
Xp	Forested peatlands	peat swamp forests
Y	Freshwater springs; oases	-
Zg	Geothermal wetlands	-
Zk(b)	Karst and other subterranean hydrological systems	-
<b><i>Human-made wetland</i></b>		
1	Aquaculture ponds	fish and shrimp ponds
2	Ponds (generally <80,000 m <sup>2</sup> )	farm ponds, stock ponds, small tanks
3	Irrigated land	irrigation channels and rice fields
4	Seasonally flooded agricultural land	intensively managed or grazed wet meadow or pasture
5	Salt exploitation sites	salt pans, salines, etc

**Table 2.1** The Ramsar Convention’s classification for wetlands (cont’d)

<b>Code</b>	<b>Classification</b>	<b>Example of wetland</b>
6	Water storage areas (generally >80,000 m <sup>2</sup> )	reservoirs/barrages/dams/impoundments
7	Excavations	gravel/brick/clay pits; borrow pits, mining pools
8	Wastewater treatment areas	sewage farm, settling ponds, oxidation basins, etc.
9	Canals and drainage channels, ditches	-
Zk(c)	Karst and other subterranean hydrological systems	

In summary, the definition of wetlands depends on the aims of study and the field of interest. Different definitions can be formulated because the ways in which individual disciplines deal with wetlands. Thailand relies on the “Ramsar Convention” for wetland definitions that are specific in name. Considering the applications of the wetland’s definition should be made for specific projects.

## **2.4 Methane cycle in wetlands**

Methanogenesis is the terminal step of carbon flow in many anaerobic environments; it plays a role in the carbon cycle . This mechanism produces methane gas as an end- or a by-product from methanogens. Methane escaping from anaerobic habitats can serve as a carbon and energy for methanotrophs, and can escape to the

atmosphere as a source of GHG (Bastviken, 2009; Fenchel et al., 2012; Schlesinger and Bernhardt, 2013; Zinder, 1993).

#### **2.4.1 Methanogenesis**

Methanogenesis involves a very unique biochemistry, distinguishing it from fermentation and respiration (Fenchel et al., 2012). This catabolic mechanism is an extreme specialization (for anaerobic habitats); and methane production through methanogenesis is unique to these microbes. They are limited to few simple compounds with a single and are dependent on other organisms as their substrates (McInerney et al., 1979). Recent study demonstrated that aerobic methanogenesis occurs by demethylation of polysaccharide esters of methyl phosphonic acid (Repeta et al., 2016). Four distinct pathways for methanogenesis include: hydrogenotrophic, acetoclastic, methylotrophic, and methyl-reducing (Kallistova et al., 2017).

Hydrogenotrophic methanogenesis reduces carbon dioxide to methane using hydrogen (or sometimes formate) as the reductant. This pathway is the most widespread catabolic reaction (Table 2.2) because hydrogen is a major fermentation product in many species of anaerobic bacteria, fungi, and protozoa, which act as important substrate for methanogens; the hydrogenophilic (hydrogen-using) methanogens have a symbiotic growth with surrounding anaerobic bacteria that able to produce hydrogen gas and maintain the low concentration of hydrogen. Horn et al., (2003) found this reaction as a precursor for methane production in peat bogs (Horn et al., 2003).

**Table 2.2** Example of methanogenic reactions (Zinder, 1993)

Reactants	Products	$\Delta G$ (kJ/mol CH <sub>4</sub> )
$4\text{H}_2 + \text{HCO}_3^- + \text{H}^+$	$\text{CH}_4 + 3 \text{H}_2\text{O}$	-135
$4\text{HCO}_2^- + \text{H}^+ + \text{H}_2\text{O}$	$\text{CH}_4 + 3\text{HCO}_3^-$	-145
$4\text{CO} + 5\text{H}_2\text{O}$	$\text{CH}_4 + 3\text{HCO}_3^- + 3\text{H}^+$	-196
$2\text{CH}_3\text{CH}_2\text{OH} + \text{HCO}_3^-$	$2\text{CH}_3\text{COO}^- + \text{H}^+ + \text{CH}_4 + \text{H}_2\text{O}$	-116
$\text{CH}_3\text{COO}^- + \text{H}_2\text{O}$	$\text{CH}_4 + \text{HCO}_3^-$	-31
$4\text{CH}_3\text{OH}$	$3\text{CH}_4 + \text{HCO}_3^- + \text{H}^+ + \text{H}_2\text{O}$	-105
$4(\text{CH}_3)_3\text{-NH}^+ + 9\text{H}_2\text{O}$	$9\text{CH}_4 + 3\text{HCO}_3^- + 4\text{NH}_4^+ + 3\text{H}^+$	-76
$2(\text{CH}_3)_2\text{-S} + 3\text{H}_2\text{O}$	$3\text{CH}_4 + \text{HCO}_3^- + \text{H}_2\text{S} + \text{H}^+$	-49
$\text{CH}_3\text{OH} + \text{H}_2$	$\text{CH}_4 + \text{H}_2\text{O}$	-113

Aceticlastic methenogenesis utilizes acetate to produce methane. In general, acetate dismutation is a type of fermentation but unlike common fermentation pathways. This pathway is most active and important in freshwater sediments and anaerobic digestors where acetate contributes about two-thirds of total methane formation (Fenchel et al., 2012).

Methylotrophic and methyl-reducing methanogens utilize methylated one-carbon compounds included methanol, methylamines, and methyl thiols. Methylotrophic methanogenesis, one of the methyl groups is oxidized to carbon dioxide while the same reactions occur in the reverse direction, hydrogenotrophic methanogenesis. Thus, they participate in reduction of the methyl groups to methane (Welte and Deppenmeier, 2014). Methylotrophic methanogenesis is important in some marine sediments and other anoxic environments where methylated substrates occur (Fenchel et al., 2012). Kallistova et al. (2017) considered the methyl-reducing methanogens as interest from the theoretical point of view because these microbes can also grow on methylated compounds, but, in contrast to methylotrophic methanogens—they cannot disproportionate these substrates, so it is strictly dependent on the presence of hydrogen and formate (Kallistova et al., 2017).

In addition, many projects have applied the oxidation reduction (redox) potential to describe methanogenesis in wetland environments. Redox reactions in wetlands are microbially mediated processes that transfer protons and electrons among redox-active components (Table 2.3).

**Table 2.3** The sequential reactions of organic matter (OM) degradation, Gibbs free energy ( $\Delta G$ ), and redox potential as hydrogen scale ( $E_h$ ) (Faulkner, 2014)

Reaction	Product	$\Delta G$ (kJ/mol CH <sub>4</sub> )	$E_h$ (mV)
OM + O <sub>2</sub>	CO <sub>2</sub> + H <sub>2</sub> O	-2,872	> +300
OM + NO <sub>3</sub> <sup>-</sup>	N <sub>2</sub> + CO <sub>2</sub> + H <sub>2</sub> O	-2,717	+250
OM + MnO <sub>2</sub>	Mn <sup>2+</sup> + CO <sub>2</sub> + H <sub>2</sub> O	-1,922	+225
OM + Fe(OH) <sub>3</sub>	Fe <sup>2+</sup> + CO <sub>2</sub> + H <sub>2</sub> O	-419	+100
OM + SO <sub>4</sub> <sup>2-</sup>	S <sup>2-</sup> + CO <sub>2</sub> + H <sub>2</sub> O	-381	-100
OM + CO <sub>2</sub>	CH <sub>4</sub> + H <sub>2</sub> O	-368	< -200

When wetland soils become gradually anaerobic with water inundation, capacity of oxygen diffusion between the waterlogged soil and the atmosphere decreases by 10,000 times. Redox potential also decreases with increasing depth leading to the chemical gradients along with the soil profiles that affect microbial activity and microbiota distribution (Stolzy et al., 1981; Sweerts et al., 1991). These events force facultative aerobes (microorganisms capable of switching from aerobic degradation to anaerobic respiration) and obligate anaerobic microorganisms that grow only in the absence of oxygen, to use nitrate, manganese, iron, sulfate, and carbon compounds as alternative electron acceptors instead of oxygen during anaerobic catabolism (Faulkner, 2014).

In conclusion, methane gas is a biological product from methanogenesis in anaerobic or even aerobic environments. Common pathways for methanogenesis by methanogenic bacteria include hydrogenotrophic, acetoclastic, methylotrophic, and



methyl-reducing process. Additionally, the oxidation reduction potential concept has been also used intensively to describe methanogenesis in the anaerobic environment such as wetland with the different levels of success.

#### **2.4.2 Methane reduction**

The amount of methane released into the atmosphere depends on the exiting ratio between its production and consumption by diverse organisms, and its transport through the different ways to which various factors are related (Bartlett and Harriss, 1993; Roslev and King, 1996). Different microbial groups carry out methane oxidation resulting in decreasing methane emissions, in both aerobic and anaerobic environment (Brune et al., 2000; Happell et al., 1994).

Aerobic oxidation of methane is carried out by methanotrophs—methane oxidizers for energy generating their biomass and carbon dioxide using oxygen as the electron acceptor and releasing methanol as an intermediate product (Kallistova et al., 2017). In wetlands, methanotrophs develop in the oxidized soil layer, in plant aerobic rhizosphere (aerenchyma), and inside the roots and the submersed aspects of leaf sheaths (Bosse and Frenzel, 1997; Gilbert and Frenzel, 1995). Oxygen availability is the main factor governing the methanotroph activity; it occurs mainly in wetlands during the dry periods (Harriss et al., 1982; Yavitt et al., 1991).

Previous studies reported that methane oxidation occurs within first 7 millimeters as a function of oxygen penetration in peatlands (Moore and Knowles, 1990; Moore and Roulet, 1993). Methane oxidation ranges from 14 to 29 percent of the total oxygen contained in the sediment (Torres-Alvarado et al., 2005). Many studies found that methanotrophs can re-oxidize 80 to 90 percent of methane produced in

anaerobic rice field environments (Conrad and Rothfuss, 1991; Frenzel et al., 1992; Oremland and Culbertson, 1992; Sass et al., 1992). Yavitt et al. (1991) reported a 80 percent methane oxidation rates of the total production in peatlands (Yavitt et al., 1991), and King et al. (1990) reported consumption of 91 percent of the total methane generated in the Florida Everglades. Thus methane oxidation occurs in different wetland types (King et al., 1990).

Nitrifying bacteria also have methane affinity—they oxidize methane under soil nitrogen limiting conditions soil as anoxic oxidation of methane (Chan and Parkin, 2001); they can compete for available oxygen with the methanogens in freshwater wetlands (Megraw and Knowles, 1987).

Anaerobic methane oxidation also plays a significant role in decreasing methane emissions. In 1976, Reeburgh first discovered this process coupled with sulfate reduction in marine sediments (Reeburgh, 1976). However, microorganisms took twenty more years to completely identify (Bian et al., 2001; Boetius et al., 2000; Orphan et al., 2002). Orphan et al. (2002) reported that this mechanism in brackish water different; archaean groups carry out this mechanism in brackish water by forming consortia with sulfate reducing bacteria, which involves a metabolic syntrophic relationship based on inter species electron transfer (Orphan et al., 2002; Valentine, 2004). Methane produced at deeper layers diffuses upward where sulfate is available and thus methane oxidation occurs in the transition zone between sulfate reduction and methanogenesis. Blair and Aller (1995) found that the reactions of anaerobic methane oxidation has syntrophic relationship between Archaea and sulfate reducing bacteria (Blair and Aller, 1995). Apparently, archaea oxidize methane and the sulfate reducing microbes use the resulting products (Table 2.4).

**Table 2.4** Anaerobic methane oxidation reactions by archaeas

<b>Methane oxidation by Archaeas</b>	<b>Reactions effectuated by sulfate reducing microbes</b>
$\text{CH}_4 + 2\text{H}_2\text{O} \rightarrow \text{CO}_2 + 4\text{H}_2$	$\text{SO}_4^{2-} + 4\text{H}_2 \rightarrow \text{S}^{2-} + 4\text{H}_2\text{O}$
$\text{CH}_4 + 4\text{HCO}_3^- + 2\text{H}^+ \rightarrow \text{CO}_2 + 4\text{HCOOH} + 2\text{OH}^-$	$\text{SO}_4^{2-} + 4\text{HCOOH} \rightarrow \text{S}^{2-} + 4\text{CO}_2 + 4\text{H}_2\text{O}$
$\text{CH}_4 + \text{CO}_2 \rightarrow \text{CH}_3\text{COOH} + 4\text{H}_2$	$\text{SO}_4^{2-} + \text{CH}_3\text{COOH} \rightarrow 2\text{HCO}_3^- + \text{H}_2\text{S}$
$2\text{CH}_4 + 2\text{H}_2\text{O} \rightarrow \text{CH}_3\text{COOH} + 4\text{H}_2$	

In 2006, Raghoebarsing reported a new anaerobic methane oxidation that couple with denitrification (Raghoebarsing et al., 2006). His work demonstrated that nitrate could also be an electron acceptor (Haroon et al., 2013). Beal et al. (2009) also suggested that the methane oxidation mechanism comes along with the reduction of manganese ( $\text{Mn}^{4+}$ ) and iron ( $\text{Fe}^{3+}$ ) in marine sediments. The three different reactions of methane oxidation depend upon different electron acceptors (Beal et al., 2009).

However, among the factors related to these mechanisms are organic material content, rate of methane production, depth of sulfate penetration, temperature, pressure, mineralogy, sediment porosity, and seasonal changes (Ojima et al., 1993). Furthermore, oxidation of new methane provides an interesting contribution to the global methane cycle, because the specific mechanism is not fully known.

### 2.4.3 Pathways of methane transport into the atmosphere

The balance between methane production in deeper layers and its oxidation after it diffuses to higher zone determines the loss of methane. Possible mechanisms for methane efflux from methanogenic environment to the atmosphere include: (1) diffusion of dissolved methane along the concentration gradient, (2) release of methane containing gas bubbles known as ebullition, and (3) transport via the aerenchyma of vascular plants (Figure 2.2) (Bogdanov et al., 2007; Whiting and Chanton, 1992). These three mechanisms vary in time and space on methane production (Lai, 2009).

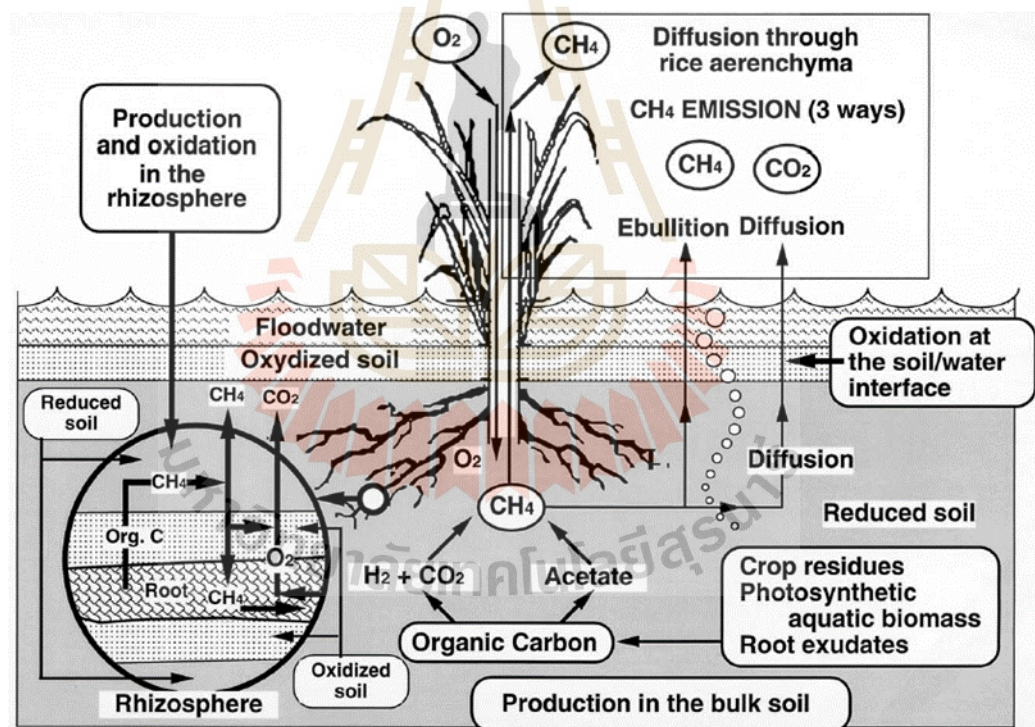


**Figure 2.2** Major transport of methane to the atmosphere (Lai, 2009)

Methane diffusion results from a concentration gradient moving upward to the lower concentration. Kelly and colleague (1990) found that methane diffusion flow corresponds to 56 percent of total emission (Kelley et al., 1990).

Methane bubbles can escape upward to the surface environments by ebullition when the concentration at lower inundated soil layer is higher than hydrostatic pressure of the covered water (Yavitt and Knapp, 1995).

Transport by plant is a response to anoxic soil conditions; plants adapt to aerate their submersed organs by creating internal ventilation systems with gas localized in the stems, roots, and rhizomes; this space (the aerenchyma) plays a role in gas channeling, among oxygen and methane (Torres-Alvarado et al., 2005). Wetland plants present two diffusion gradients: (1) oxygen flux from the atmosphere to the submersed roots and rhizomes where methane is generated, (2) methane diffusion from anoxic regions to the atmosphere—introducing methane to the aerenchyma of the roots facilitates this mechanism. Methane transport through plants includes diffusion inside the root; conversion of the dissolved form to the gaseous form in the root cortex; diffusion passes through the cortex and aerenchyma; and finally releases to the atmosphere through the leaf micropores.

In summary, the deep wetland layers contain trapped methane due to the hydrostatic pressure of the overlaying water layer. Methane trapped in sediments can periodically release through the three major pathways including diffusion, ebullition, and plant mediation.

## **2.5 Potential factors affecting methanogenesis and methane emission**

### **2.5.1 Water level**

Water level determines the depth at which aerobic and anaerobic conditions occur in wetlands and thus controls methanogenesis and methane oxidation processes (Kelley et al., 1995). A study on methane emissions from North American wetlands found that methane flux has a positive corresponding relationship between water level (Figure 2.3) and soil temperature (Klinger et al., 1994; Moore and Roulet, 1993; Shannon and White, 1994). Harris et al. (1982) determined that peat from Great Dismal swamp lowers methane emissions when water level is below the surface of the peat during dry periods; when peat is well-saturated with water, it becomes methane emission source (Harriss et al., 1982). Wang and Bettany (1995) supports findings from Harris et al. (1982) that temporarily submerged upland soils may become methane sources because snow melt and heavy summer storms create a waterlogged layer suitable for producing methane (Harriss et al., 1982; Wang and Bettany, 1995).

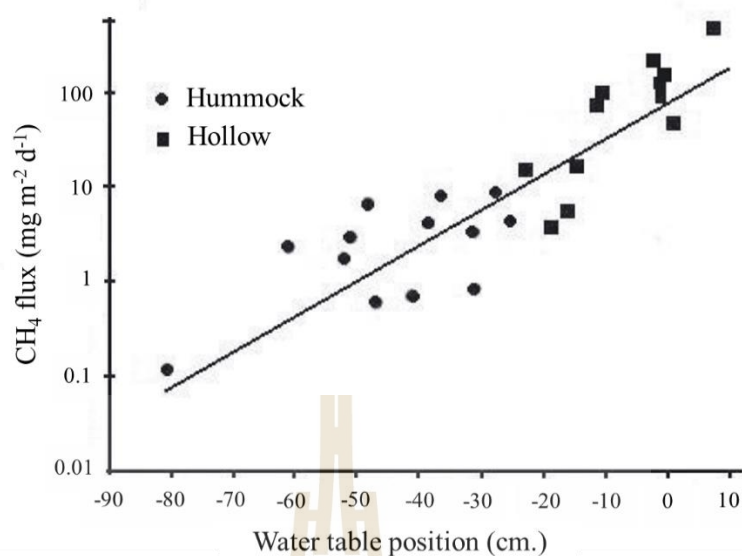


**Figure 2.3** Methane emissions and water table level (Bubier et al., 1993). The methane flux data come from two site: Hummock (circle) and Hollow (square). The figure provides the correlation trend between methane fluxes and water levels.

### 2.5.2 Oxygen and reducing condition as redox potential

Hungate and Macy (1973) reported that methanogens are strictly anaerobes and need a redox potential of at least -0.3V (Hungate and Macy, 1973). In methanogenic environments, mainly oxygen controls methanotrophy in rice fields (Joulian et al., 1997). Kumaraswamy et al. (1997) found that methane oxidation was higher in rhizosphere followed by the surface soil with the level of 0.1 cm, and bulk soil ranged from 10 to 20 cm in depth (Kumaraswamy et al., 1997).

Kludze and Delaune (1995) planted grasses and rice in submerged soil in a laboratory experimental setting with maintained redox potential at 100, 0, -100, and -200 mV. The redox potential affected both methanogenesis and gas transfer through the

plant (Kludze and Delaune, 1995). When redox potential decreased from -200 mV to -300 mV methane production increased by 10-fold (Figure 2.4) and soils emitted 17 times more methane because the plants form more aerenchyma (Kludze et al., 1993).

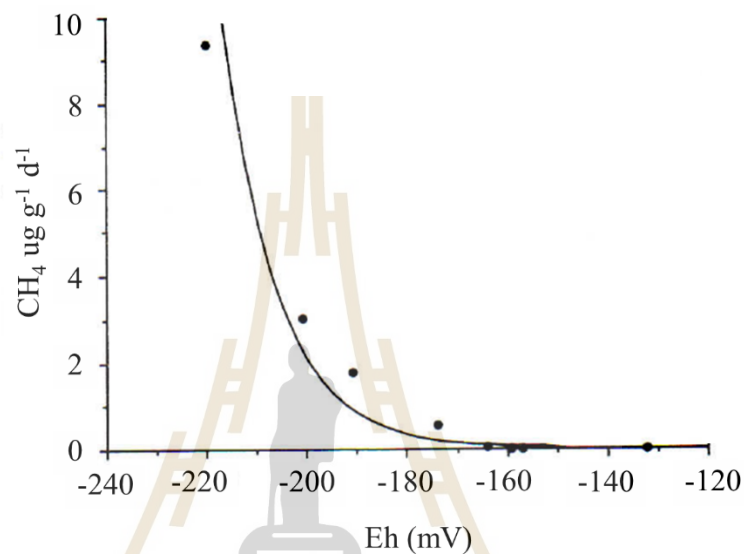


**Figure 2.4** Methane flux decreased with redox potential increase (Wang et al., 2009)

### 2.5.3 Soil texture

In undated environments, soil texture influences generating anaerobiosis needed for methanogenesis, the decomposition of organic matter, transport and trapping of methane into the atmosphere, and the depth of oxidized soil layer hosting methanotroph. Greater clay content affects methane emission based on its nature, because some clay types limit organic matter from mineralizing (Oades, 1988), which delays methanogenesis. The results from Brye et al. (2013) were in line with Oades (1988). Figure 2.5 demonstrates the results that methane fluxes were found higher in the silt loam than in the clay soil (Brye et al, 2013). However, some study showed that



soils rich in swelling clays with high organic material are usually more favorable to methanogenesis than sandy soils, silty soils, or soils abundant in kaolinite (Neue and Roger, 1994).

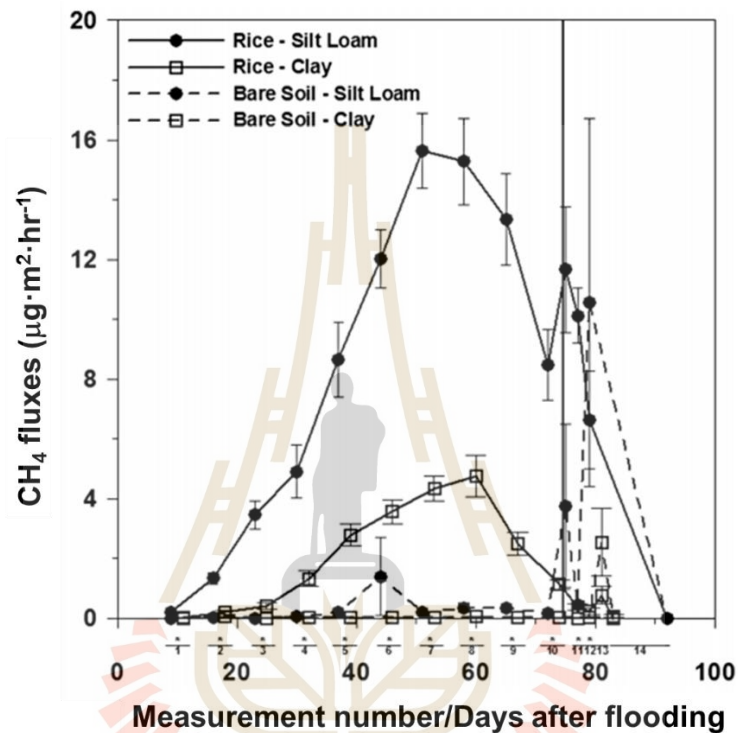


**Figure 2.5** Temporal distribution of methane fluxes (Brye et al., 2013)

High clay content can also trap methane bubbles in soils (Sass et al., 1994) resulting in emission decreases. A study from the Philippines demonstrated that methane emission and methane production during three crop cycles were markedly higher in calcareous (soil contains more than 15%  $\text{CaCO}_3$ ) sandy silt than in clay soil (Denier van der Gon et al., 1996). In calcareous soils, methane production may be partly stimulated by carbonate buffering (Neue and Roger, 1994). Sass et al. (1994) reported

a positive correlation between sand content and average methane emission during the crop (Sass et al., 1994).

Methane emission varied with soil texture. Wangnera et al. (1999) observed that high negative surface charge increased methane production under both anaerobic and anoxic conditions. Methane production rates in marshland soils increased in this order: sand < gravel < clayey silt < clay (Wagner et al., 1999).

#### **2.5.4 Organic matter content as a substrate**

Methanogenesis intensity in flooded soils depends upon the content and the nature of organic matter (Annisa et al., 2014), the ability of microflora (to decompose the organic material), and electron acceptors (Zhao et al., 2018). In wetlands, availability of organic carbon susceptible to be consumed during methanogenesis varies based on net production of flooded organic material by other organisms (Schlesinger and Bernhardt, 2013). When the water column depth raises, decomposition of organic material is greater under anaerobic conditions and, since these processes are slower, the generated organic substrates are of better quality, for instant, carbohydrates and proteins. With a lower water column depth, there is less flood vegetal cover, favoring aerobic mineralization processes, which generate biologically inert humic-substances that are difficult to degrade (Cicerone et al., 1992).

In freshwater wetlands, Crozier and DeLaune (1996) found that organic matter concentration increased total methane production (Crozier and DeLaune, 1996). In marshes, methane concentration was positively associated with organic carbon content (Ding et al., 2002). More recent study, a positive correlation between methane

production and organic material content was observed only in soil exhibiting a high methanogenic activity (Wang et al., 2009).

Morrissey et al. (2013) investigated eight tidal wetland soils in Virginia and found salinity increases microbial decomposition rates in low salinity wetlands. Their findings suggested that ecosystems may experience decreased soil organic matter accumulation, accretion, and carbon sequestration rates even with modest saltwater intrusion levels because of the inhibitory effect of salinity on methanogenesis (Morrissey et al., 2013).

In peat soils, the nature of the organic matter determines both methane production and methane consumption. Methanogenesis capacity strongly decreases with depth; the layer ranged from 0 centimeter to 5 centimeter contributed 70 percent of the total methane generated, indicating that recent plant residues are a main substrate for methanogens (van den Pol-van Dasselaar and Oenema, 1999).

#### **2.5.5 Chemical properties**

The reducers; nitrate, ferric ion, and sulfate compete for substrate and electrons with methanogens (Chidthaisong and Conrad, 2000). A high ferric ion content in soils allows for fast decreasing redox potential after flooding favors methanogenesis (Joulian et al., 1997; Wang et al., 2009). Ferric ions can also have a chemical impact, because of the re-oxidation in the rhizosphere, and a biological impact, by increasing carbon oxidation into carbon dioxide (Frenzel et al., 1999; Yao et al., 1999). Additionally, Wassmann and colleagues (1993) found ferrous ions may reduce methane production in rice field soils by maintaining microorganism activity, thus delaying substrate availability for methanogenesis (Wang et al., 2009).

Sulfate and acidic sulfate soils have less methane emissions than other soil types (Jernsawatdipong et al., 1994; Yagi et al., 1994). Hydrogen is limited because sulfate reducing microbes compete with methanogens. In sulfur rich soils rice productivity is also lower which may contribute to methanogenic decreases. A Thailand based study found ten times lower methane emissions in sulfate rich soils (Yagi et al., 1994). Brackish wetlands, characterized by constant supply of sulfates, also negative correlations between sulfate concentration and methane emission (Ramachandran and Ramachandran, 2001). Sulfate reducing bacteria compete more efficiently for the available substrates, in particular, acetate and hydrogen, as compared to methanogenic bacteria so the sulfate reduction process is favored (Lovley and Klug, 1986). Thus whenever sulfates are abundant, methane production decreases and methanogenesis is restricted to deep areas of sediments where sulfate supplies are limited (Sinke et al., 1992).

However, thermodynamic experiments on soil samples from 16 rice fields revealed methane production depends mainly upon degradable organic material availability rather than the amount of sulfate and ferric ions (Yao et al., 1999; Yao and Conrad, 1999). Phosphorus addition onto planted rice soils as fertilizer significantly decreased methane emission likely by increasing methanotrophic potential (Lu et al., 1999). Phosphate concentrations also inhibited acetotrophic (in acetoclastic pathways) methanogen activity in the roots of rice plants (Chin et al., 2004). The effects of heavy metals on methane production are complicated but usually act as inhibitors (Mishra et al., 1997).

### 2.5.6 Salinity

Methanogens are present from fresh water to hypersaline environments. Freshwater methanogens require at least 1 millimolar (mM) sodium ions ( $\text{Na}^+$ ) since an sodium motive force involved inwardly in the bioenergetics of methanogenesis (Kaesler and Schönheit, 1989; Müller et al., 1987). Kreisl and Kandler (1986) found that some methanogens genera can grow in marine media after a period of adaptation. Methanogens adapt to salinity by accumulating compatible solutes in their cytoplasm to equalize the external and internal osmolarity (Kreisl and Kandler, 1986).

### 2.5.7 pH

Most methanogens have pH optima near neutrality (Jones et al., 1987) and are very sensitive to soil pH variation (Wang et al., 2009). Figure 2.6 shows the 68 experimental methanogenic species were unable to grow below 5.6 pH (Wang et al., 2009).

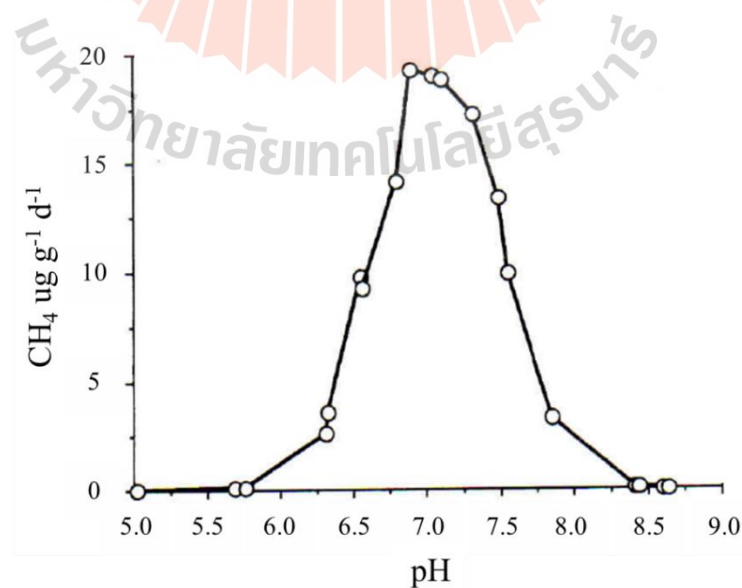


**Figure 2.6** pH and methane fluxes (Wang et al., 2009)

Methanogens can adapt to extreme environments. Peat samples where the initial pH equals 3.9 still show significant methanogenic activity when incubated at pH 3.0 (Dunfield et al., 1993; Williams and Crawford, 1984). Additionally, Williams and Crawford found that a hydrogenotrophic methanogen from peat bogs was able to grow at pH 5.0 and continued to produce some methane until pH 3.0 (Williams and Crawford, 1984). Goodwin and Zeikus (1987) demonstrated that both carbon dioxide reduction and methanogenesis from acetate can occur in sediments pH 4.0 or higher (Goodwin and Zeikus, 1987).

There are some moderately alkaliphilic methanogens that grow optimally near pH 8.0 and can still grow at pH 9.0 (Blotevogel et al., 1985; Garcia et al., 2000). Some methanogens belonging to this group from an alkaline hypersaline lake in Egypt have an optimum pH value of 9.2 (Mathrani et al., 1988).

#### **2.5.8 Temperature in methanogenic environments**

Temperature is important factor affected methanogenic activity (Chin and Conrad, 1995; Conrad et al., 1987; Schütz et al., 1990; Yamane and Sato, 1967). Increasing soil temperature can enhance methane emission, due to its influence on microbial metabolism and reducing soil temperature reduces methanogenic activity (Butterbach-Bahl et al., 2013). In methanogenic rice soil incubation, a temperature reduction from 35°C to 15°C induced a decrease in methane production and changed the organic matter degradation pathways (Chin and Conrad, 1995). When temperature diminishes the hydrogen partial pressure decreases with acetate, propionate, caproate, lactate, and isopropanol accumulation therefore, methanogenesis from hydrogen decreases and acetate consumption increases (Conrad et al., 1987). Laboratory studies

with soil cores from swamps and peatlands in Canada showed methane emission increases by 6.6 times with temperature increases from 10°C to 23°C (Moore and Dalva, 1993). However, Fang and Moncrieff (2001) noted that effects of temperature were overlapped with effects of moisture under field conditions, thus possibly making it hard to observe clear correlations (Fang and Moncrieff, 2001).

Methanogens are found in a wide variety of thermal regimes, from marine sediments which permanently remain at 2°C to geothermal areas above 100°C (Zinder, 1993). There is a great diversity of both mesophilic and thermophilic methanogens. In general, thermophilic species grow more rapidly than corresponding mesophiles. Temperatures below 15°C can limit methanogenesis in fresh water habitats, for example, lake sediments and rice paddies (Conrad et al., 1987; Zeikus and Winfrey, 1976). The optimum for methanogenesis temperature in this sediments is often near 35°C. Zeikus and Wolf (1972) isolated the first thermophilic methanogen in 1972 (Zeikus and Wolfe, 1972). This group of methanogens grows optimally at 65°C in hot springs (Zeikus et al., 1980). Hyperthermophiles are also present in an undersea spreading center, an Icelandic hot spring, and a shallow marine hydrothermal system with a temperature optimum of 80°C (Jones et al., 1983), near 83°C, and near 100°C, respectively.

#### **2.5.9 Temperature as an influencing factor**

There is a direct relationship between rising temperature methanogens growth (Westermann, 1993). As soil temperature increases an exponential increase in methane flux also occurs (Hargreaves and Fowler, 1998). Therefore, there are large emissions from marshes and alluvial floodplains in tropical regions with the optimal temperature

of decomposition of 35°C (Miyajima et al., 1997). Seasonal variations in methane emission correlating with soil temperature in temperate regions and subtropical regions (Boon and Mitchell, 1995; Klinger et al., 1994; Prieme, 1994). However, significant methane emission still occur in swamps during winter, and methane emission even continues beneath the snow (Dise, 1992).

Brooks Avery et al. (2002) discovered that methanogenic activity increases in wetlands from mid and high latitudes during high temperature seasons. Figure 2.7 shows the experimental results supported these observations; increases temperature induce an exponential increase in the acetoclastic, and hydrogenotrophic methanogenesis (Brooks Avery et al., 2003).

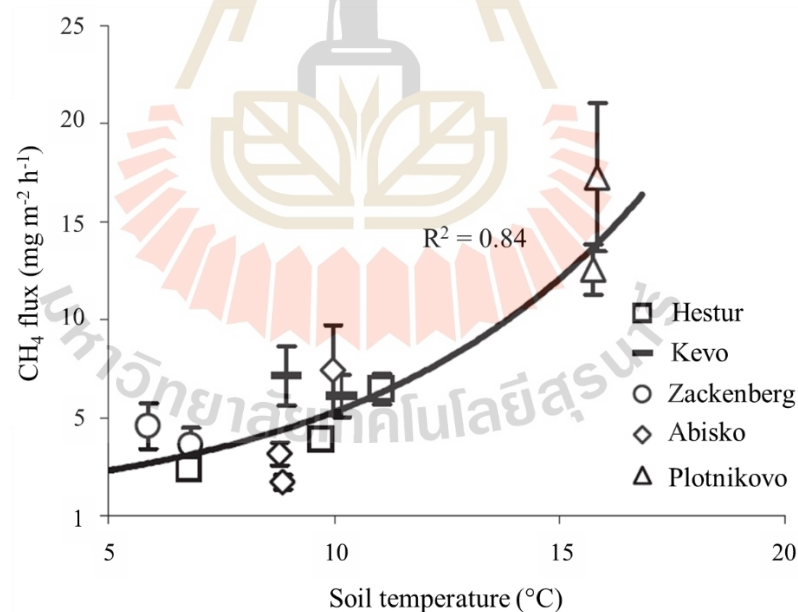


**Figure 2.7** Exponential increase in methane flux with soil temperature from different five observations (Brooks Avery et al., 2003)



Methanotrophy seem to be less sensitive to temperature than methanogens. Both methane production-consumption in temperate and sub-arctic peats were optimal from 20°C to 30°C, with a broader tolerance to temperature for methanotrophs (Dunfield et al., 1993). Soil cores from temperate forests did not show large variation in methanotrophic activity between -1°C and 30°C in an experimental setting (King and Adamsen, 1992) while Castro and colleagues found that the temperature between -5°C and 10°C affect methanotrophic bacteria in Massachusetts forests (Castro et al., 1995).

Temperature also influences methane transport through rice plants; at 5 cm depths. There is a positive correlation between soil temperature and methane conductance in rice plants (Hosono and Nouchi, 1997; Nouchi et al., 1994). Figure 2.8 from Minamikawa et al. (2015) demonstrated that daily variations of methane emission in rice fields co-occur with daily temperature variation (Brooks Avery et al., 2003; Sass et al., 1994; Wassmann et al., 1994; Hosono and Nouchi, 1997). The methane flux increased rapidly from the morning to the peak at about midday, and decreased suddenly in the evening, then remained steady throughout the night. Study in the Philippines evidenced that the highest methane emissions occurred early afternoon and lowest rates in early mornings (Wassmann et al., 1994).

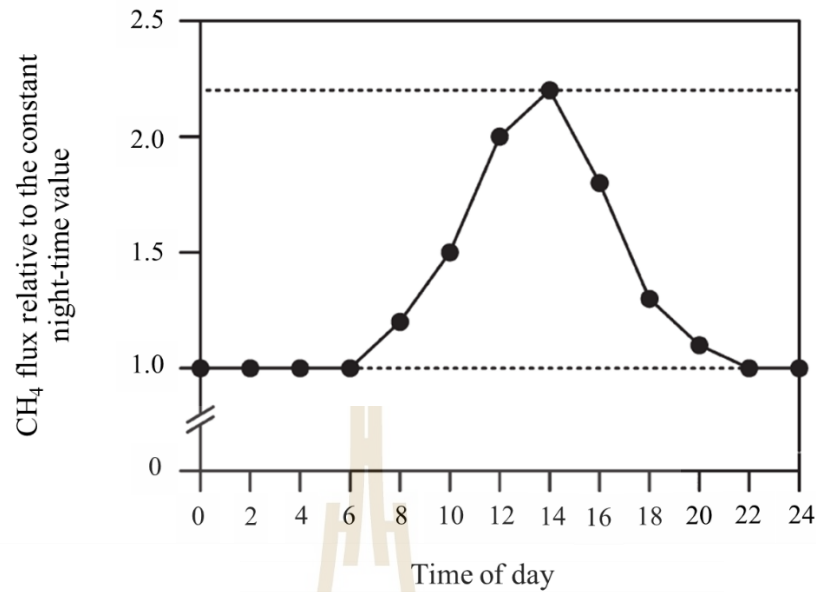


**Figure 2.8** Relative methane flux in a day (Minamikawa et al., 2015)

#### 2.5.10 Seasonal variation

In Australian river sediments, methane emission ranged from less than 0.01 milli-mole/m<sup>2</sup>/hr in winter to 2.75 milli-mole/m<sup>2</sup>/hr in summer (Boon and Mitchell, 1995). In addition to a direct effect of the temperature, seasonal variation of the methane emission from temperate wetlands also related to plant vegetative cycles (processing an aerenchyma, and non-rooted floating vegetation), which may play an important role in methane oxidation, as in the North Carolina swamps (Kelley et al., 1995).

## 2.6 Quantification of methane emission from wetlands

Chamber methods can quantify methane emission at the smallest scale. These methods yield information on processes such as photosynthesis light response, dark respiration and soil carbon efflux and their environmental dependencies. Mass balance techniques are suitable for small, defined source areas, typically ranging from tens to

thousands of square meters in extent, for instance, landfill (Harper et al., 1999), cattle (Leuning et al., 1999), pasture (Laubach and Kelliher, 2004; Wilson et al., 1983), and farm (Denmead et al., 1982). The micrometeorological eddy-covariance technique is more appropriate for the ecosystem scale or large landscape, i.e. at whole-forest scale instead of standard monitoring tools. Eddy-covariance relies on the mass balance approach (Launiainen, 2011). This method uses fast response anemometers and gas sensors to make direct measurements of vertical gas fluxes at a point, several times a second, but it is costly.

### 2.6.1 Chamber techniques

Chambers are used to measure gas fluxes. Their operating principle is simple, and they offer flexibility, portability and low cost. Chambers restrict the volume of air with which gas exchange occurs so as to magnify changes in concentration of gas in the head space. There are two approaches to the chamber technique: open and closed (Pavelka et al., 2018).

In the opened-chamber, a constant flow of outside air occurs through the chamber head space, record the difference in concentration between the air entering and leaving the head space, and then calculate the gas flux at the surface ( $F_g$ ) from the equation (2.1) where  $V$  is volumetric flow rate ( $\text{m}^3/\text{s}$ ),  $C_o$  is gas concentration in the air leaving the chamber,  $C_i$  is gas concentration in the air entering the chamber, and  $A$  is the surface area covered by the chamber ( $\text{m}^2$ ).

$$F_g = V \frac{(C_o - C_i)}{A} \quad (2.1)$$

However, when fluxes are small, the use of opened chambers could be limited by the small magnitude of the concentration increase. For closed-chambers, there is no replacement of air in the chamber head space, so the gas concentration consistently increases. In equation (2.2),  $V$  is the volume of the head space,  $A$  is the surface area covered by the chamber ( $m^2$ ),  $dP/dt$  is the change in gas concentration by the time ( $mg/s$ ) produces the gas flux ( $F_g$ ) estimate.

$$F_g = \left(\frac{V}{A}\right)\left(\frac{dP}{dt}\right) \quad (2.2)$$

Closed-chambers experiments are more common than opened-chambers because the larger gas concentration changes are easier to detect and usually, are simple to operate. They can be static or dynamic. In static chambers, there is no air circulation between the sensor and chamber, hence no power needs. A common practice is to take periodic air samples from the head space with a syringe and subsequently measure gas concentrations in laboratory. Dynamic chambers are more sophisticated. Air is circulated in a closed loop between the head space and a gas analyzer.

### 2.6.2 Meteorological techniques

Meteorological techniques are based on assumption that fluxes are nearly constant with height and that concentrations change vertically but not in the horizontally. Launiainen (2011) explained that the principle of meteorological eddy covariance bases on the mass balance approach (Figure2.9). In horizontally, homogenous and stationary conditions the turbulent vertical flux at upper edge of the

box ( $Z_{ref}$ ) should equal the integral over all sources and sinks,  $S(z)$  within the studied volume. Eddies create correlated variations in vertical wind speed ( $w'$ ) and scalar concentration ( $S'$ ) and thus efficiently transport mass and energy in vertical direction. Schematic concentration profile  $C_s(z)$  is shown in right (Launiainen, 2011).

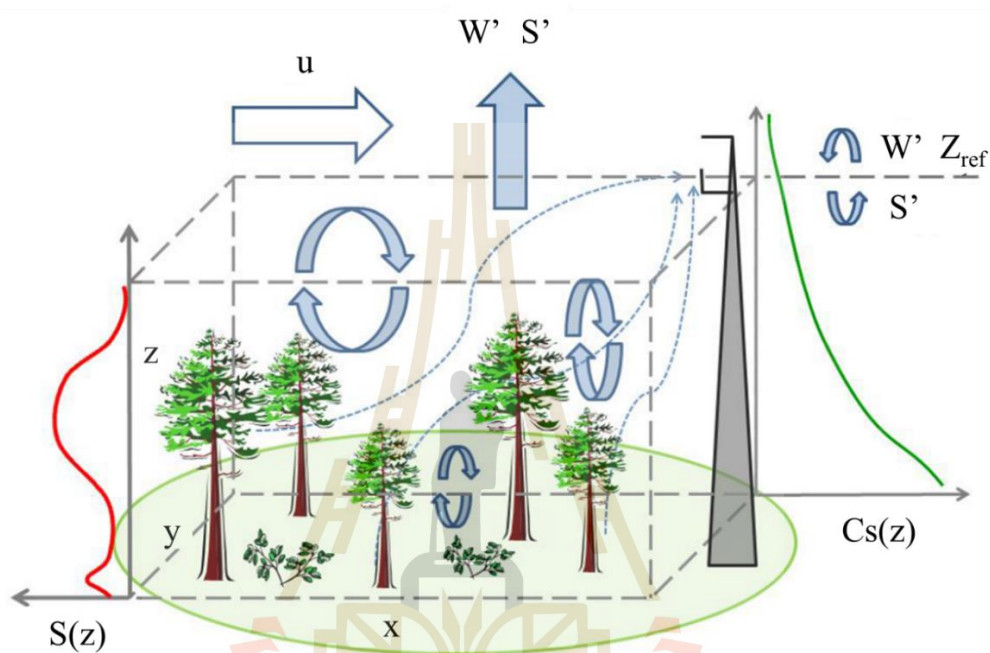


**Figure 2.9** The principle of meteorological eddy covariance based on mass balance (Launiainen, 2011)

The fluxes at a particular height ( $Z$ ) results from many ground level sources upwind. The contributions of sources at different distances from the sensor can be predicted by footprint analyses which use theories of atmospheric dispersion to predict trajectories of parcels of air transported by the wind. Surface roughness and thermal stability are important influences on the footprint.

Conventional meteorological techniques to measure gas fluxes at large landscape scales of many thousands of square meters include eddy covariance, eddy

accumulation, and flux gradient methods. Eddy covariance (Figure 2.9) makes direct measurements of the rate of vertical transport of the gas of interest. The instantaneous flux density across a horizontal plane in the atmosphere is the product of vertical wind speed and the gas concentration at that level. Yu and colleagues (2013) described that this technique requires fast response instrumentation operating at frequencies of 10 hertz (real time reading in every 10 seconds) or higher to measure both the vertical wind speed and the gas concentration. The Eddy accumulation technique substitutes a fast response solenoid valve for a fast response gas sensor. This technique is similar to eddy covariance except that a fast response gas sensor is unnecessary, and air samples can be preconditioned before the gas analyzer. In flux gradient approaches, fluxes are the product of an eddy diffusivity and the vertical concentration gradient of the gas, or the product of transfer coefficient and the difference in gas concentration between two heights. However, eddy covariance is often used for quantifying gas flux from wetlands (Yu et al., 2013).

The Eddy covariance technique is most common for carbon dioxide and water vapor fluxes evaluation. The technique is widely used in micrometeorology over a number of surface (Baldocchi, 2003; Lund et al., 2010). Novel commercial sensors have expanded the available gases for measurement to include methane and also other greenhouse gases (Hargreaves et al., 2001; Rinne et al., 2007). Despite the readily available equipment, the eddy covariance method still requires understanding of atmospheric turbulence, and a variety of corrections are necessary to report accurate fluxes (Foken, 2008). Although, the eddy covariance method is a widely used and a well-accepted technique, there are some limitations. There is a potential for systematic errors in the energy balance closure, and a possibility of under estimation of night time

fluxes in low wind speeds (Baldocchi, 2003; Twine et al., 2000). In summary, there are two main methods commonly used: chamber based and micrometeorological methods. Chamber methods are simpler and more practical than micrometeorological methods (Table 2.5).

**Table 2.5** Examples for advantages and limitations of each method

Advantage/ Limitation	Method	
	chamber	Micrometeorological
Operation level	Simple	Sophisticated
Power	Need from small battery	Need
Scale of study	Small to large area	Ecosystem scale
Cost	Low	High to very high

## 2.7 Statement of conclusion

GHGs in the atmosphere play key roles on the Earth's climatic systems. Three important GHGs are of concern; carbon dioxide, methane, and nitrous oxide. These gases emit from various sources.

Apart from carbon dioxide, methane gas is the second most important GHGs due to its contribution to the greenhouse effects and the GWP of 87 times with 20-year time horizon. In natural environment, methane is biologically produced from methanogenesis by methanogenic bacteria in anaerobic or even aerobic environment. These conditions are found in wetlands.

Methanogenesis has four major pathways: (1) by using carbon dioxide with hydrogen, (2) by using acetic acid, (3) by directly using methylated compound, and (4)

by subsequent process from reducing methylated compounds. Methane is oxidized by methanotroph (methane consuming bacteria) resulting in methane reduction before escaping into the atmosphere. Trapped methane in methanogenic environment can transport by three different pathways: diffusion upward (by concentration gradient), air bubble as ebullition (by disturbing, and changing in hydrostatic pressure), and through the aerenchyma of vascular plants (air vascular).

Methane emissions from wetlands vary greatly in time and space. Many factors influence the emissions, such as: pH, temperature, water table level, soil property, salinity, organic carbon content, and climatic conditions. Many studies have shown the evidences on the correlation of methane emissions and these factors.

The quantification of gas fluxes usually uses two major techniques: chamber-based techniques and meteorological approaches. Each technique has advantages and limitations in different studies. The chamber-based technique is simple to operate and adaptable to a wide variety of studies from local to global spatial scales while the meteorological technique is more sophisticate and suitable for a pilot scale study. Objectives and practicality are the basic criteria for selecting the specific technique.



## CHAPTER III

### METHODS

Quantification of seasonal methane fluxes from a natural wetland in Nakhon Ratchasima consists of 4 parts: (1) study area description, (2) sample collection, (3) sample analysis, and (4) data analysis. The overview content is in Figure 3.1.

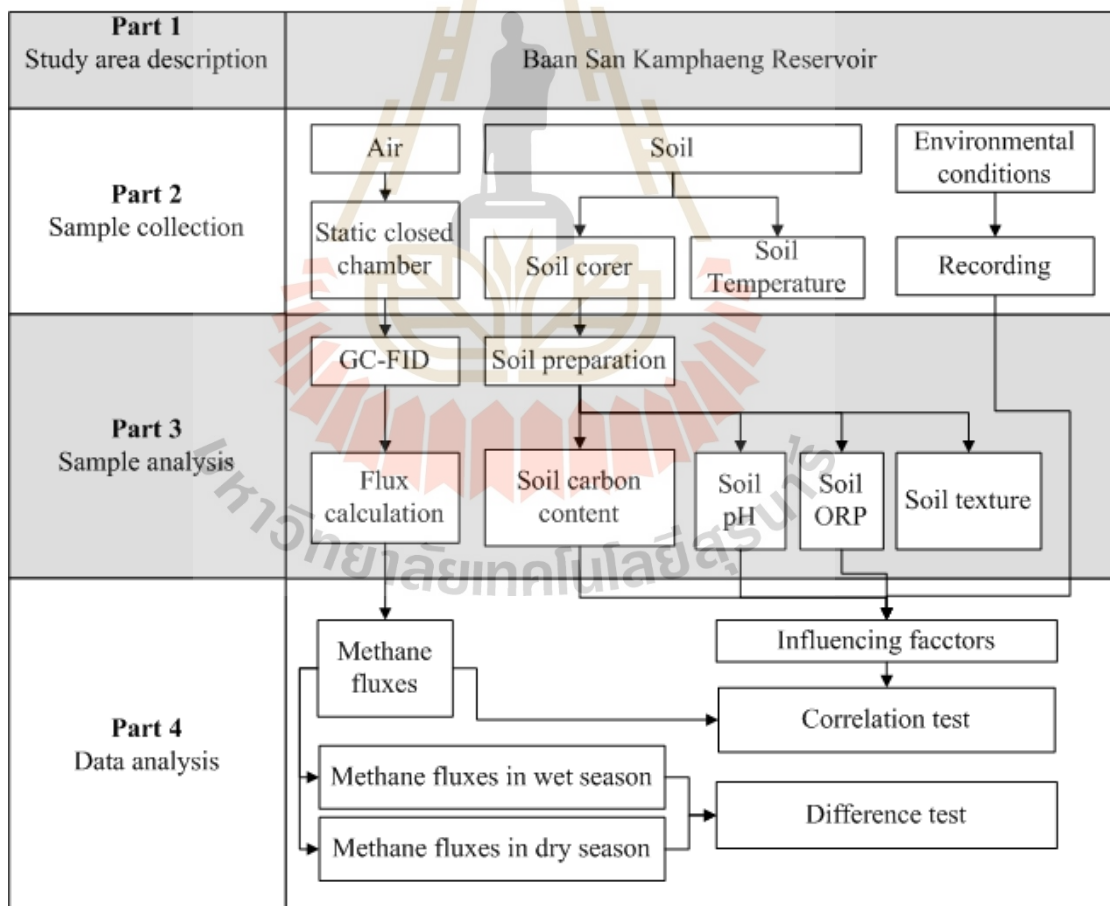


**Figure 3.1** The overview content

### 3.1 Study area

Baan San Kumphaeng Reservoir is located near the Phanom Dong Rak's foothills at Wang Numkheaw district, Nakhon Ratchasima province (14°23'18" N 101°42'30" E). Lam Prapleng stream discharges water into the reservoir year-round. The stream channel is almost stagnant in some months, especially during dry season. Table 3.1 shows general information of Baan San Kumphaeng reservoir (Regional Irrigation Office 8, 2000).

**Table 3.1** General information of Baan San Kumphaeng Reservoir

List of information	Details
Surface area of reservoir (at Retention water level)	1.632 (km) <sup>2</sup>
Surface area of water	2.115 (km) <sup>2</sup>
Reservoir basin	51.20 (km) <sup>2</sup>
Annual rainfall (average)	1,136.00 mm.
Annual stream flow input	8,066,000 m <sup>3</sup> / year
Storage capacity (at Dead storage)	760,000 m <sup>3</sup>
Storage capacity (at Maximum Runoff)	8,500,000 m <sup>3</sup>
Flood surcharge	2,000,000 m <sup>3</sup>
Dead storage level	+ 433.60 m. (MSL)
Retention water level	+ 438.50 m. (MSL)
Bed level	+ 426.00 m. (MSL)
Maximum runoff level	+ 439.60 m. (MSL)

**Note:** MSL is Mean Sea Level

Gas sampling location was performed at a certain point but the variations water level of the wetland had changed throughout the year, impractical to fix at a certain location. A set of requirement was established to justify the relocation of the sampling point to be as close as possible in each month (Table 3.2) (de Klein and Harvey, 2012). Figure 3.2. shows the sampling area in this study.



Figure 3.2 Sampling area

**Table 3.2** Considerations for chamber deployment in this study

<b>Issue</b>	<b>Objective</b>	<b>Minimum requirement</b>
Site disturbance	Minimize effect of site disturbance on fluxes estimate.	<ul style="list-style-type: none"> <li>○ Insert a chamber base at least 2 hours prior to the first sampling.</li> <li>○ Avoid the soil disturbance around the chambers.</li> <li>○ Relocate chambers when the water level differs from surroundings within 0-5 cm.</li> <li>○ Remain the chamber deployment onto the constant soil texture.</li> </ul>
Chamber deployment	Minimize changes the physical conditions and leaks.	<ul style="list-style-type: none"> <li>○ Deploy chamber in the period of 60-120 minute for a chamber with height of 120 cm.</li> </ul>

## 3.2 Sample collection

The sample was collected monthly for 12 months. The sample included: (1) gas samples, (2) soil samples, and (3) other environmental parameters.

### 3.2.1 Gas sample collection

The static closed rectangular chambers were used for gas sampling (Hutchinson and Mosier, 1981). The chamber is made from clear acrylic with a 0.25m x 0.25m x 1.20m as shown in Figure 3.3. A thermometer and a small fan are installed inside the chamber to determine the temperature and uniformly mixed the emitted gas (Collier et al., 2014). A rectangular base of a chamber is made of aluminum with groove to fit the acrylic box and leak proof.

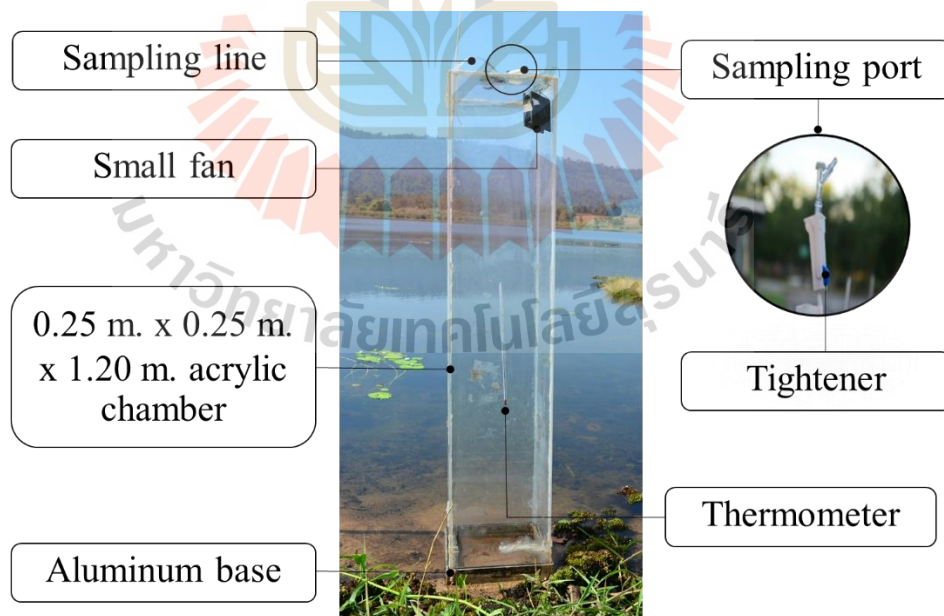


**Figure 3.3** An acrylic chamber and an aluminum base configuration

Gas samples were collected once a month, with five replicated chambers, over one year (Figure 3.4).



**Figure 3.4** A set up of five replicated chambers

The sampling periods began at 2, 22, 42, 62, and 82 minute intervals from 8.30 to 11.00 AM to represent daily average of methane fluxes (Minamikawa et al., 2015).

The steps of gas sampling were as follow.

1. Pushed a chamber base in the soil, at 5 cm depth of soil.
2. After two hours, placed the acrylic chamber on top to trap gas and filled the groove with water to prevent gas leak.
3. Drew gas from the chamber headspace using syringes at predetermine time intervals and transferred into evacuated vials.

4. Sealed the vial cap with silicon sealant.
5. Kept and stored gas samples under 4°C until they were analyzed in laboratory.

### 3.2.2 Soil sample collection

The soil corer made from iron with 4.5 cm diameter and 35 cm height was used for soil sampling. The points of soil sampling were adjacent to the chamber replacement as much as possible. Three replications of soil sampling were performed after the gas collection was completely carried out each month. The steps of soil sampling were as follow (Pennock et al., 2007).

1. Inserted a soil corer into the ground at the maximum depth of 15 cm.
2. Pulled a soil corer up from the ground.
3. Pushed soil samples from a soil corer with plunger.
4. Separated soil sample into three sections: 0.0 – 5.0 cm, 5.0 – 10.0 cm, and 10.0 – 15.0 cm.
5. Transferred each soil section into plastic bags.
6. Kept and stored gas samples under freezing condition until they were analyzed in laboratory.

Soil temperature was measured next to the chamber during the gas sampling (Figure 3.4). The steps of soil sampling were as follow.

1. Inserted a thermometer into the soil at the depth intervals of 2.5, 7.5, and 12.5 cm.
2. Recorded soil temperature after at least 1 minute for constant reading.

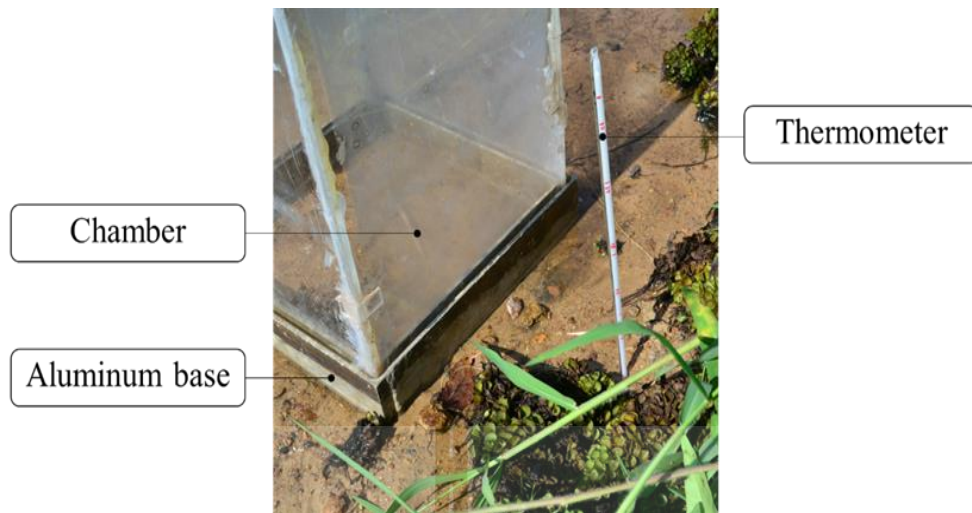


**Figure 3.5** Soil temperature measurement

### 3.3 Sample analysis

#### 3.3.1 Methane fluxes

A gas chromatography (Agilent®, Model 7890A, USA) equipped with a flame ionization detector and a 3.05 m of stainless-steel packed column (Molecular Sieve 13X) was used for quantifying methane concentrations under the conditions described in Table 3.2.



**Table 3.3** Conditions of GC-FID for methane gas analysis.

Parameter	Value
<b>Inlet</b>	
- Heater	- 250°C
- Pressure (total flow)	- 41.3 psi (28 ml/ min)
- Septum Purge Flow	- 3 ml/ min
- Split ratio	- 20 : 1
<b>Oven</b>	
- Temperature	- 50°C
- Equilibration time	- 1 min
- Rate	- 30°C/ min, 150°C
<b>Detector</b>	
- Heater	- 250°C
- H <sub>2</sub> Flow	- 30 ml/ min
- Air Flow	- 400 ml/ min
- Makeup Flow (N <sub>2</sub> )	- 10 ml/ min

Agilent OpenLAB CDS Chemstation Edition A.01.03[024] was operated and acquired the signal for quantifying gas concentration against 19.5 ppmv of standard methane gas (Air Liquide, Thailand, Co., Ltd).

The linear regression model was performed with Microsoft Excel<sup>®</sup> for plotting methane concentrations (ppm) versus time (minute). The derivative of the regression represents the rate of change in gas concentration (ppmv/min) Methane emission rates were calculated based on linear change of gas concentration over time and converted to flux rate (mg/m<sup>2</sup>/day) based on the chamber volume and temperature (Healy et al., 1996). Gas flux rate (mg/m<sup>2</sup>/day) was calculated by the following equation at STP condition.

$$E = \frac{XhM}{RT} \quad (3.1)$$

Where

- $E$  = emission on the aerial basis ( $\text{mg}/\text{m}^2/\text{day}$ ),  
 $X$  = rate of change in gas concentration ( $\text{ppmv}/\text{min}$ ),  
 $h$  = chamber height (m),  
 $M$  = molecular weight (g/mol),  
 $R$  = universal gas constant ( $0.0821 \text{ atm}\cdot\text{L}/\text{K}/\text{mol}$ ), and  
 $T$  = absolute temperature (K).

### 3.3.2 Soil preparation

Soil samples were prepared and analyzed based on procedures described by Tan (2005). All soil samples were completely air-dried at room temperature for at least 1 week. Dried soil samples were later sieved to select the sample with less than 2 mm for further analysis (Tan, 2005).

### 3.3.3 Analysis of soil carbon

A LECO<sup>®</sup> analyzer was used to determine soil carbon content. The steps of soil carbon content analysis were as follow.

1. Weighed  $0.2000 \pm 0.0500$  g of prepared soil
2. Created the calibration curve with EDTA LRCM<sup>®</sup>
3. Analyzed the samples with LECO<sup>®</sup> analyzer

### 3.3.4 Analysis of soil pH

A pH meter (METLER<sup>®</sup>) was used for measuring soil pH. Measurement of soil pH was carried out in an aqueous matrix of 0.01 M calcium chloride (CaCl<sub>2</sub>). The steps of soil pH measurement were as follow.

1. Weighed 10 g of prepared soil into a 25 ml beaker.
2. Added 20 ml of 0.01 M CaCl<sub>2</sub>.
3. Stirred the suspension intermittently for 30 min.
4. Immersed the pH probe in the suspension with simultaneously mixing.
5. Recorded the pH once the reading was constant.

### 3.3.5 Analysis of soil oxidation reduction potential (ORP)

A YSI<sup>®</sup> with ORP sensor was used for measuring soil ORP. The steps of soil ORP measurement were as follow.

1. Weighed 20 g of prepared soil into a 25 ml beaker.
2. Added 20 ml of deionized water.
3. Stirred the suspension for 5 min.
4. Immersed the soil ORP probe in the suspension with simultaneously mixing.
5. Recorded the soil ORP once the reading was constant.

### 3.3.6 Analysis of soil texture

The hydrometer method was applied for soil texture analysis. The 2M of sodium hydroxide was used as the dispersion reagent. The steps of soil texture analysis were as follow.

1. Weighed 100 g of prepared soil into a 1,000 ml beaker.
2. Added 800 ml of deionized water.
3. Added drop-wise of 2 M NaOH under constant stirring until the suspension had a pH of 10 - 11.
4. Transferred the suspension into an ASTM soil testing cylinder.
5. Washed the remaining soil residue into the cylinder with deionized water.
6. Filled the A.S.T.M. soil testing cylinder with deionized water until the marked line.
7. Mixed the suspension thoroughly and recorded the time when mixing was stopped.
8. Placed a hydrometer into the suspension carefully at the exactly 40 s after the mixing was stopped.
9. Read the top of the meniscus in the hydrometer stem.
10. Removed and rinsed the hydrometer.
11. Repeated the steps of 7. to 10., took the two reading as the results.
12. Determined the temperature of the suspension after the hydrometer have been removed.
13. Mixed the suspension again thoroughly.
14. Took a third hydrometer and temperature reading after 120 min.

15. Calculated the soil texture as the following steps.

a. Corrected reading of the temperature

$$C_r = H + 0.2(T_s - 68) \quad (3.2)$$

Where

$C_r$  = Corrected reading

$H$  = Hydrometer reading

$T_s$  = The temperature of the suspension ( $^{\circ}F$ )

b. 40s reading

$$\%(silt + clay) = (C_r/G_s) \times 100 \quad (3.3)$$

Where

$G_s$  = g of weighed soil

$$\% \text{ sand} = 100 - \%(silt + clay) \quad (3.4)$$

c. 120 min reading

$$\% \text{ clay} = (C_r/G_s) \times 100 \quad (3.5)$$

d. % silt

$$\% \text{ silt} = b. - c. \quad (3.6)$$

e. Classified the soil texture with USDA textural triangle

### 3.4 Data analysis

R with packages “base” and Microsoft Excel® for Windows® were performed for statistical analysis. Data were tested for normal distribution by Shapiro-Wilk’s Test. If data were normally distributed, independent-samples t-test and analysis of variances (ANOVA) was carried out. Otherwise, non-parametric Mann-Whitney U test and Kruskal-Wallis were applied. Table 3.4 demonstrates summary of all statistics used in this study.

**Table 3.4** Statistics used in the present study.

Purpose	Parametric test	Non-parametric test	Significant level ( <i>p</i> )
Normality		Shapiro-Wilk’s Test	>0.05
Difference	- t-test	- Mann-Whitney U	<0.05
	- ANOVA	- Kruskal-Wallis	<0.05
Relationship	- Pearson	- Spearman’s rho	<0.05

Pearson and Spearman’s rho test were used for determining the correlation between methane fluxes and influencing factors. Table 3.5 shows the criteria of determination for correlation test in this study. All results were considered statistically significant if *p* value was less than 0.05.

**Table 3.5** Association level and *r* value for correlation test.

Association level	weak	moderate	strong
<i>r</i> value	0.00 to ± 0.39	± 0.40 to ± 0.59	± 0.60 to ± 1

## **CHAPTER IV**

### **RESULTS AND DISCUSSIONS**

Gas and soil samplings from the natural wetland were collected from December 2018 to November 2019 to characterize levels and relationships of the methane emissions, soil pH, soil ORP, soil texture, and soil carbon content. This chapter explains the results of methane concentrations from the natural wetland, the methane fluxes and the relationships on temperature and other parameters such as soil texture, soil pH, etc.

#### **4.1 Methane concentrations from the natural wetland**

Gas sampling was carried out on a monthly basis, providing 64 chambers deployment in total but only 61 deployments provided data in this study. Three chambers were disqualified from fall over due to strong wind during field sampling. The total gas samples were 308 but 16 gas samples were unaccounted for due to errors during laboratory analysis. Only 292 gas samples were used to determine the methane fluxes between 2018 and 2019. Data on methane concentrations collected in February 2020 and flux determination are shown as an example in Table 4.1. Gas samples collected in time interval ( $T_i$ ) in all five chambers were analyzed for corresponded methane concentrations ( $C$ ) and were plotted to determine regression coefficient. Data on other months were in appendix A.

**Table 4.1** Methane concentration, temperature recorded, and graph of methane emissions in February 2019

$C_n$	$T_i$ (min)	$T_c$ (°C)	C (ppmv)	Regressions of methane emissions	X
1	2	28.0	2.48		0.0098
	22	28.0	2.86		
	42	29.0	2.92		
	62	30.0	3.11		
	82	28.8	2.84		
	<b>avg.</b>		28.0		
2	2	n.a.	n.a.		0.0031
	22	27.5	n.a.		
	42	27.5	2.74		
	62	28.1	2.71		
	82	30.0	2.86		
	<b>avg.</b>		28.3		
3	2	n.a.	n.a.		0.0017
	22	27.0	2.78		
	42	27.5	2.80		
	62	28.0	2.81		
	82	31.5	2.89		
	<b>avg.</b>		28.5		



**Table 4.1** Methane concentration, temperature recorded, and graph of methane emissions in February 2019 (cont'd)

<b>C<sub>n</sub></b>	<b>T<sub>i</sub> (min)</b>	<b>T<sub>c</sub> (°C)</b>	<b>C (ppmv)</b>	<b>Regressions of methane emissions</b>	<b>X</b>
4	2	n.a.	n.a.		0.0593
	22	27.0	25.72		
	42	27.5	27.14		
	62	26.5	28.09		
	82	29.0	n.a.		
	<b>avg.</b>	27.5	26.98		
5	2	n.a.	n.a.		0.0138
	22	27.0	4.15		
	42	27.0	n.a.		
	62	27.0	4.59		
	82	29.1	5.00		
	<b>avg.</b>	27.5	4.58		

**Note:** C<sub>n</sub> = chamber number  
T<sub>i</sub> = Time intervals of gas sampling (min)  
avg. = average  
T<sub>c</sub> = chamber's temperature at time interval of gas sampling (°C)  
C = methane concentration (ppmv)  
X = slope of graph; represents methane emissions rate (ppmv/min)  
n.a. = unaccounted sample

The derivative of regressions (X in Table 4.1) represented the methane emission rate of each plot was used to calculate methane fluxes and only valid with the determination coefficient  $\geq 0.85$  ( $R^2$ ). The lower determination coefficient ( $< 0.85$ ) may indicate the disturbed and leaked system during sampling (Altor and Mitsch, 2006). The chamber height (1.20 m) was used for flux calculation and the recorded temperature of sample for each time interval were used to correct methane

concentration into standard conditions (equation 4.1) where 16.04 g/mol is molecular weight of methane, 1440 is the constant value for flux rate on a day basis, and 0.0821 is the universal gas constant. The results from calculation of monthly methane flux are in Table 4.2.

$$\text{Methane flux rate, } E_{\text{day}} \text{ (mg/m}^2\text{/day)} = 1440X \frac{(1.20 \text{ m})(16.04 \text{ g/mol})}{(0.0821)K} \quad (4.1)$$



**Table 4.2** Monthly data on methane flux rate

Month	C <sub>n</sub>	X	T <sub>c</sub>	K (T <sub>c</sub> + 273.15)	E <sub>day</sub>
2018, December	1	0.0049	30.1	303.3	5.46
	2	n.a.	31.3	304.5	n.a.
	3	n.a.	n.a.	n.a.	n.a.
	4	0.0027	29.5	302.7	3.01
	5	0.0043	31.9	305.1	4.76
	6	0.0059	31.9	305.1	6.53
2019, January	1	0.0070	30.0	303.2	7.80
	2	n.a.	29.0	302.2	n.a.
	3	n.a.	29.0	302.2	n.a.
	4	n.a.	29.0	302.2	n.a.
	5	0.4475	29.0	302.2	500.01
	6	0.0041	29.0	302.2	4.58

**Table 4.2** Monthly data on flux rate (cont'd)

Month	C <sub>n</sub>	X	T <sub>c</sub>	K (T <sub>c</sub> + 273.15)	E <sub>day</sub>
February	1	0.0098	28.8	301.9	10.96
	2	n.a.	28.3	301.4	n.a.
	3	0.0017	28.5	301.7	1.90
	4	0.0593	27.5	300.7	66.59
	5	0.0138	27.5	300.7	15.49
March	1	0.0058	31.3	304.4	6.43
	2	0.0017	30.4	303.6	1.89
	3	0.0612	32.9	306.0	67.52
	4	0.0081	31.8	305.0	8.97
	5	0.0033	31.2	304.4	3.66
	6	0.0463	31.9	305.1	51.24
April	1	0.0090	31.8	305.0	9.96
	2	0.0140	33.0	306.2	15.44
	3	0.0151	32.5	305.7	16.68
	4	0.0112	31.6	304.8	12.41
	5	0.0134	33.0	306.1	14.78
May	1	0.0199	33.5	306.7	21.91
	2	0.0133	35.4	308.6	14.55
	3	0.0113	34.7	307.9	12.39
	4	0.1269	33.2	306.4	139.83
	5	0.0062	34.2	307.4	6.81

**Table 4.2** Monthly data on flux rate (cont'd)

Month	C <sub>n</sub>	X	T <sub>c</sub>	K (T <sub>c</sub> + 273.15)	E <sub>day</sub>
June	1	0.0079	31.2	304.3	8.76
	2	0.0144	29.5	302.7	16.06
	3	0.0087	28.5	301.7	9.74
	4	0.0045	30.2	303.3	5.01
	5	0.0047	29.8	302.9	5.24
July	1	0.0090	28.7	301.8	10.07
	2	n.a.	27.5	300.6	n.a.
	3	0.0174	28.7	301.9	19.46
	4	0.0149	29.2	302.4	16.64
	5	0.0203	28.4	301.6	22.73
August	1	0.0052	28.7	301.9	5.82
	2	0.0047	29.9	303.1	5.24
	3	0.0144	29.0	302.1	16.09
	4	0.0106	30.5	303.7	11.79
	5	0.0133	29.3	302.4	14.85
September	1	0.0123	23.8	296.9	13.99
	2	0.0061	23.9	297.0	6.93
	3	0.0128	23.4	296.6	14.57
	4	0.0105	23.8	296.9	11.94
	5	0.0126	24.8	298.0	14.28

**Table 4.2** Monthly data on flux rate (cont'd)

Month	C <sub>n</sub>	X	T <sub>c</sub>	K (T <sub>c</sub> + 273.15)	E <sub>day</sub>
	1	7.7701	30.6	303.8	8634.92
	2	4.9766	30.2	303.4	5538.52
October	3	2.9737	29.3	302.5	3319.32
	4	3.3293	31.7	304.9	3686.75
	5	1.5199	30.3	303.5	1690.96
	1	n.a.	n.a.	n.a.	n.a.
	2	n.a.	30.6	303.8	n.a.
November	3	n.a.	38.6	311.8	n.a.
	4	0.138	32.9	306.1	152.23
	5	n.a.	35.2	308.4	n.a.

**Note:** C<sub>n</sub> = chamber number

X = methane emission rate (ppmv/min)

T<sub>c</sub> = chamber's temperature (°C)

K = absolute temperature (K)

E<sub>day</sub> = methane flux per day (mg/m<sup>2</sup>/day)

n.a. = missing value e.g. coefficient of determination less than 0.85 and leakage of gas in a vial

#### 4.1.1 Methane fluxes

All gas samples ( $n=292$ ) were analyzed for methane concentration and calculated for methane fluxes over the year, providing valid 52 fluxes of methane (Table 4.2). Methane fluxes varied from 2 to 8,635  $\text{mg}/\text{m}^2/\text{day}$  with the mean  $\pm$  SD of  $476 \pm 1,559 \text{ mg}/\text{m}^2/\text{day}$  and the median of  $14 \text{ mg}/\text{m}^2/\text{day}$ . The lowest methane flux was found in February while the highest methane flux was in October. A histogram showed the distribution of methane flux values (Figure 4.1). About 87% of methane fluxes had the values less than  $150 \text{ mg}/\text{m}^2/\text{day}$ .

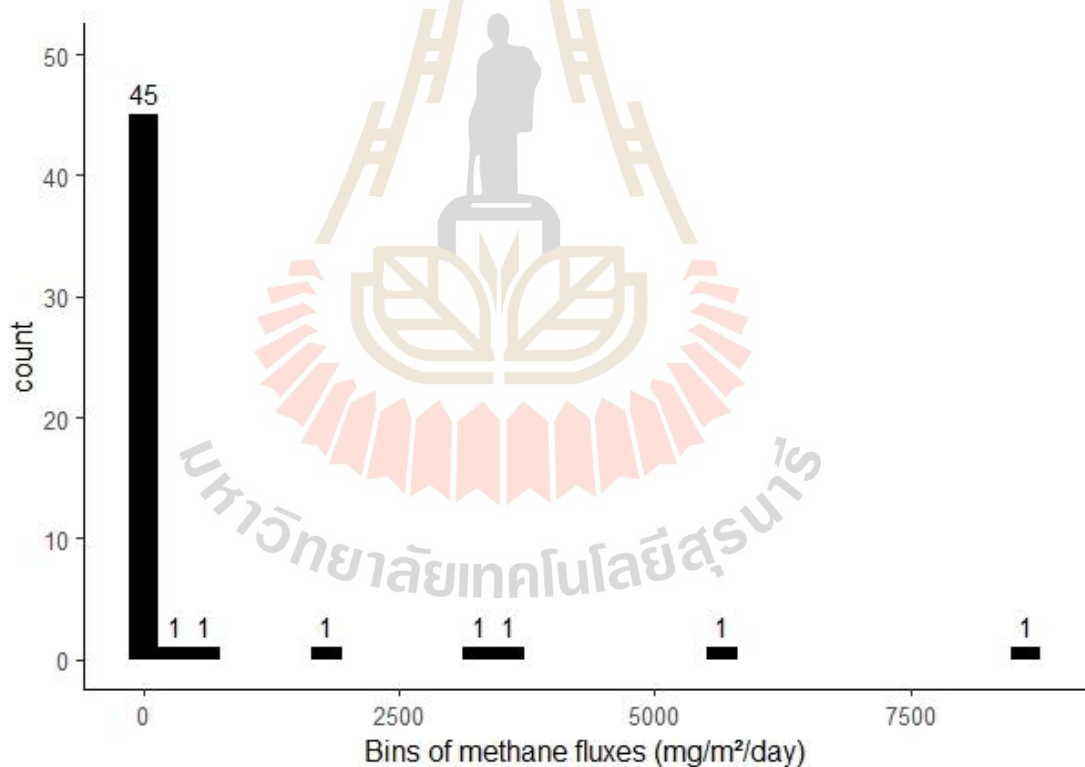


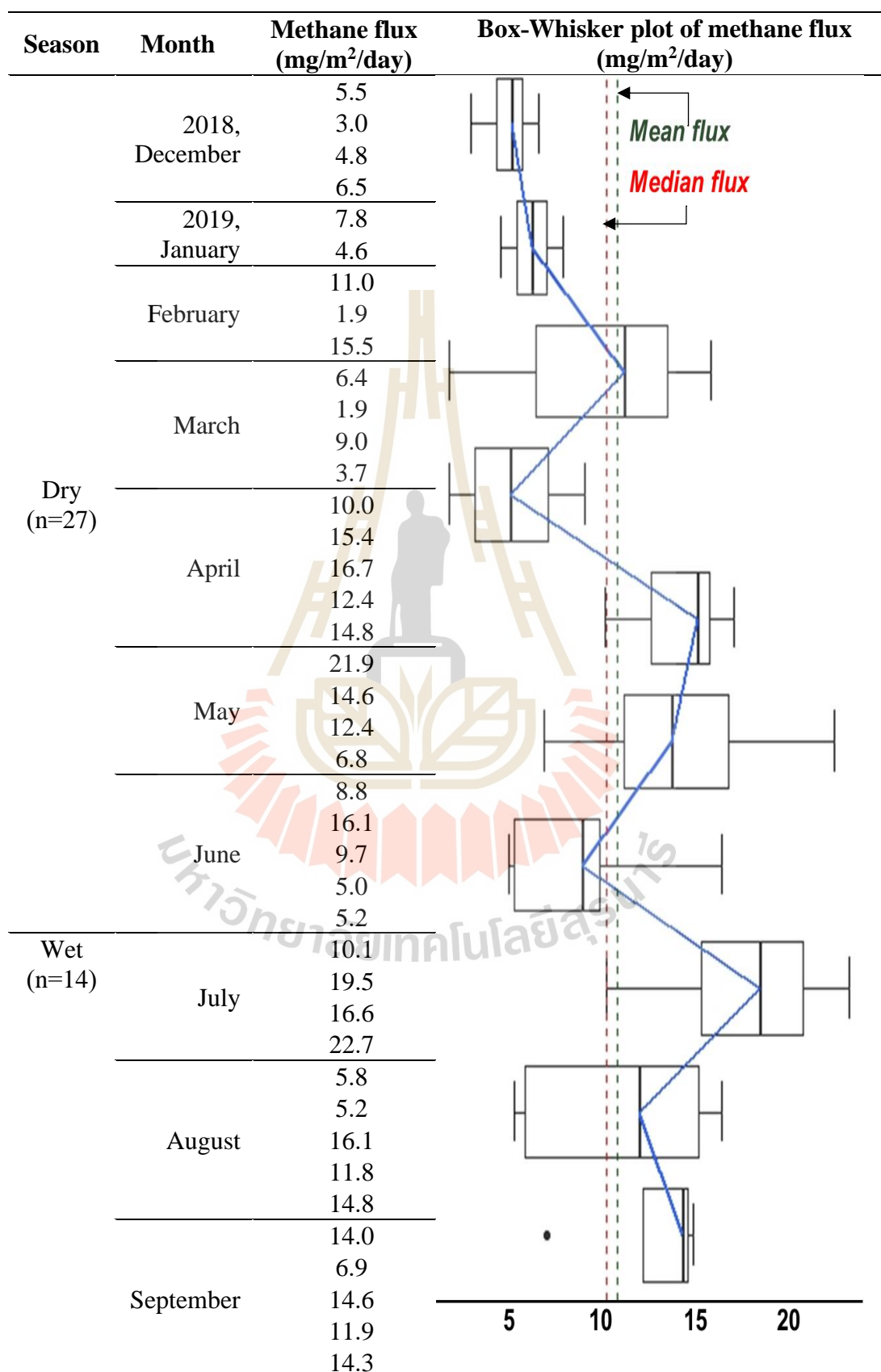
**Figure 4.1** Histogram of methane fluxes ( $n=52$ )

Very extreme values of methane fluxes affected the overall statistics of the dataset ( $n=52$ ). Purposely, the Box-Whisker plot was used to observed and determine

the outliers in the dataset, providing the upper fence of 40.7 mg/m<sup>2</sup>/day. Therefore, methane fluxes over the upper fence were considered as outliers or extreme values and thus excluded from the statistical analysis, deriving the new dataset with a total number of 41 fluxes (n) before the data were classified seasonally. Of the 41 fluxes, it should be noted that all methane flux values in October and November were not included because they were classified as outliers.

Wet and dry seasons were classified by the water levels in the wetland and meteorological conditions—including air temperature and rain, observed during the sampling period. Wet season started from July to September (3 months), while dry season started from December to June (7 months). The water level in the wetland reached the maximum storage capacity in wet season while the water level gradually decreased during dry season. Methane fluxes varied from 1.9 to 22.7 mg/m<sup>2</sup>/day with the mean  $\pm$  SD of 10.6  $\pm$  5.4 mg/m<sup>2</sup>/day and the median of 10.1 mg/m<sup>2</sup>/day. The methane fluxes during wet season ranged from 5.2 to 22.7 mg/m<sup>2</sup>/day with the mean  $\pm$  SD of 13.2  $\pm$  5.0 mg/m<sup>2</sup>/day and the median of 14.1 mg/m<sup>2</sup>/day while the methane fluxes during dry season was between 1.9 and 21.9 mg/m<sup>2</sup>/day with the mean  $\pm$  SD of 9.3  $\pm$  5.2 mg/m<sup>2</sup>/day and the median of 8.8 mg/m<sup>2</sup>/day (Table 4.3).



**Table 4.3** Monthly methane fluxes (n=41) during wet dry seasons

To estimate methane emission, the wet season accounted for 161 days and the dry season accounted for 204 days. The methane emission rate in the wet and dry season were 9.1-19.5 and 1.5-14.0 mg/m<sup>2</sup>/day (derived median  $\pm$  SD), respectively. Seasonal estimates of methane emissions are in Table 4.4.

**Table 4.4** Seasonal estimates of the median methane emissions

Period	Day	Methane flux rate	Methane emissions (kg/m <sup>2</sup> /period)		
		(mg/m <sup>2</sup> /day) Median $\pm$ SD	lower	Upper	Median
Wet season	161	14.1 $\pm$ 5.0	1.5	3.1	2.3
Dry season	204	8.8 $\pm$ 5.2	0.7	2.9	1.8
Annual	365	10.1 $\pm$ 5.4	1.7	5.7	3.7

The overall median of methane flux was 10.1  $\pm$  5.4 mg/m<sup>3</sup>/day. The median methane fluxes in wet (14.1  $\pm$  5.0 mg/m<sup>3</sup>/day) and dry season (8.8  $\pm$  5.2 mg/m<sup>3</sup>/day) were statistically significantly different with t-test ( $p < 0.05$ ). Estimated methane emissions in wet season were 1.5-3.1 kg/m<sup>2</sup> and 0.7-2.9 kg/m<sup>2</sup> in dry season. Annually, the natural wetland emitted methane about 1.7-5.7 kg/m<sup>2</sup>/year. Despite dry season covered more months, the methane emissions during dry season (n=27) were significantly lower than wet season (n=14) with t-test ( $p < 0.05$ ). In the wet season, higher water level of the wetland from the rain events may lead to more flood condition, resulting in higher organic content from plant decomposition in the wetland soil. Thus, higher rate of methane flux was found during this season (Laanbroek, 2010). The overall seasonal methane flux is compared in Figure 4.2.

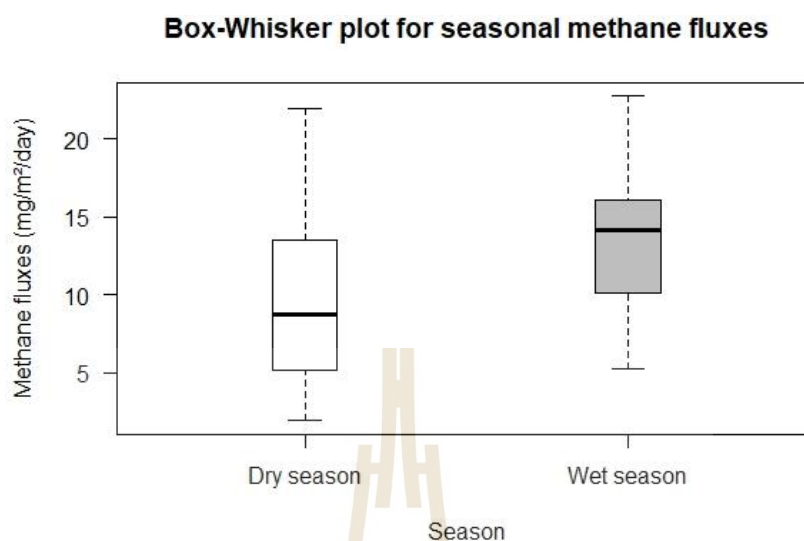


**Figure 4.2** Box-Whisker plot between dry and wet season of methane fluxes

#### 4.1.2 Spatiotemporal dynamics of seasonal methane fluxes

Using the median methane flux obtained from this study,  $10.1 \pm 5.4$  mg/m<sup>2</sup>/day, the median was relatively comparable to the number derived from the freshwater marsh in 2001 study in Prachin Buri province (18.4 mg/m<sup>2</sup>/day), and much higher than the mangrove area in 2005 study in Ranong province (0.12, 0.27, and 0.52 mg/m<sup>2</sup>/day) (Table 4.5). However, several studies indicated that methane fluxes varied temporally and spatially as seen in Table 4.5. When comparing the results to those studies, large differences of methane fluxes were observed, probably due to spatiotemporal variations.

**Table 4.5** Examples of methane fluxes from wetlands in Asia

Country	Wetland	Mean CH <sub>4</sub> flux (mg/m <sup>2</sup> /day)	Method used	Authors
Thailand	Reservoir	10.6 10.1 ± 5.4 (median ± SD)	static closed chamber	this study, 2019
Thailand	Freshwater marsh	18.4	static closed chamber	Khemjaroen, K., 2001
Thailand	Mangrove	0.19 <sup>*</sup> , 0.27 <sup>**</sup> , 0.52 <sup>***</sup>	Static closed chamber	Lekphet et al., 2005
India	Reservoir -exposed soil zone -shallow water zone -deep water zone	61.1 (47.7-74.5) 209.8 (170.3-249.3) 23.3 (20.8-25.8)	Semi-static closed chamber	Bansal et al., 2015
China	Reservoir -Zhigui upstream -Badong upstream -Wanzhou upstream -Xiangxi river	3.7 (-0.6-8.0) 2.9 (0.3-5.5) 146.3 (138.4-154.2) 9.1 (-6.9-25.1)	Close-ended chamber	(Zhao et al., 2013)

**Note:** <sup>\*</sup> = cold season, <sup>\*\*</sup> = summer season, <sup>\*\*\*</sup> = rainy season

The methane flux results from Khemjaroen (2001) were obtained from a 4-month study, February to May, while the methane flux results from Lekphet et al. (2005) was obtained over the year, same as this research. Year-long studies showed different levels of methane fluxes which could be the results from various factors, such as different area of study, time of the study, specific property of the wetland. The results from Lekphet et al. (2005) can be an indicative of seasonal and temporal fluctuation of methane fluxes.

In India, the methane fluxes varied spatially among the wetland area: exposed soil zone, shallow water zone, and deep-water zone. The results demonstrated that higher rate of methane fluxes was found in shallow water zone of wetland (Bansal et al., 2015). Similarly, spatial dynamics of methane fluxes can be observed from four main streams of a reservoir in China (Zhao et al., 2013).

In China, the methane fluxes were largely different between two different plants dominated in a wetland (Liu et al., 2008). Similarly, spatial dynamics of methane fluxes can be observed from various wetlands in China (Liu et al., 2008; Xing et al., 2005; Zhao et al., 2013).

Additionally, methane flux variation could be attributed to the differences in climate zone of a wetland that affected the balance between methane production and methane reduction, causing variations in spatiotemporal of the methane emissions (Table 4.6).

**Table 4.6** Methane flux rate from wetland in different climate zone

Country	Climate	Wetland type	Flux (mg/m <sup>2</sup> /day)	Authors
Thailand	Tropical	Natural reservoir	5.2 ± 16.0 (mean ± SD)	This study, 2019
Thailand	Tropical	Mangrove area	0.19 (cold), 0.27 (summer), 0.52 (rainy); (mean)	Lekphet et al., 2005
Thailand	Tropical	Freshwater marsh	18.2 ± 11.2 (mean ± SD)	Khemjaroen, 2001
Brazil	Tropical	Lake/reservoir	13.8 (mean)	Dos Santos, 2006
France	Tropical	reservoir	44.8 (mean)	Guerin et al., 2006
India	Tropical	reservoir	116.6 (mean)	Bansal et al., 2015

**Table 4.6** Methane flux rate from wetland in different climate zone (cont'd)

Country	Climate	Wetland type	Flux (mg/m <sup>2</sup> /day)	Authors
U.K.	Temperate	Natural pond	1.0-22.5 (range)	Casper et al., 2000
U.S.	Temperate	reservoir	4.4 (mean)	Soumis et al., 2004
Finland	Boreal	reservoir	33.6 (mean)	Huttunen et al., 2003
Canada	Boreal	reservoir	27.36 (mean)	Tremblay et al., 2005
China	Subtropical	Lake	0.06-5.5 (range)	Xing et al., 2005
China	Subtropical	Meadow	270.5 ± 271.0 (mean ± SD)*	Liu et al., 2008
			71.8 ± 40.1 (mean ± SD)**	
Australia	Subtropical	reservoir	93.5 (mean)	Sturm et al., 2013
China	Subtropical	reservoir	5.12 (mean)	Zhao et al., 2013
Taiwan	Subtropical	reservoir	4.8 (mean)	Wang et al., 2013

**Note:** \* = wetland was dominated by *Carex cinerascens*

\*\* = wetland was dominated by *Artemisia selengensis*

## 4.2 Temperature effects on methane fluxes

Air temperatures during the gas sampling campaign from December 2018 to September 2019 showed that the average temperature was 27.3°C, ranging from 22.3 to 30.5°C with the median  $\pm$  SD of  $28.4 \pm 2.5^\circ\text{C}$ . The median air temperatures reached maximum in May while the lowest median air temperature was found in September (Figure 4.3)—the minimum of air temperature was possibly affected by the rainstorm during August to late September 2019.

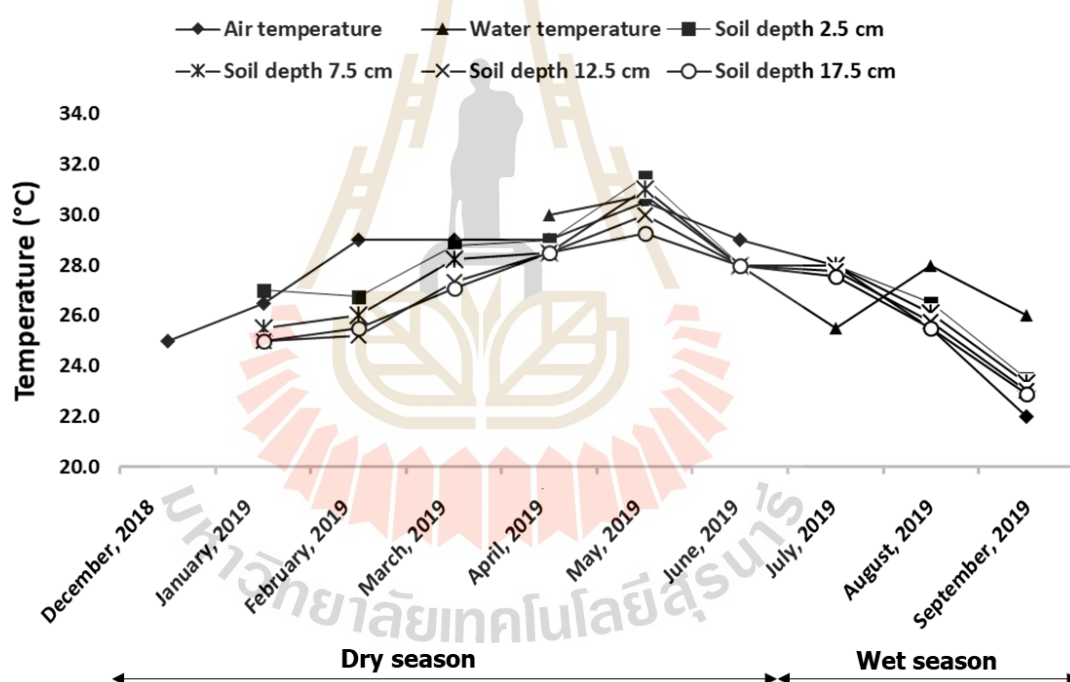


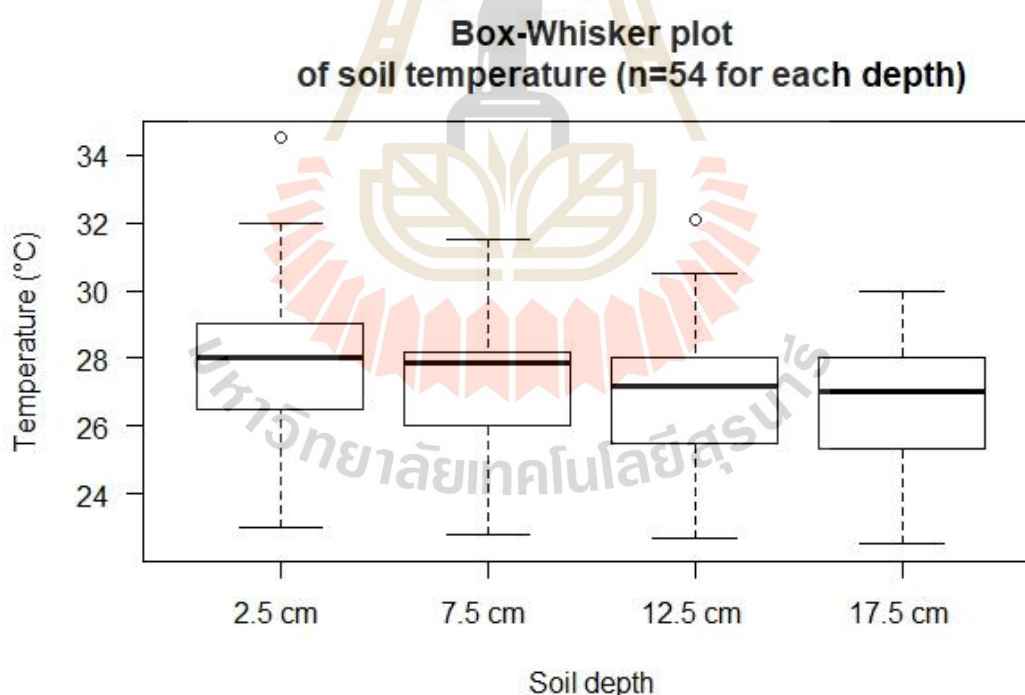
**Figure 4.3** Observed temperature during sampling periods

Average of water temperatures was 28.0°C, ranged from 25.5 to 30.8°C with the median  $\pm$  SD of  $28.0 \pm 2.1^\circ\text{C}$  during April and September 2019. The maximum water temperature in May was 30.8°C, and the minimum of 25.5°C in July. It should



be noted that the lowest water temperature was possibly due to rain event at the start of wet season.

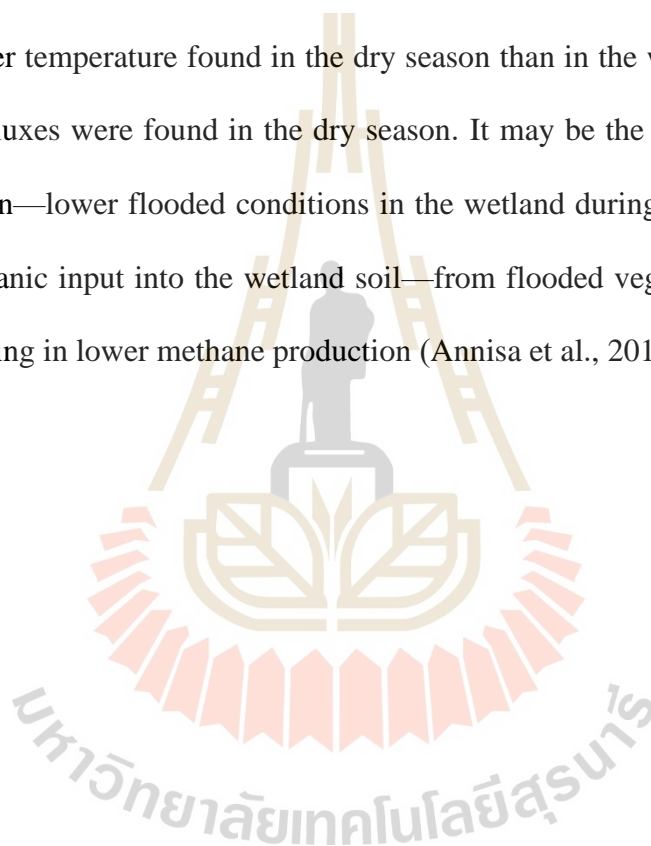
Soil temperature was measured simultaneously during gas sampling. Median soil temperature at 2.5 cm depth was 28.0°C varied between 23.0 and 34.5°C. Median soil temperature at 7.5 cm depth was 27.9°C ranged from 22.8 to 31.50°C. At the 12.5 and 17.5 cm depth, median soil temperatures were 27.2 and 27.0°C, respectively. Soil temperature at 12.5 cm depth ranged between 22.7 and 32.1°C while soil temperature at 17.5 ranged from 22.5 to 30.0°C (Figure 4.4). Soil temperatures at each depth were significantly differed ( $p < 0.05$ ), the results from a non-parametric Kruskal-Wallis test.



**Figure 4.4** Statistics of soil temperature at each depth

The correlation test between monthly methane fluxes and soil temperatures was performed. The outliers of the extreme fluxes were excluded from the correlation test.

Soil temperatures at various depths were not correlated with methane fluxes in the dry season (n=23), but they were, in the wet season, statistically significant at 0-5 and 5-10 cm depth (n=14), as shown in Figure 4.5. Butterbach-Bahl et al. (2013) showed in an experiment that methane production increases with increasing in temperature at a certain range. Under field conditions, temperature and other influencing factors overlap, causing difficulty to observe clear correlations (Fang and Moncrieff, 2001). Despite higher temperature found in the dry season than in the wet season, lower rate of methane fluxes were found in the dry season. It may be the influences from more oxic condition—lower flooded conditions in the wetland during the dry period along with low organic input into the wetland soil—from flooded vegetations, grasses, and weeds, resulting in lower methane production (Annisa et al., 2014; Zhao et al., 2018).



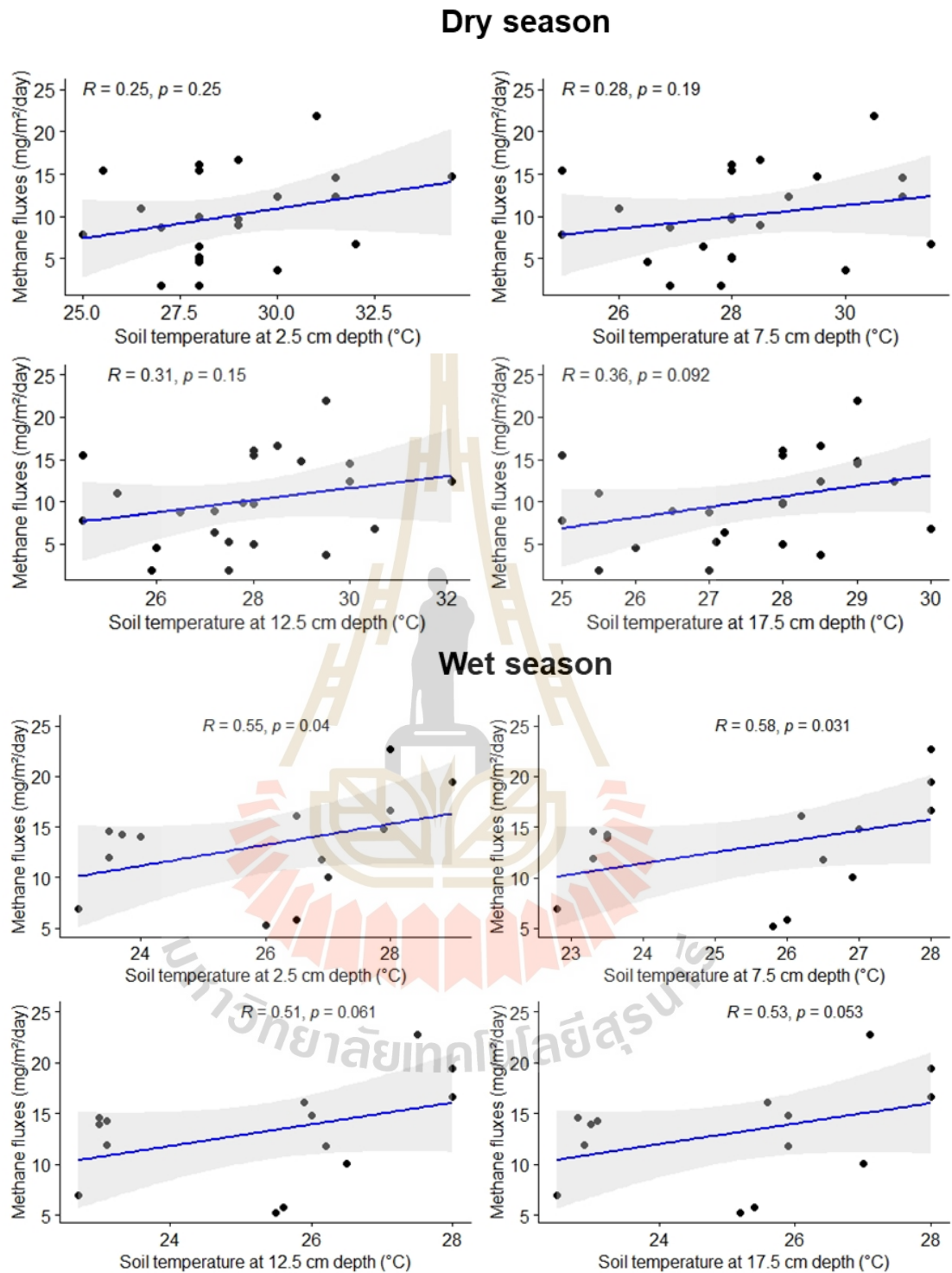
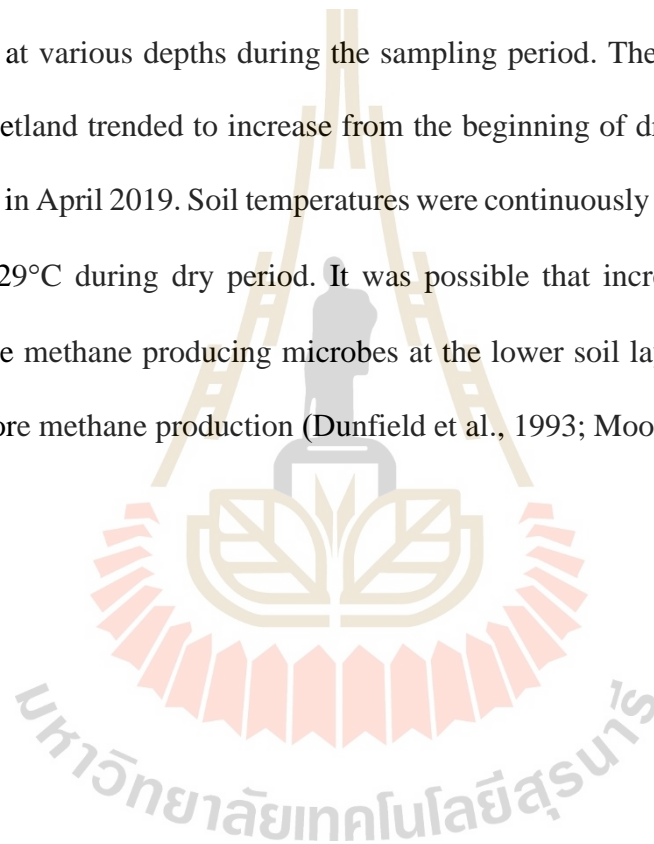


**Figure 4.5** Pearson's correlation test on soil temperature and methane fluxes by season.

Color bands show 95% confident interval.

Monthly methane fluxes varied throughout the year in this study. The lowest methane flux was found in March while the highest methane flux was in July (Figure 4.6). The variations in climatic conditions such as precipitation and temperature also affect the biogeochemical process influenced the methane production and reduction (Christiansen et al., 2017; Fatumah et al., 2019; Shi et al., 2012; Zhou et al., 2006).

Figure 4.6 demonstrates the trend of monthly methane fluxes among the soil temperatures at various depths during the sampling period. The methane fluxes from the natural wetland trended to increase from the beginning of dry season and reached to the highest in April 2019. Soil temperatures were continuously increased, in the range of about 25-29°C during dry period. It was possible that increasing in temperature influenced the methane producing microbes at the lower soil layers to become active leading to more methane production (Dunfield et al., 1993; Moore and Dalva, 1993).



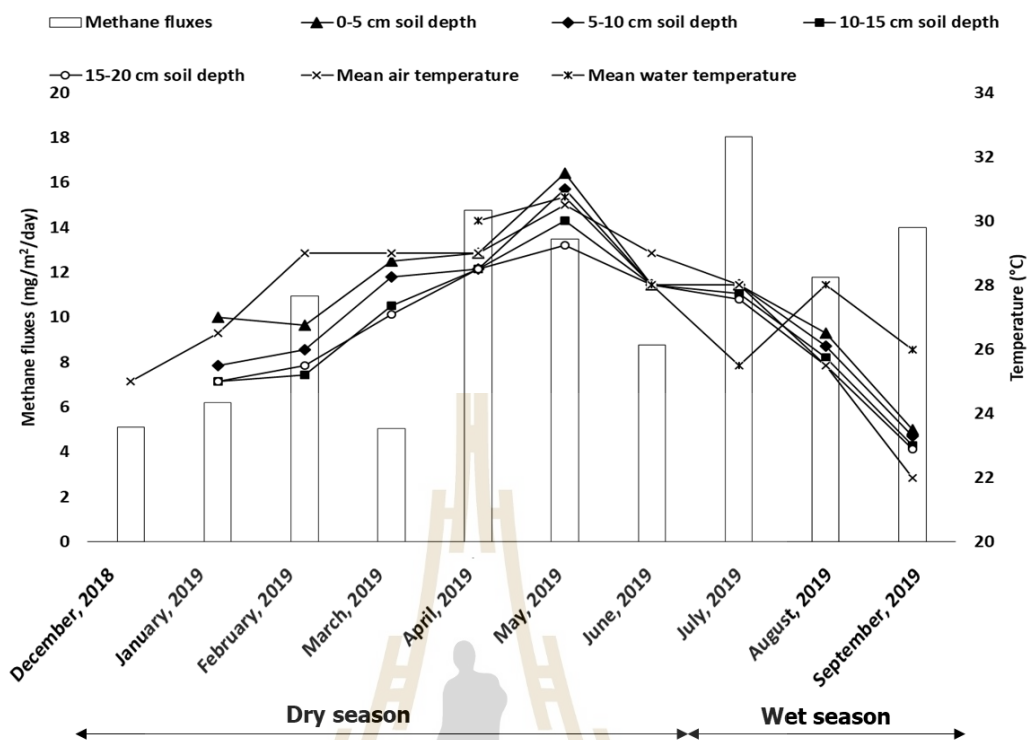


**Figure 4.6** Trend of temperature and methane fluxes. Air temperature were recorded during December 2018 to September 2019, water temperatures were observed from March to September, and soil temperature were recorded from January to September.

From December 2018 to April 2019, the slightly lower rate of methane fluxes in March may be resulted from changes in temperature, about 25-29°C, coincided with lower water level causing more oxic conditions in the lower soil layers and affecting microbial activity (Dise, 1992; King and Adamsen, 1992). The median methane fluxes decreased about 1.7 times from April in June, as the end of the dry season (14.8 mg/m<sup>2</sup>/day down to 8.8 mg/m<sup>2</sup>/day).

The methane fluxes fluctuated more when the weather approached the wet season in July 2019. During this period, the level of water in the wetland remained near the lowest capacity of water storage. Similarly, the soil temperatures decreased continuously until September 2019 due to more rain events. From July to September, the methane fluxes remained higher, between 11.8 and 18.1 mg/m<sup>2</sup>/day. Obviously, the monthly methane fluxes peaked to 3,687 mg/m<sup>2</sup>/day and decreased to 152 mg/m<sup>2</sup>/day in November. It should be noted that the wetland during this period was disturbed from both natural and human activities (Figure 4.7). It was speculated that the re-wetted or flooded conditions from the rains may cause the change in biogeochemical properties of the wetland environment (Kelley et al., 1995; (Klinger et al., 1994; Moore and Roulet, 1993; Shannon and White, 1994).



**Figure 4.7** The appearance of disturbed wetland in October and November 2019

### 4.3 Soil texture effects on methane fluxes

Three replicated of monthly soil were collected at the depth of 0-15 cm and were thoroughly mixed for soil texture analysis (n = 12). The results of soil texture analysis showed that all the samples were sandy soil (Table 4.7), sand ranging from 84.6 to 96.8%. The monthly methane fluxes in this study were from the samples in the area in the sandy wetland only.

**Table 4.7** Soil texture classified by USDA classification

Year	Month	Soil texture (%)			Soil class
		Sand	Silt	Clay	
2018	December	96.8	0.4	2.8	sand
2019	January	96.8	0.4	2.8	sand
	February	84.6	11.9	3.5	loamy sand
	March	96.6	0.2	3.2	sand
	April	96.5	0.3	3.2	sand
	May	93.6	3.4	3.0	sand
	June	97.2	0.0	2.8	sand
	July	97.1	0.1	2.8	sand
	August	96.1	0.4	3.5	sand
	September	93.0	0.4	6.6	sand
	October	93.0	3.8	3.2	sand
	November	96.8	0.2	3.0	sand

Khemjaroen (2001) studied the methane fluxes from the soil classified as clay texture, with the fluxes of 7.1-29.7 mg/m<sup>2</sup>/day. Some studies suggested the effects of soil texture on methane emission. Wagner and colleagues (1999) found that methane production increased with the following order: sand < gravel < clayey silt < clay (Wagner et al., 1999). The methane production may be limited in sandy soil for this study, possibly from more water percolation and redox potential (150-326 mV). However, the result from Wagner et al. (1999) was contradicted with the older study (Oades, 1988). Clay content affected methane emission by inhibit mineralizing of organic matter (Oades, 1988). Similarly, clays with high organic material were more favorable to methanogenesis but it also should be noted that clayey soil may delay the release of methane, therefore the reduction of methane emissions can occur due to the oxidation before it can escape to the atmosphere (Neue and Roger, 1994). These discrepancies may suggest that the soil texture effects on the methane fluxes in the wetlands.

#### **4.4 Soil pH effects on methane fluxes**

All 104 soil samples collected at three depths between December 2018 and November 2019 were determined for pH. All soil samples had pH less than 7.5 (Figure 4.8). About 77% of soil samples had pH less than 6.5. Soil samples at 0-5 cm depth had pH in the range of 4.83-7.33 with the mean  $\pm$  SD of 5.93  $\pm$  0.72, while soil samples at 5-10 cm and 10-15 cm showed slightly lower ranges, 4.50-7.27 and 4.60-7.40, with the mean  $\pm$  SD of 5.81  $\pm$  0.0.83 and 5.68  $\pm$  0.74, respectively. The medians pH for 0-5, 5-10, and 10-15 cm soil depth were 6.00, 5.57, and 5.40, respectively.



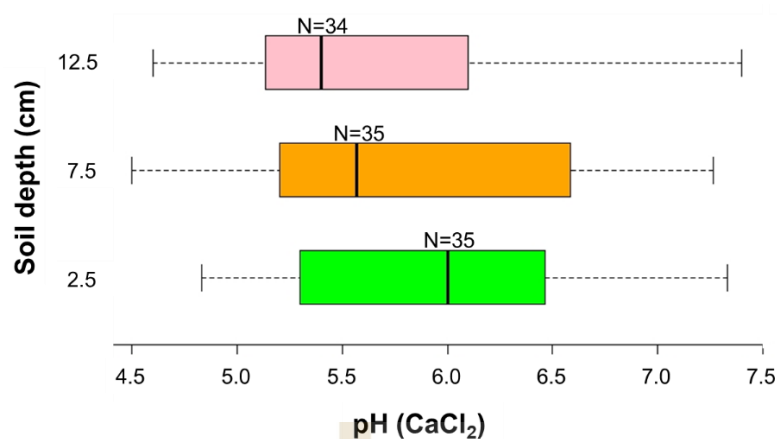


**Figure 4.8** Statistics of soil pH at each depth

The minimum median soil pH at 0-5 cm depth was found from soil sample in January, pH 4.8, while the maximum median soil pH was in July sample, pH 7.3. The 5-10 cm soil depth had the lowest median soil pH in June, pH 4.5, while the highest median soil pH was in September and July samples, pH 7.3. The 10-15 cm soil depth had the maximum median soil pH in September, pH 7.4, while the minimum median soil pH was in August, pH 4.6.

Correlations between soil pH and methane fluxes are in Figure 4.9. Soil pH at all depths was not statistically significant ( $n=29$ ) testing with a Pearson's correlation.

However, the results suggest that the monthly methane fluxes trend to conform more with soil pH at less than 10 cm depth. Data show that during the study period methane fluxes changed widely from December 2018 to September 2019 (Figure 4.10). Wang et al., (2009) suggested that most methanogens are very sensitive to soil pH variation, about 0.2 unit higher than the natural soil suspension pH could slightly increase in methane production (Wang et al., 2009).

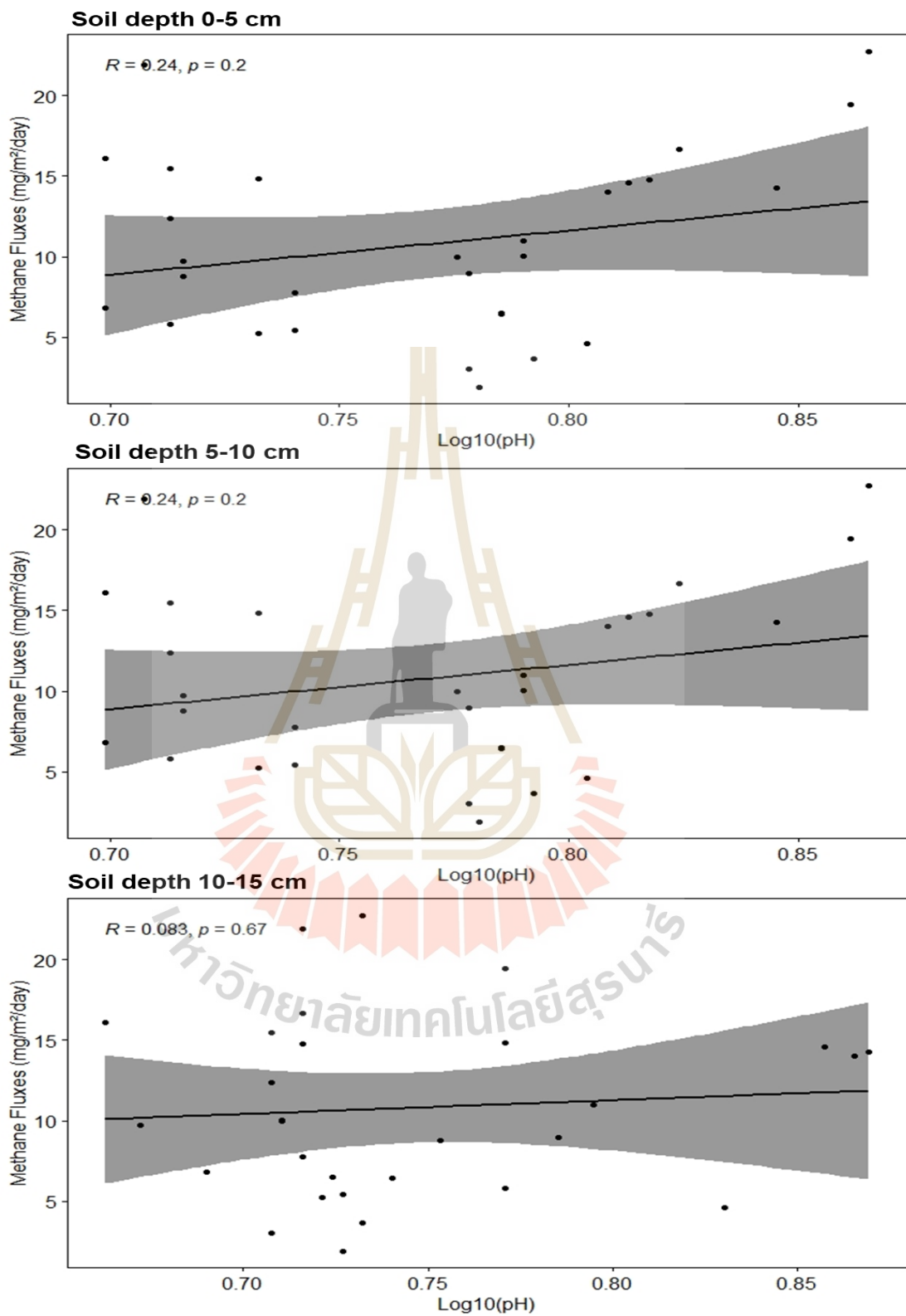


**Figure 4.9** Pearson's correlation test of soil pH and methane fluxes. Color bands show 95% confident interval.

Figure 4.10 displays the trend of methane fluxes versus soil pH at each depth. The lowest median soil pH at 10-15 cm depth was in June sample with the number of pH 5.1, while the highest median was in October, pH 7.3.

In the dry season, soil pH at 0-5 and 10-15 cm depths had the opposite trend with methane fluxes while soil pH at 5-10 cm depth showed the positive trend. In the wet season, soil pH at 0-5 and 5-10 cm depths were coincident with the methane fluxes. No such trend was observed with the soil pH at 10-15 cm depth.

The relationship between soil pH and methane fluxes was unclear in this study. The methane fluxes in dry season remained in the range of 5.1-14.8 mg/m<sup>2</sup>/day with an unusually high flux in October (Table 4.2). When excluded this flux data in October and November, the maximum value of soil pH was found in July and September with the number of 7.3. It can be highlighted that the higher methane fluxes can also be observed in July and September too (Figure 4.10).

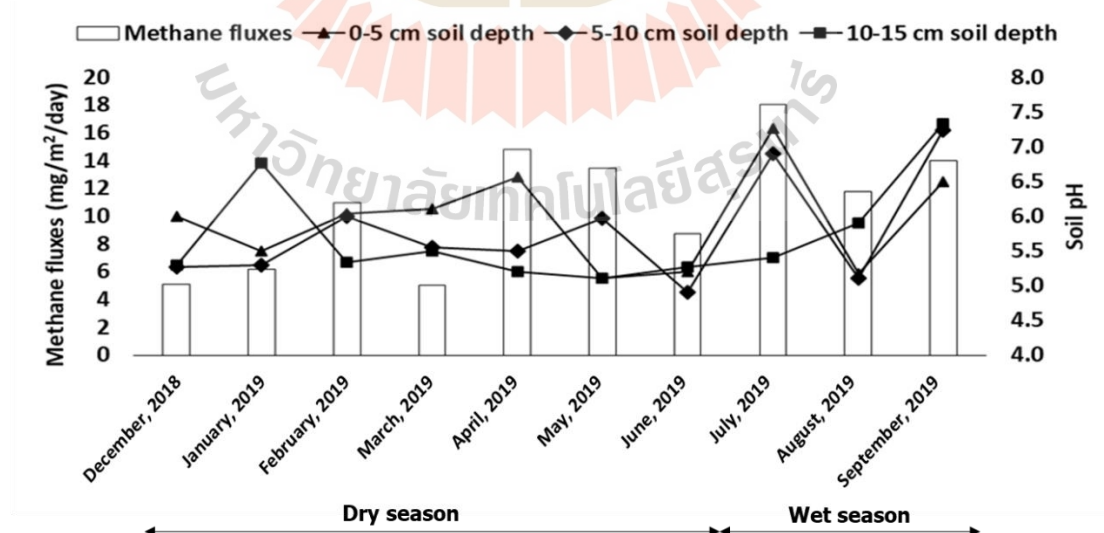


**Figure 4.10** Trend of soil pH and methane fluxes

The results suggested that the monthly methane fluxes in the dry months changed conversely with soil pH at specific soil depths, 0-5 and 10-15 cm, while the results were positive with soil pH at 5-10 cm (Figure 4.10). Wet season showed higher association between soil pH at soil layers less than 10 cm, and the monthly methane fluxes. Similar results were reported by Lekphet et al. (2005) that no statistically significant could be observed on methane fluxes and soil pH in the mangrove area in the eastern and southern Thailand (Lekphet et al, (2005).

However, Jones and colleagues (1978) found that most methanogens have pH optima near neutrality (Jones et al., 1987) while the later studies found that methanogens can also grow in acidic (Dunfield et al., 1993; Williams and Crawford, 1984) and alkaline environment (Blotevogel et al., 1985; Garcia et al., 2000).

#### **4.5 Soil ORP effects on methane fluxes**

All soil samples (n = 104) were analyzed for soil reducing status as ORP (mV). The ORP of soil samples at 0-5 cm depth ranged from 192 to 294 mV with the mean  $\pm$  SD of  $223 \pm 36$  mV. The ORP of soil sample at 5-10 cm depth ranged from 150 to 315 mV with the mean  $\pm$  SD of  $229 \pm 41$  mV, while the ORP of soil sample at 10-15 cm depth ranged between 157 and 326 mV with the mean  $\pm$  SD of  $235 \pm 42$  mV (Figure 4.11). It should be noted that the soil samples from this study were not flood soil, they were the upland soil of the wetlands, resulting in positive value of soil ORP.

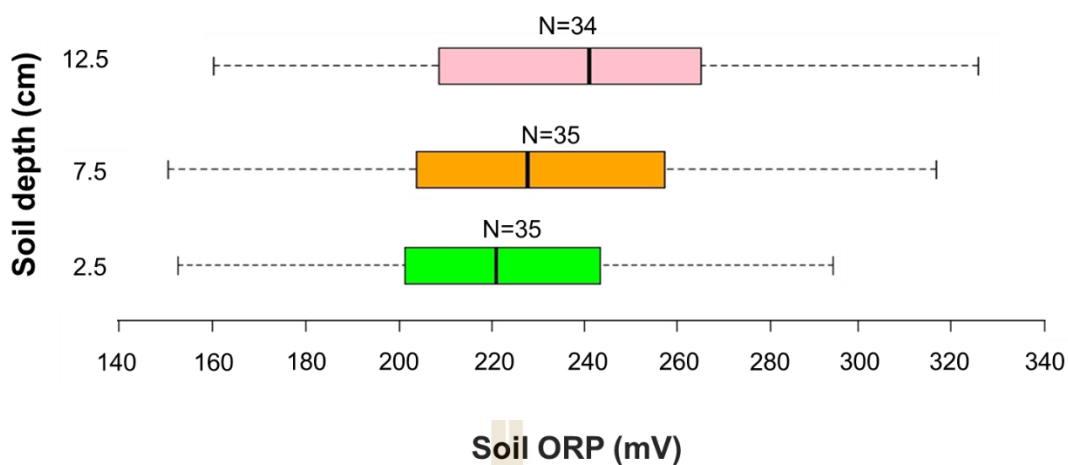


**Figure 4.11** Statistics of soil ORP each depth

The highest soil ORP at 0-5 cm depth was found from soil sample in June (294 mV) while the lowest ORP was in July (152 mV). The maximum soil ORP at 5-10 cm depth was found from soil sample in June (315 mV) while the minimum soil ORP was in September (150 mV). The highest soil ORP at 10-15 cm depth was in June (326 mV) while the lowest soil ORP was in September (15.7 mV) (Figure 4.12).

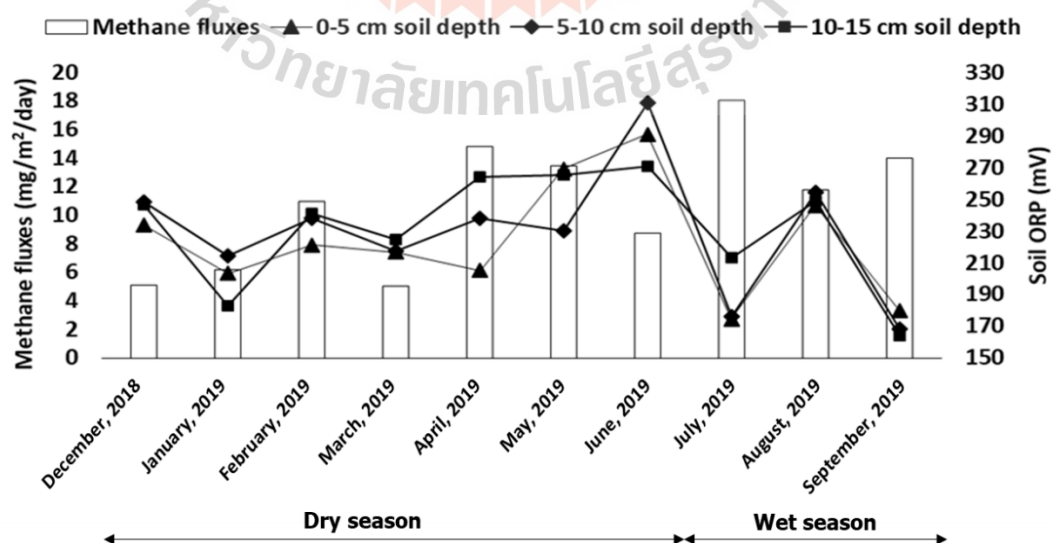


**Figure 4.12** Trend of soil ORP and methane fluxes

Figure 4.12 shows the trend of monthly methane fluxes and soil ORP at each depth. In dry season, the methane fluxes and soil ORP had similar direction during January to March; when the soil ORP increased from about 180-280 mV to about 220-240 mV in February, the methane fluxes also increased from 6.2 mg/m<sup>2</sup>/day in January to 11.0 mg/m<sup>2</sup>/day in February, while the methane fluxes later decrease to 5.0 mg/m<sup>2</sup>/day with decreasing in soil ORP to 210-210 mV in March. In April to June, methane fluxes decreased from 14.8 to 8.8 mg/m<sup>2</sup>/day with increasing in soil ORP about 230-310 mV. This negative association between methane fluxes and soil ORP was observed in the wet season too. In the wet season, large increasing of soil ORP from about 170-210 mV in July to 240-260 mV in August led to decrease in methane from 18.0 mg/m<sup>2</sup>/day to 11.8 mg/m<sup>2</sup>/day. The methane fluxes raised again in September with the number of 14.0 mg/m<sup>2</sup>/day, when the soil ORP dropped to about 160-180 mV (Figure 4.12). Correlations between soil ORP and methane fluxes are in Figure 4.13. The soil ORP only at 5-10 cm soil depth was statistically significant with the monthly methane fluxes (Fig.4.13).

Yaki et al. (1998) found that the soil ORP and methane emission had negative relationship at 0-5 cm soil depth only while Pun and Yamaji (2016) indicated that the soil ORP had positive relationship with methane fluxes at soil depth 0-15 cm, and only soil ORP at 15-20 cm depth showed the negative association (Pun and Yamaji, 2016).

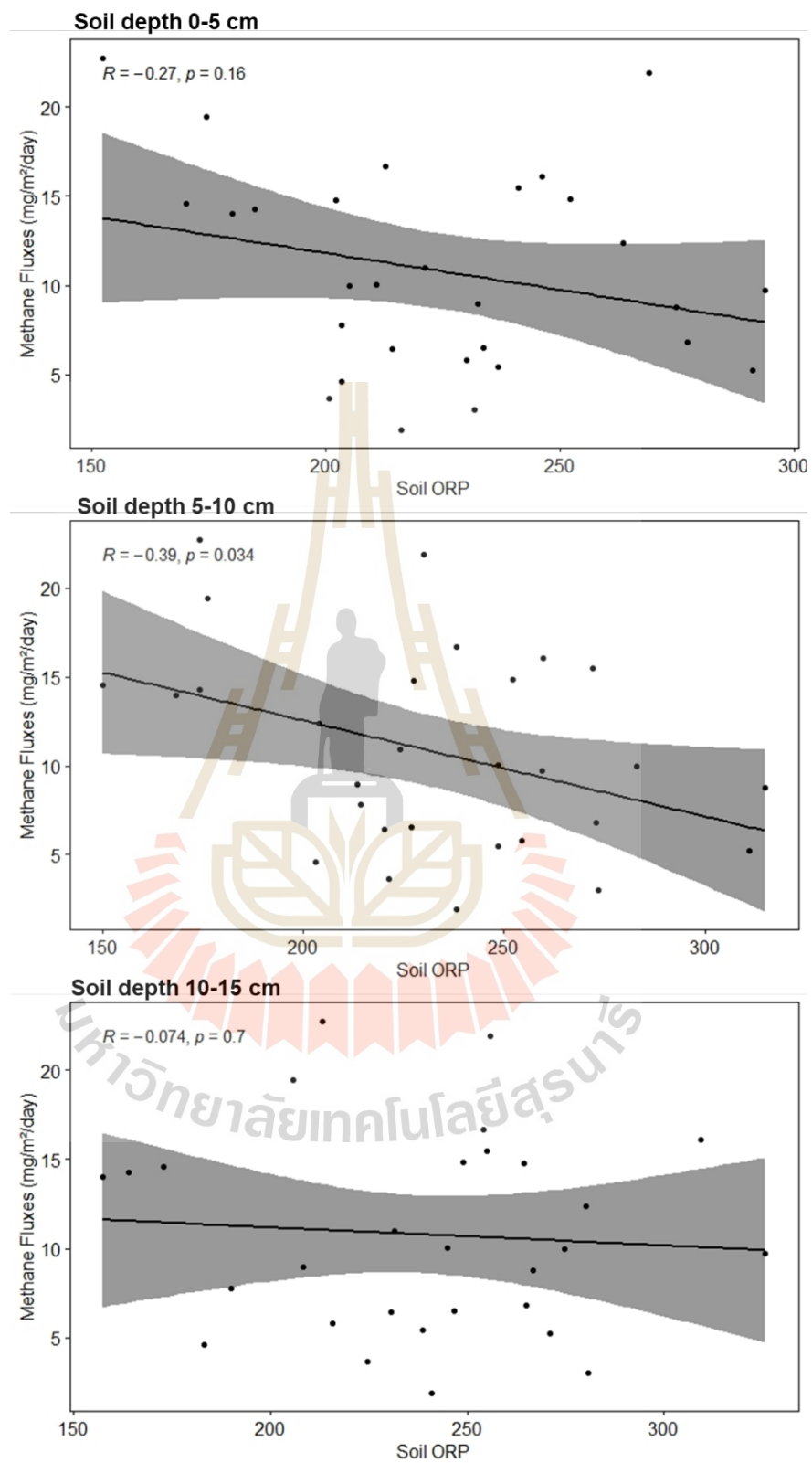


**Figure 4.13** Pearson's correlation test of soil ORP and methane fluxes. Color bands show 95% confident interval.

#### 4.6 Soil carbon (%C) effects on methane fluxes

All soil samples (n = 104) were analyzed for carbon content. The soil carbon content at 0-5 cm depth ranged widely from 0.04 to 2.97% with the mean  $\pm$  SD of 0.63  $\pm$  0.75%. The soil carbon content at 5-10 cm depth ranged from 0.06 to 1.62% with the mean  $\pm$  SD of 0.51  $\pm$  0.45% while the soil carbon content at 10-15 cm depth ranged between 0.05 and 1.60% with the mean  $\pm$  SD of 0.38  $\pm$  0.35% (Figure 4.14).

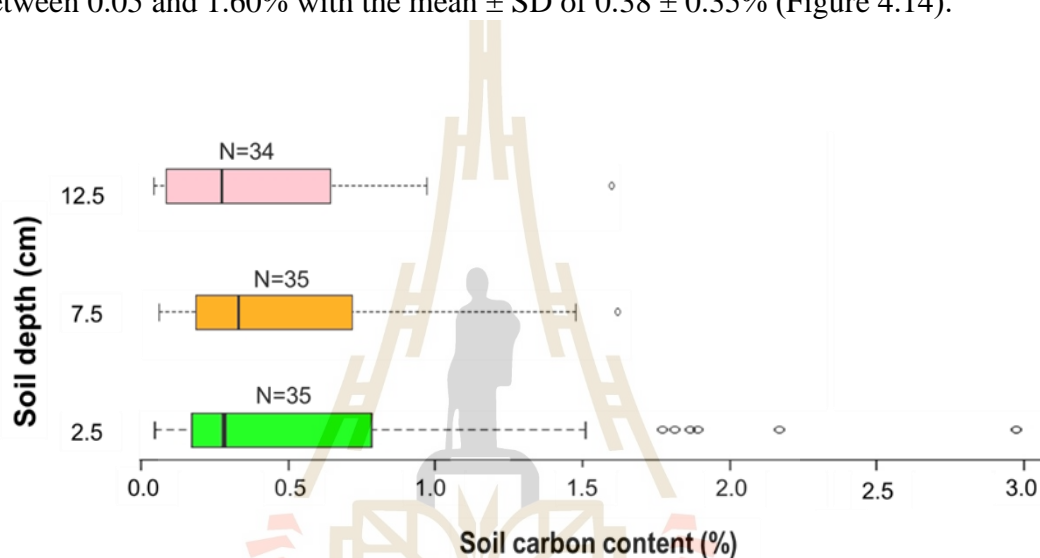


**Figure 4.14** Statistics of soil carbon content at each depth

Correlations between soil carbon content and methane fluxes are in Figure 4.15. All of soil carbon content was not significantly associated with the monthly methane fluxes in this study (Fig. 4.15). It should be noted that carbon content was a total carbon in the wetland soil. Therefore, it would be assumed that some of carbon forms in the wetland may be not easily consumed by methanogens, thus no correlation can be observed in this study.



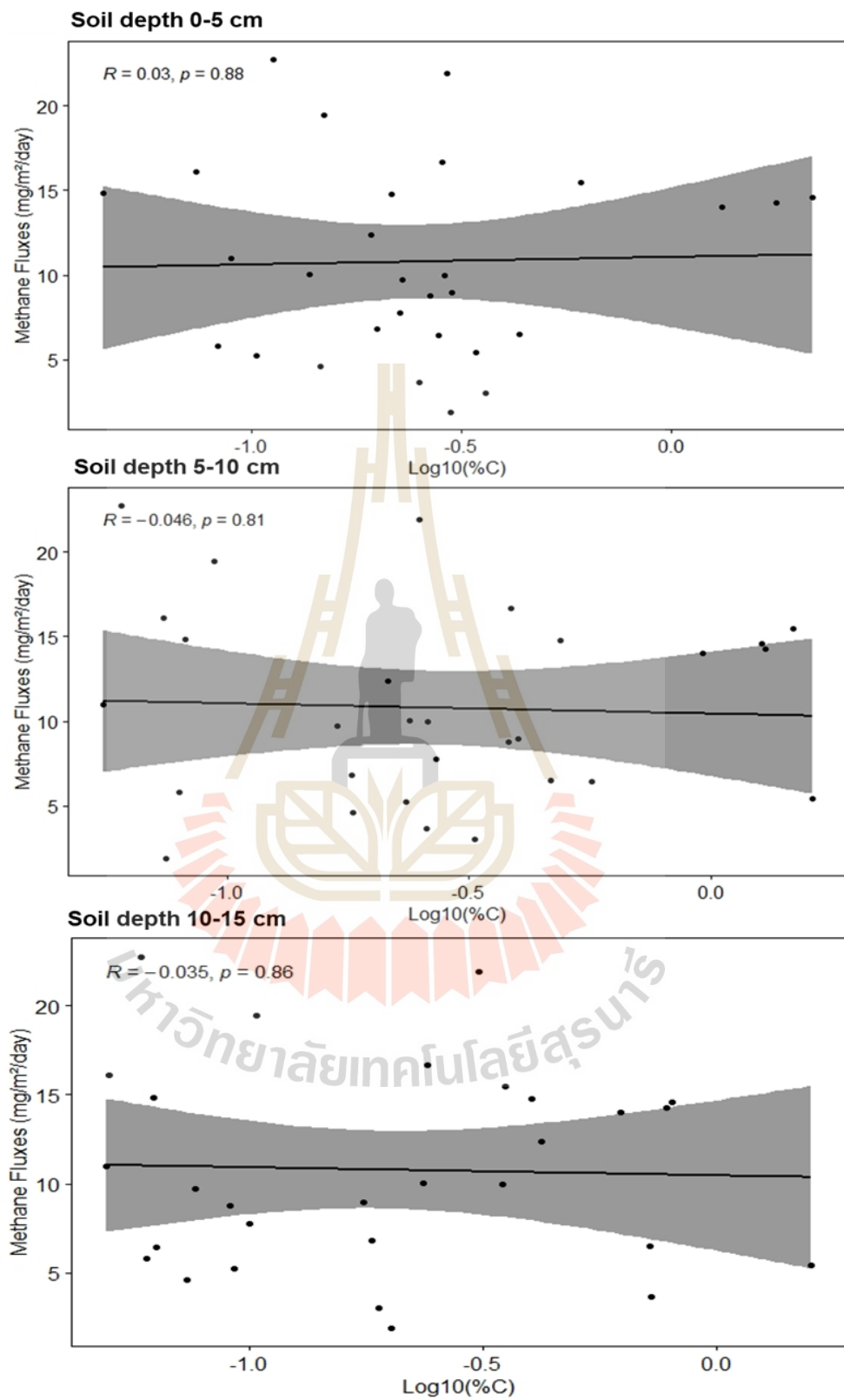


**Figure 4.15** Pearson's correlation test of soil carbon content and methane fluxes. Color bands show 95% confident interval.

The highest soil carbon content at 0-5 cm depth was found in September, 1.77%, while the lowest soil carbon content was in August, 0.07%. The maximum soil carbon content at 5-10 cm depth was in September, 1.27%, while the minimum soil carbon content was in February, 0.07%. The highest soil carbon content at 10-15 cm depth was in September, 0.78% while the lowest soil carbon content was in January, 0.07% (Figure 4.16).

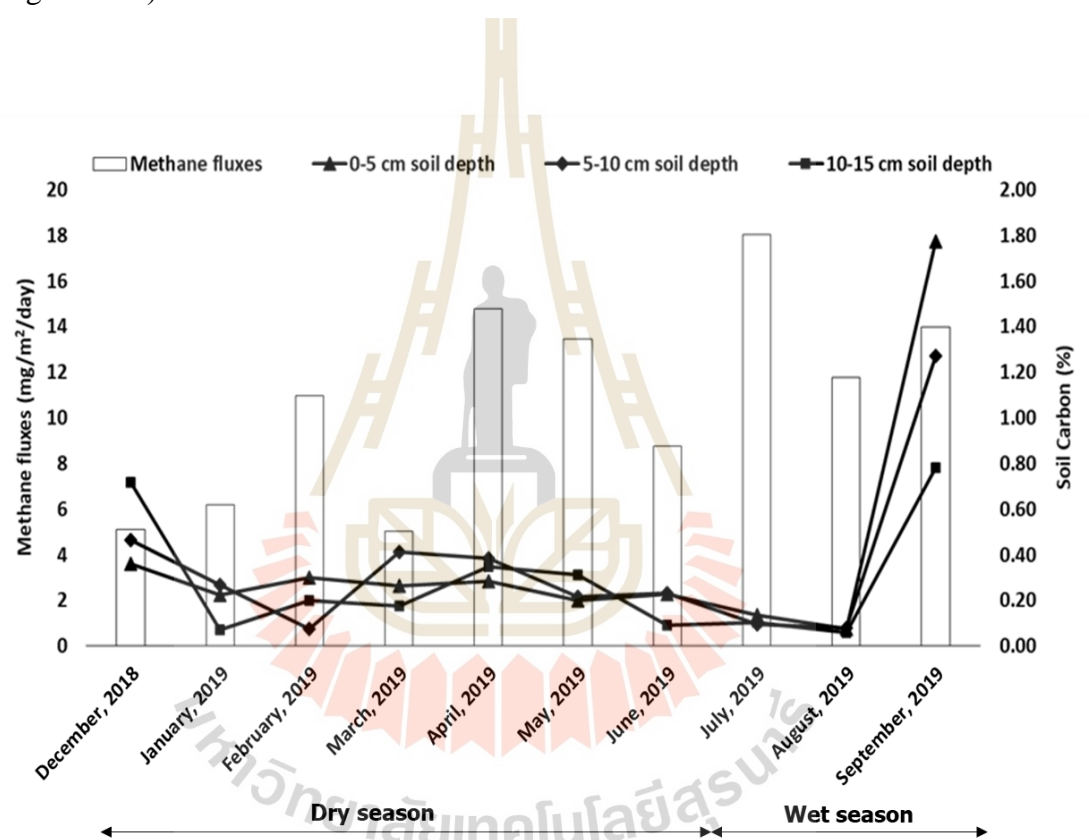


**Figure 4.16** Trend of soil carbon content and methane fluxes

During dry season, monthly methane fluxes increased from 5.1 to 11.0 mg/m<sup>2</sup>/day and gradually decreased in the median soil carbon content from about 0.47% in December 2018 to 0.20% in February 2019 with the mean  $\pm$  SD of  $0.30 \pm 0.20\%$ . From March to June, the carbon content was barely changed,  $0.26 \pm 0.09$  (mean  $\pm$  SD), compared to the previous periods. Later change in soil carbon content to about 0.26

percent from February to March with rising median soil temperature from 25.75°C in February to 28.5°C in April led to sudden increase methane fluxes and reached the maximum flux in the dry season, 14.8 mg/m<sup>2</sup>/day. It was probably due to increase in soil temperature as co-influencing factor induced methanogens to produce higher methane gas (Dunfield et al., 1993; Moore and Dalva, 1993). Coincidentally, slowly decreased in methane fluxes with soil carbon reduction until the start of wet season in July may be resulted from methane production—carbon substrate consumed continually during methanogenesis by methanogens—with decreasing in soil temperature from about 30.5°C in April to 26.0°C in July.

Wet season had high median of the methane fluxes, 14.1 mg/m<sup>2</sup>/day, from July to September. The water level in the wetland increased and reached the maximum storage capacity in July 2019. Large increase of carbon content from 0.1% in July to 1.27% in September (Figure 4.16) was probably from flooded and decomposed grass, thus more substrate for methanogenesis, resulting in higher methane fluxes during wet season (Laanbroek, 2010; Macdonald et al., 1998; van den Pol-van Dasselaar and Oenema, 1999).

## CHAPTER V

### CONCLUSIONS AND RECOMMENDATIONS

The closed chamber method was successfully used to collect monthly gas samples from the natural wetland in Nakhon Ratchasima between December 2018 and November 2019. Methane gas concentrations were quantified with a GC-FID against the standard gas. Properties of soil; texture, temperature, pH, ORP and carbon content; were collected and analyzed to provide additional information of this natural wetland. Soil texture of the wetland is sandy in nature. Water levels in the wetland changed seasonally over the year. The air temperature fluctuated between 22.3 and 30.5°C, lowest in wet season. The temperature of the soil at 2.5 and 7.5 cm depth, associated positively and significantly with methane fluxes in the wet season only. The soil ORP had positive value, 150-326 mV, and associated negatively and significantly with the methane fluxes at 5-10 cm soil depth only. The soil pH varied in the range of 4.5-7.4, with the highest in September and the lowest in June. The soil carbons varied greatly, 0.04-3.00%, and were of high number in wet season. No correlation could be observed for soil pH and soil carbon at all soil depths in this study. Table 5.1 shows the summary of parameters in this study.

**Table 5.1** Summary of parameter in this study

<b>Parameters</b>	<b>Divisions</b>	<b>Details</b>
<b>Season</b>	Wet season	161 days (Jul-Nov)
	Dry season	204 days (Dec-Jun)
<b>Methane flux rate</b> (mg/m <sup>2</sup> /day)	Yearly flux	10.1 ± 5.4 (median ± SD)
	Dry season flux	8.8 ± 5.2 (median ± SD)
	Wet season flux	14.1 ± 5.0 (median ± SD)
<b>Methane emissions</b> (kg/m <sup>2</sup> )	Annual emissions	1.7-5.7 (lower-upper bound)
	Dry season emissions	0.7-2.9 (lower-upper bound)
	Wet season emissions	1.5-3.1 (lower-upper bound)
<b>Air temperature (°C)</b>	Yearly	28.4 ± 2.5 (median ± SD)
<b>Water temperature (°C)</b>	Yearly	28.0 ± 2.1 (median ± SD)
<b>Soil temperature</b> (°C)	0-5 cm depth	28.0 ± 2.3 (median ± SD)
	5-10 cm depth	27.9 ± 2.1 (median ± SD)
	10-15 cm depth	27.2 ± 2.1 (median ± SD)
	15-20 cm depth	27.0 ± 1.8 (median ± SD)
<b>Soil texture</b>	%sand	96.5 ± 3.7 (median ± SD)
	%silt	0.4 ± 3.6 (median ± SD)
	%clay	3.2 ± 1.1 (median ± SD)
	<b>soil class</b>	<b>sandy texture</b>
<b>Soil pH:</b>	0-5 cm depth	6.00 ± 1.2 (median ± SD)
	5-10 cm depth	5.57 ± 1.3 (median ± SD)
	10-15 cm depth	5.40 ± 1.5 (median ± SD)

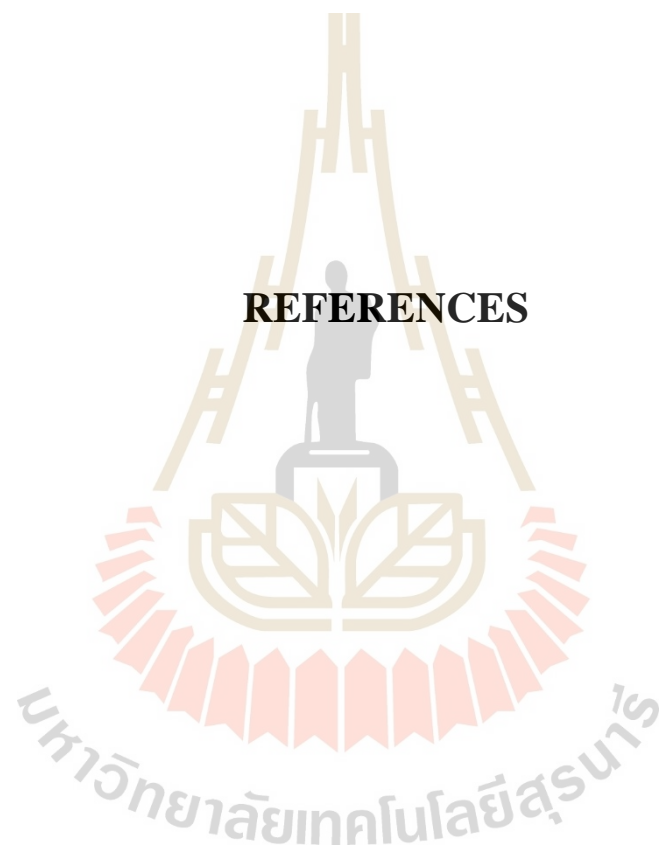
**Table 5.1** Summary of parameter in this study (cont'd)

<b>Parameters</b>	<b>Divisions</b>	<b>Details</b>
<b>Soil ORP (mV)</b>	0-5 cm depth	210 ± 52 (median ± SD)
	5-10 cm depth	227 ± 56 (median ± SD)
	10-15 cm depth	240 ± 69 (median ± SD)
<b>Soil carbon (%)</b>	0-5 cm depth	0.28 ± 0.75 (median ± SD)
	5-10 cm depth	0.33 ± 0.46 (median ± SD)
	10-15 cm depth	0.28 ± 0.36 (median ± SD)

Wet and dry seasons were classified based on physical and meteorological conditions observed during the sampling periods. Dry season had lower rate of methane fluxes, 8.8 mg/m<sup>2</sup>/day, compared to wet season, 14.1 mg/m<sup>2</sup>/day, differed with statistically significant with t-test. The estimates seasonal methane emissions in wet and dry season were 1.5-3.1 and 0.7-2.9 kg/m<sup>2</sup>, respectively with the annual emissions of 1.7-5.7 kg/m<sup>2</sup>.

Further study on seasonal methane fluxes from a natural wetland should be carried out in different type of natural wetlands. Influencing factors of wetland environments should be included in the study, e.g. ionic properties of soil, soil textures, soil microbes, soil pH, precipitations, vascular plant species, etc. The appropriate methodology for the study would base on the balance between good procedure and field practicality with cost effectiveness. A static closed chamber was at least appropriate and recommend for quantification of methane fluxes from a wetland because it is easy to operate, cost effectiveness, and yields good results. The aspects of applicable and comparable data should be of focus.

## REFERENCES



## REFERENCES

- Altor, A. E, and Mitsch, W. J. (2006). Methane flux from created riparian marshes: Relationship to intermittent versus continuous inundation and emergent macrophytes. **Ecological Engineering**, 28: 224-234.
- Annisa, W., Maas, A., Purwanto, B., and Widada, J. (2014). Effect of organic matter level on methane emission in acid sulfate soil from Belandean, South Kalimantan. **Asian Research Publishing Network (ARPN), Journal of Agricultural and Biological Science**, 9 (4): 146-151.
- Atique, L., and Mahmood, I. (2014). Disturbances in atmospheric radiative balance due to anthropogenic activities and its implications for climate change. **American-Eurasian Journal of Agricultural & Environmental Science**, 14 (1): 73-84.
- Baldocchi, D.D. (2003). Assessing the eddy covariance technique for evaluating carbon dioxide exchange rates of ecosystems: past, present and future. **Global Change Biology**, 9: 479–492.
- Bartlett, K.B., and Harriss, R.C. (1993). Review and assessment of methane emissions from wetlands. **Chemosphere**, 26 (1-4): 261-320.
- Bastviken, D. (2009). Methane, in Encyclopedia of inland waters, Likens, G.E. (ed). **Academic Press, Oxford**, pp: 783–805.
- Beal, E.J., House, C.H., and Orphan, V.J. (2009). Manganese- and iron-dependent marine methane oxidation. **Science**, 325 (5937): 184–187.



- Bian, L., Hinrichs, K.U., Xie, T., Brassell, S.C., Iversen, N., Fossing, H., Jørgensen, B.B., and Hayes, J.M. (2001). Algal and archaeal polyisoprenoids in a recent marine sediment: Molecular isotopic evidence for anaerobic oxidation of methane. **Geochemistry, Geophysics, Geosystems**, 2 (1): 22 pp.
- Blair, N.E., and Aller, R.C. (1995). Anaerobic methane oxidation on the Amazon shelf. **Geochimica et Cosmochimica Acta**, 59: 3707–3715.
- Blotevogel, K.H., Fischer, U., Mocha, M., and Janssen, S. (1985). *Methanobacterium thermoalcaliphilum* spec. nov., a new moderately alkaliphilic and thermophilic autotrophic methanogen. **Archives of Microbiology**, 142: 211–217.
- Boetius, A., Ravensschlag, K., Schubert, C.J., Rickert, D., Widdel, F., Gieseke, A., Amann, R., Jørgensen, B.B., Witte, U., and Pfannkuche, O. (2000). A marine microbial consortium apparently mediating anaerobic oxidation of methane. **Nature**, 407: 623-626.
- Bogdanov, G., Vlizlo, V., Solohub, L., Janovich, V., Antonyak, H., and Luchka, I. (2007). Biochemical aspects of mitigation of methane emission in atmosphere by ruminants. **In proceeding of The 3rd International Conference Greenhouse Gases and Animal Agriculture (GGAA2007)**. Christchurch, New Zealand.
- Boon, P.I., and Mitchell, A. (1995). Methanogenesis in the sediments of an Australian freshwater wetland: Comparison with aerobic decay, and factors controlling methanogenesis. **FEMS Microbiology Ecology**, 18: 175–190.
- Bosse, U., and Frenzel, P. (1997). Activity and distribution of methane-oxidizing bacteria in flooded rice soil microcosms and in rice plants (*Oryza sativa*). **Applied and environmental microbiology**, 63: 1199–207.

- Brooks Avery, G., Shannon, R.D., White, J.R., Martens, C.S., and Alperin, M.J. (2003). Controls on methane production in a tidal freshwater estuary and a peatland: methane production via acetate fermentation and CO<sub>2</sub> reduction. **Kluwer Academic Publishers, Biogeochemistry**, 62: 19–37.
- Brune, A., Frenzel, E., and Cypionka, H. (2000). Life at the oxic–anoxic interface: Microbial activities and adaptations. **FEMS Microbiology Review**, 24 (5): 691–710.
- Brye, K.R., et al. (2013). Soil texture effects on methane emissions from direct-seeded, delayed-flood rice production in Arkansas. **Lippincott & Wilkins, Chemistry, Soil Science**, 178 (10): 519-529.
- Bubier, J., Moore, T., and Roulet, N. (1993). Methane emissions from wetlands in the midboreal region of Northern Ontario, Canada. **Ecological Society of America (ESA), Ecology**, 74 (8): 2240–2254.
- Butterbach-Bahl, K., Baggs, E.M., Dannenmann, M., Kiese, R., Zechmeister-Boltenstern, S., 2013. Nitrous oxide emissions from soils: how well do we understand the processes and their controls? **The Royal Society Publishing, London, Philosophical Transactions, B: Biological Science**, 368 (1621): 20130122, 13 pp.
- Castro, M.S., Steudler, P.A., Melillo, J.M., Aber, J.D., and Bowden, R.D. (1995). Factors controlling atmospheric methane consumption by temperate forest soils. **American Geophysical Union (AGU), Global Biogeochemical Cycles**, 9 (1): 1–10.

- Chan, A.S.K., and Parkin, T.B., 2001. Methane oxidation and production activity in soils from natural and agricultural ecosystems. **Journal of environmental quality**, 30: 1896–903.
- Chidthaisong, A., and Conrad, R. (2000). Turnover of glucose and acetate coupled to reduction of nitrate, ferric iron and sulfate and to methanogenesis in anoxic rice field soil. **FEMS Microbiology Ecology**, 31 (1): 73–86.
- Chin, K.J., Lueders, T., Friedrich, M.W., Klose, M., and Conrad, R. (2004). Archaeal community structure and pathway of methane formation on rice roots. **Microbial Ecology**, 47 (1): 59–67.
- Chuersuwan, S., Suwanwaree, P., and Chuersuwan, N. (2014). Estimating greenhouse gas fluxes from constructed wetlands used for water quality improvement. **Songklanakarin Journal of Science and Technology**, 36 (3): 367–373.
- Cicerone, R.J., Delwiche, C.C., Tyler, S.C., and Zimmerman, P.R. (1992). Methane emissions from California rice paddies with varied treatments. **American Geophysical Union (AGU), Global Biogeochemical Cycles**, 6 (3): 233–248.
- Collier, S.M., Ruark, M.D., Oates, L.G., Jokela, W.E., and Dell, C.J. (2014). Measurement of greenhouse gas flux from agricultural soils using static chamber. **Journal of Visualized Experiments** 90: 52110.
- Conrad, R., Lupton, F.S., and Zeikus, J.G. (1987). Hydrogen metabolism and sulfate-dependent inhibition of methanogenesis in a eutrophic lake sediment (Lake Mendota). **FEMS Microbiology Ecology**, 3 (2): 107–115.
- Conrad, R., and Rothfuss, F. (1991). Methane oxidation in the soil surface layer of a flooded rice field and the effect of ammonium. **Biology and Fertility of Soils**, 12: 28–32.

- Cowardin, L., Carter, V., Golet, F., and LaRoe, E. (1979). Classification of wetlands and deepwater habitats of the United States. **Fish and Wildlife Service, United States: 142 PP.**
- Crozier, C.R., and DeLaune, R.D., 1996. Methane production by soils from different Louisiana marsh vegetation types. **The Society of Wetland Scientists, Wetlands**, 16 (2): 121–126.
- de Klein, C. A. M., and Harvey, M. J. (2012). Nitrous oxide methodology guidelines. **Ministry for Primary Industries, New Zealand: 146 PP.**
- Denier van der Gon, H.A.C., van Breemen, N., Neue, H.U., Lantin, R.S., Aduna, J.B., Alberto, M.C.R., and Wassmann, R. (1996). Release of entrapped methane from wetland rice fields upon soil drying. **American Geophysical Union (AGU), Global Biogeochemical Cycles**, 10 (1): 1-7. 10.
- Denmead, O.T., Freney, J.R., and Simpson, J.R. (1982). Atmospheric dispersion of ammonia during application of anhydrous ammonia fertilizer. **Journal of Environmental Quality**, 11 (4): 568–572.
- Ding, W., Cai, Z., Tsuruta, H., and Li, X. (2002). Effect of standing water depth on methane emissions from freshwater marshes in northeast China. **Atmospheric Environment**, 36 (33): 5149–5157.
- Dise, N.B. (1992). Winter fluxes of methane from Minnesota peatlands. **Kluwer Academic Publishers, Biogeochemistry**, 17: 71–83.
- Dunfield, P., Knowles, R., Dumont, R., and Moore, T.R. (1993). Methane production and consumption in temperate and subarctic peat soils: Response to temperature and pH. **Soil Biology and Biochemistry**, 25 (3): 321–326.
- Emiliani, C. (1981). The oceanic lithosphere. **Harvard University Press, USA: 3-5.**

- Fang, C., and Moncrieff, J.B. (2001). The dependence of soil CO<sub>2</sub> efflux on temperature. **Soil Biology and Biochemistry**, 33 (2): 155–165.
- Faulkner, K. (2014). Understanding wetland biogeochemistry: soils and sediment, In wetlands (Edited by Spray, S. L., and McGlothlin, K. L.). **Rowman and Littlefield Publisher, Inc, United States**: 126 PP.
- Fenchel, T., Blackburn, T.H., and King, G.M. (2012). Bacterial Biogeochemistry, Third ed. **Academic Press, Elsevier Ltd.**, 312 PP.
- Foken, T. (2008). Micrometeorology. **Springer-Verlag Berlin Heidelberg**: 306 PP.
- Fourier, J.B.J. (1824). General remarks on the temperature of the terrestrial globe and the planetary spaces, translation from the French by Burgess, E., 1837. **American Journal of Science**, 32: 1-20.
- Frenzel, P., Bosse, U., and Janssen, P.H. (1999). Rice roots and methanogenesis in a paddy soil: ferric iron as an alternative electron acceptor in the rooted soil. **Soil Biology and Biochemistry**, 31 (3): 421–430.
- Frenzel, P., Rothfuss, F., and Conrad, R. (1992). Oxygen profiles and methane turnover in a flooded rice microcosm. **Biology and Fertility of Soils**, 14: 84–89.
- Garcia, J.L., Patel, B.K.C., and Ollivier, B. (2000). Taxonomic, phylogenetic, and ecological diversity of methanogenic archaea. **Anaerobe**, 6 (4): 205–226.
- Gilbert, B., and Frenzel, P. (1995). Methanotrophic bacteria in the rhizosphere of rice microcosms and their effect on pore water methane concentration and methane emission. **Biology and Fertility of Soils**, 20: 93–100.
- Goodwin, S., and Zeikus, J. (1987). Ecophysiological adaptations of anaerobic bacteria to low pH: Analysis of anaerobic digestion in acidic bog sediments. **Applied and environmental microbiology**, 53 (1): 57–64.

- Happell, J., Chanton, J.P., and Showers, W. (1994). The influence of methane oxidation on the stable isotopic composition of methane emitted from Florida swamp forests. **Geochimica et Cosmochimica Acta**, 58 (20): 4377–4388.
- Hargreaves, K.J., and Fowler, D. (1998). Quantifying the effects of water table and soil temperature on the emission of methane from peat wetland at the field scale. **Atmospheric Environment**, 32 (19): 3275–3282.
- Hargreaves, K.J., Fowler, D., Pitcairn, C.E.R., and Aurela, M. (2001). Annual methane emission from Finnish mires estimated from eddy covariance campaign measurements. **Theoretical and Applied Climatology**, 70: 203–213.
- Haroon, M.F., Hu, S., Shi, Y., Imelfort, M., Keller, J., Hugenholtz, P., Yuan, Z., and Tyson, G.W. (2013). Anaerobic oxidation of methane coupled to nitrate reduction in a novel archaeal lineage. **Nature**, 500: 567–570.
- Harper, L.A., Denmead, O.T., Freney, J.R., and Byers, F.M. (1999). Direct measurements of methane emissions from grazing and feedlot cattle. **Journal of Animal Science**, 77 (6): 1392–1401.
- Harriss, R.C., Sebacher, D.I., and Day, F.P. (1982). Methane flux in the Great Dismal swamp. **Nature**, 297: 673-674.
- Healy, M.G., Devine, C.M., and Murphy, R. (1996). Microbial production of biosurfactants. **Resources, Conservation and Recycling**, 18 (1-4): 41–57.
- Horn, M., Matthies, C., Küsel, K., Schramm, A., and Drake, H. (2003). Hydrogenotrophic methanogenesis by moderately acid-tolerant methanogens of a methane-emitting acidic peat. **American Society for Microbiology, Applied and Environmental Microbiology**, 69 (1):74–83.

- Hosono, T., and Nouchi, I. (1997). The dependence of methane transport in rice plants on the root zone temperature. **Kluwer Academic Publishers, Plant and Soil**, 191: 233–240.
- Hungate, R.E., and Macy, J. (1973). The roll-tube method for cultivation of strict anaerobes. **Bulletins from the Ecological Research Committee**: 123–126.
- Hutchinson, G.L., and Mosier, A.R. (1981). Improved soil cover method for field measurement of nitrous oxide fluxes. **Soil Science Society of America Journal**, 45 (2): 311-316.
- IPCC. (2014). Climate Change 2014: Synthesis Report. Contribution of Working Groups I, II and III to the Fifth Assessment Report of the Intergovernmental Panel on Climate Change. Edited by Core Writing Team, Pachauri, R. K., and Meyer, L.A. **IPCC, Geneva, Switzerland**: 151 PP.
- IPCC, (2018). Summary for Policymakers. In: Global warming of 1.5°C. An IPCC Special Report on the impacts of global warming of 1.5°C above pre-industrial levels and related global greenhouse gas emission pathways, in the context of strengthening the global response to the threat of climate change, sustainable development, and efforts to eradicate poverty, Masson-Delmotte, V., Zhai, P., Pörtner, Roberts, H.D., Skea, J., Shukla, P.R., Pirani, A., Moufouma-Okia, W., Péan, C., Pidcock, R., Connors, S., Matthews, J.B.R., Chen, Y., Zhou, X., Gomis, M.I., Lonnoy, E., Maycock, T., Tignor, M., and Waterfield, T. (eds). **World Meteorological Organization, Geneva, Switzerland**: 32 PP.
- Jalota, S.K., Vashisht, B.B., Sharma, S., and Kaur, S. (2018). Understanding Climate Change Impacts on Crop Productivity and Water Balance. **Academic Press, Elsevier Inc.**, pp: 1–53.

- Jermasawatdipong, P., Murase, J., Prabuddham, P., Hasathon, Y., Khomthong, N., Naklang, K., Watanabe, A., Haraguchi, H., and Kimura, M. (1994). Methane emission from plots with differences in fertilizer application in Thai paddy fields. **Soil Science and Plant Nutrition**, 40 (1): 63–71.
- Jones, W.J., Nagle, D.P., and Whitman, W.B. (1987). Methanogens and the diversity of archae bacteria. **American Society for Microbiology, Microbiology Review**, 51 (1): 135–177.
- Jones, W.J., Whitman, W.B., Fields, R.D., and Wolfe, R.S. (1983). Growth and plating efficiency of methanococci on agar media. **American Society for Microbiology, Applied and Environmental Microbiology**, 46 (1): 220–226.
- Joulian, C., Escoffier, S., Le Mer, J., Neue, H.U., and Roger, P. (1997). Populations and potential activities of methanogens and methanotrophs in rice fields: Relations with soil properties. **Federation of European Biochemical Societies (FEBS) Press, European Journal of Soil Biology**, 33 (2): 105–116.
- Kaesler, B., and Schönheit, P. (1989). The role of sodium ions in methanogenesis: Formaldehyde oxidation to  $\text{CO}_2$  and  $2\text{H}_2$  in methanogenic bacteria is coupled with primary electrogenic  $\text{Na}^+$  translocation at a stoichiometry of 2-3  $\text{Na}^+/\text{CO}_2$ . **Federation of European Biochemical Societies (FEBS) Press, European journal of biochemistry**, 184 (1): 223–232.
- Kaewgamtong, N. (2002). Methane Emission form Constructed Wetland. **Master thesis, King Mongkut's University of Technology Thonburi, Bangkok.**
- Kallistova, A.Y., et al. (2017). Methane formation and oxidation by prokaryotes. **Pleiades Publishing, Ltd., Microbiology**, 86 (6): 671-691.



- Kelley, C., Martens, C.S., and Chanton, J.P. (1990). Variations in sedimentary carbon remineralization rates in the White Oak River estuary, North Carolina. **Association for the Sciences of Limnology (ASLO), Limnology and Oceanography**, 35 (2): 372–383.
- Kelley, C.A., Martens, C.S., and Ill, W.S. (1995). Methane dynamics across a tidally flooded riverbank margin. **Association for the Sciences of Limnology (ASLO), Limnology and Oceanography**, 40 (6): 1112–1129.
- Khemjaroen, K. (2001). Methane emissions from natural and man-made wetlands: a comparative study on freshwater marsh, paddy field, and shrimp farm in Bansang district. **Master thesis of Environmental Management, Mahidol University, Bangkok.**
- King, G., Roslev, P., and Skovgaard, H. (1990). Distribution and rate of methane oxidation in sediments of the Florida everglades. **Applied and environmental microbiology**, 56 (9): 2902–11.
- King, G.M., and Adamsen, A.P.S. (1992). Effects of temperature on methane consumption in a forest soil and in pure cultures of the methanotroph *Methylomonas rubra*. **Applied and Environmental Microbiology**, 58 (9): 2758–2763.
- Klinger, L.F., Zimmerman, P.R., Greenberg, J.P., E. Heidt, L.E., and Guenther, A.B. (1994). Carbon trace gas fluxes along a successional gradient in the Hudson-Bay lowland. **American Geophysical Union, Journal of Geophysical Research: Atmospheres**, 99(1): 1469–1494.

- Kludze, H., and Delaune, R. (1995). Gaseous exchange and wetland plant response to soil redox intensity and capacity. **Soil Science Society of America Journal, Wetland Soil**, 59 (3): 939-945.
- Kludze, H., Delaune, R., and Patrick Jr., W.H. (1993). Aerenchyma formation and methane and oxygen exchange in rice. **Soil Science Society of America Journal, Soil Microbiology & Biochemistry**, 57 (2): 386-391.
- Kreisl, P., and Kandler, O. (1986). Chemical structure of the cell wall polymer of methanosarcina. **Systematic and Applied Microbiology**, 7 (2): 293–299.
- Kumaraswamy, S., Ramakrishnan, B., Satpathy, S.N., Rath, A.K., Misra, S., Rao, V.R., and Sethunathan, N. (1997). Spatial distribution of methane-oxidizing activity in a flooded rice soil. **Kluwer Academic Publishers, Plant and Soil**, 191: 241–248.
- Lai, D.Y.F. (2009). Methane dynamics in Northern peatlands: A review. **Pedosphere**, 19 (4): 409–421.
- Laubach, J., and Kelliher, F.M. (2004). Measuring methane emission rates of a dairy cow herd by two micrometeorological techniques. **Agricultural and Forest Meteorology**, 125 (3-4): 279–303.
- Launiainen, S. (2011). Canopy processes, fluxes and microclimate in a pine forest. **Report Series in Aerosol Science**, 117: 56 pp.
- Lekphet, S., Adsavakulchai, S., and Nitorisavut, S. (2005). Estimating methane emissions from mangrove area in Ranong province, Thailand. **Songklanakarin Journal of Science and Technology**, 27 (1): 153-163.
- Leuning, R., Baker, S.K., Jamie, I.M., Hsu, C.H., Klein, L., Denmead, O.T., and Griffith, D.W.T. (1999). Methane emission from free-ranging sheep: a

- comparison of two measurement methods. **Atmospheric Environment**, 33 (9): 1357–1365.
- Lovley, D.R., and Klug, M.J. (1986). Model for the distribution of sulfate reduction and methanogenesis in freshwater sediments. **Geochimica et Cosmochimica Acta**, 50 (1): 11–18.
- Lu, Y., Wassmann, R., Neue, H.U., and Huang, C. (1999). Impact of phosphorus supply on root exudation, aerenchyma formation and methane emission of rice plants. **Kluwer Academic Press, Biogeochemistry**, 47: 203–218.
- Lund, M., Lafleur, P.M., Roulet, N.T., Lindroth, A., Christensen, T.R., Aurela, M., Chojnicki, B.H., Flanagan, L.B., Humphreys, E.R., Laurila, T., Oechel, W.C., Olejnik, J., Rinne, J., Schubert, P., and Nilsson, M.B. (2010). Variability in exchange of CO<sub>2</sub> across 12 Northern peatland and tundra sites. **Blackwell Publishing Ltd., Global Change Biology**, 16: 2436–2448.
- Mathrani, I., Boone, R.D., Mah, R., Fox, G., and Lau, P.P. (1988). *Methanohalophilus zhilinae* sp. nov., an Alkaliphilic, Halophilic, Methylotrophic Methanogen. **In proceeding International journal of systematic bacteriology**, 38 (2): 139–142.
- McInerney, M.J., Bryant, M.P., and Pfennig, N. (1979). Anaerobic bacterium that degrades fatty acids in syntrophic association with methanogens. **Archives of Microbiology**, 122: 129–135.
- Megraw, S.R., and Knowles, R. (1987). Methane production and consumption in a cultivated humisol. **Biology and Fertility of Soils**, 5: 56–60.
- Meinshausen, M., et al. (2017). Historical greenhouse gas concentrations for climate modelling (CMIP6). **Copernicus Publications on behalf of the European**

- Geosciences Union (EGU), Geoscientific Model Development**, 10: 2057-2116.
- Miller, B.G. (2005). CHAPTER 4 - Coal-fired emissions and legislative action in the United States, in *Coal Energy Systems, Sustainable World*, Miller, B.G. (Ed.). **Academic Press, Burlington**, pp: 123–194.
- Minamikawa, K., Tokida, T., Sudo, S., Padre, A., and Yagi, K. (2015). Guidelines for measuring CH<sub>4</sub> and N<sub>2</sub>O emissions from rice paddies by a manually operated closed chamber method. **National Institute for Agro-Environmental Sciences, Tsukuba, Japan**: 80 PP.
- Mishra, S., Rath, A.K., Adhya, T.K., Rao, V.R., and Sethunathan, N. (1997). Effect of continuous and alternate water regimes on methane efflux from rice under greenhouse conditions. **Biology and Fertility of Soils**, 24: 399–405.
- Mitsch, W.J., and Gosselink, J.G. (2015). *Wetlands* (5th edition). **John Wiley & Sons, Inc., United States of America**: 456 PP.
- Miyajima, T., Wada, E., Hanba, Y.T., and Vijarnsorn, P. (1997). Anaerobic mineralization of indigenous organic matters and methanogenesis in tropical wetland soils. **Geochimica et Cosmochimica Acta**, 61 (17): 3739–3751.
- Moore, T.R., and Dalva, M., 1993. The influence of temperature and water table position on carbon dioxide and methane emissions from laboratory columns of peatland soils. **Federation of European Biochemical Societies (FEBS) Press, European Journal of Soil Science**, 44 (4): 651–664.
- Moore, T.R., and Knowles, R. (1990). Methane emissions from fen, bog and swamp peatlands in Quebec. **Kluwer Academic Press, Biogeochemistry**, 11 (1): 45–61.

- Moore, T.R., and Roulet, N.T. (1993). Methane flux: Water table relations in northern wetlands. **American Geophysical Union, Geophysical Research Letters**, 20: 587–590.
- Morrissey, E., Gillespie, J., Morina, J., and Franklin, R. (2013). Salinity affects microbial activity and soil organic matter content in tidal wetlands. **Global Change Biology**, 20 (4): 1351-1362.
- Müller, V., Blaut, M., and Gottschalk, G. (1987). Generation of a transmembrane gradient of Na<sup>+</sup> in *Methanosarcina barkeri*. **Federation of European Biochemical Societies (FEBS) Press, European Journal of Biochemistry**, 162: 461–6.
- Myhre, G., Shindell, D., Bréon, F.M., Collins, W., Fuglestedt, J., Huang, J., Koch, D., Lamarque, J.F., Lee, D., Mendoza, B., Nakajima, T., Robock, A., Stephens, G., Takemura, T., and Zhang, H. (2013). Anthropogenic and natural radiative forcing, in *Climate Change 2013: The Physical Science Basis. Contribution of Working Group I to the Fifth Assessment Report of the Intergovernmental Panel on Climate Change*, Stocker, T.F., D. Qin, G.K. Plattner, M. Tignor, S.K. Allen, J. Boschung, A. Nauels, Y. Xia, V. Bex and P.M. Midgley (eds.). **Cambridge University Press, Cambridge, United Kingdom and New York, USA.**: 82 PP.
- Neue, H.U., and Roger, P.A. (1994). Potential of methane emission in major rice ecologies, in *Climate biosphere interaction: biogenic emissions and environmental effects of climate change*, Zepp, R.G. (ed). **Wiley and Sons, New York**: 65-93.

- NOAA/ESRL. (2020). Carbon cycle greenhouse gases. **Online**. Available at: [https://esrl.noaa.gov/gmd/ccgg/trends\\_ch4/](https://esrl.noaa.gov/gmd/ccgg/trends_ch4/) (accessed 19 June 2020).
- Nouchi, I., Hosono, T., Aoki, K., and Minami, K. (1994). Seasonal variation in methane flux from rice paddies associated with methane concentration in soil water, rice biomass and temperature, and its modelling. **Kluwer Academic Press, Plant and Soil**, 161: 195–208.
- Oades, J.M. (1988). The retention of organic matter in soils. **Martinus Nijhoff/ Dr W. Junk Publishers, Biogeochemistry**, 5: 35–70.
- Ojima, D.S., Valentine, D.W., Mosier, A.R., Parton, W.J., and Schimel, D.S. (1993). Effect of land use change on methane oxidation in temperate forest and grassland soils. **Chemosphere**, 26 (1-4): 675–685.
- Oremland, R.S., and Culbertson, C.W. (1992). Importance of methane-oxidizing bacteria in the methane budget as revealed by the use of a specific inhibitor. **Nature**, 356: 421-423.
- Orphan, V., House, C., Hinrichs, K.U., Mckeegan, K., and DeLong, F.E. (2002). Multiple archaeal groups mediate methane oxidation in anoxic cold seep sediments. **Proceedings of the National Academy of Sciences of the United States of America**, 99 (11): 7663-7668.
- Pavelka, M., et al. (2018). Standardisation of chamber technique for CO<sub>2</sub>, NO<sub>2</sub>, and CH<sub>4</sub> fluxes measurements from terrestrial ecosystems. **Institute of Agrophysics, Polish Academy of Sciences, International Agrophysics**, 32: 569-587.
- Pennock, D., et al. (2007). Soil sampling designs, in Soil sampling and method of analysis (2<sup>nd</sup> Edition), Carter, M.R., and Gregorich, E.G. (eds). **Taylor &**

**Francis Group, LLC/CRC Press, Canadian Society of Soil Science, USA:**  
25-38.

Pietikäinen, J., Pettersson, M., and Bååth, E. (2005). Comparison of temperature effects on soil respiration and bacterial and fungal growth rates. **FEMS Microbiology Ecology**, 52 (1): 49–58.

Prieme, A. (1994). Production and emission of methane in a brackish and a freshwater wetland. **Soil Biology and Biochemistry**, 26 (1): 7–18.

Raghoebarsing, A.A., Pol, A., van de Pas-Schoonen, K.T., Smolders, A.J.P., Ettwig, K.F., Rijpstra, W.I.C., Schouten, S., Damsté, J.S.S., Camp, H.J.M.O. den, Jetten, M.S.M., and Strous, M. (2006). A microbial consortium couples anaerobic methane oxidation to denitrification. **Nature**, 440: 918-921.

Ramachandran, P., and Ramachandran, R. (2001). Natural and anthropogenic methane emission from coastal wetlands of South India. **Environmental Management**, 27 (4): 547–57.

Ramsar Convention Secretariat, 2016. An introduction to the convention on wetlands. **Ramsar Convention Secretariat, Gland, Switzerland**, 110 pp.

Reay, D.S., Hewitt, C.N., and Smith, K.A. (2007). Nitrous oxide: Importance, source and sinks. **Athenaeum Press Ltd, Gateshead, UK**, 249 pp.

Reeburgh, W.S. (1976). Methane consumption in Cariaco trench waters and sediments. **Earth and Planetary Science Letters**, 28 (3): 337–344.

Repeta, D.J., Ferrón, S., Sosa, O.A., Johnson, C.G., Repeta, L.D., Acker, M., DeLong, E.F., and Karl, D.M. (2016). Marine methane paradox explained by bacterial degradation of dissolved organic matter. **Nature Geoscience**, 9: 884–887.

- Rinne, J., Riutta, T., Pihlatie, M., Aurela, M., Haapanala, S., Tuovinen, J.P., Tuittila, E.S., and Vesala, T. (2007). Annual cycle of methane emission from a boreal fen measured by the eddy covariance technique. **Taylor & Francis Online, Tellus B: Chemical and Physical Meteorology**, 59 (3): 449–457.
- Roslev, P., and King, G.M. (1996). Regulation of methane oxidation in a freshwater wetland by water table changes and anoxia. **FEMS Microbiology Ecology**, 19: 105-115.
- Sass, R.L., Fisher, F.M., Lewis, S.T., Jund, M.F., and Turner, F.T. (1994). Methane emissions from rice fields: Effect of soil properties. **American Geophysical Union (AGU), Global Biogeochemical Cycles**, 8 (2): 135–140.
- Sass, R.L., Fisher, F.M., Wang, Y.B., Turner, F.T., Jund, M.F., 1992. Methane emission from rice fields: The effect of floodwater management. **American Geophysical Union (AGU), Global Biogeochemical Cycles**, 6 (3) 249–262.
- Schlesinger, W.H., and Bernhardt, E.S. (2013). Chapter 7 - Wetland Ecosystems, in *Biogeochemistry (Third Edition)*, Schlesinger, W.H., Bernhardt, E.S. (eds.). **Academic Press, Boston**, pp: 233–274.
- Shannon, R.D., and White, J.R. (1994). A three-year study of controls on methane emissions from two Michigan peatlands. **Kluwer Academic Publishers, Biogeochemistry**, 27: 35–60.
- Sinke, A.J.C., Cornelese, A.A., Cappenberg, T.E., and Zehnder, A.J.B. (1992). Seasonal variation in sulfate reduction and methanogenesis in peaty sediments of eutrophic Lake Loosdrecht, The Netherlands. **Kluwer Academic Press, Biogeochemistry**, 16: 43–61.



- Stephens, G.L., and Tjemkes, A.S. (1993). Water vapour and its role in the Earth's greenhouse. **Australian Journal of Physics**, 46: 149-166.
- Stolzy, L.H., Focht, D.D., and Flühler, H. (1981). Indicators of soil aeration status. **Flora**, 171 (3): 236–265.
- Strategy of Regional Irrigation Office 8. (2000). Baan San Kumphaeng operation and maintainance project. **Online**. Available at: <http://lamprapleng.com/index.php> (19 February 2019)
- Sweerts, J.P.R.A., Bär-Gilissen, M.J., Cornelese, A.A., and Cappenberg, T.E. (1991). Oxygen-consuming processes at the profundal and littoral sediment-water interface of a small meso-eutrophic lake (Lake Vechten, The Netherlands). **Association for the Sciences of Limnology and Oceanography (ASLO), Limnology and Oceanography**, 36 (6): 1124–1133.
- Tan, K.H. (2005). Soil sampling, preparation, and analysis (2<sup>nd</sup> Edition). **Taylor & Francis, CRC Press, Boca Raton: 672 PP.**
- Thailand Office of Natural Resources and Environmental Policy and Planning (ONEP). (2013). A little knowledge of “Wetland”. **Online**. Available at: [http://wetland.onep.go.th/w\\_mean.html](http://wetland.onep.go.th/w_mean.html) (accessed 19 June 2019)
- Torres-Alvarado, R., Ramírez-Vives, F., Fernández, F.J., Barriga-Sosa, I. de los A. (2005). Methanogenesis and methane oxidation in wetlands. **Implications in the global carbon cycle, Hidrobiológica**, 15 (3): 327-349.
- Twin, T.E., et al. (2000). Correcting eddy covariance flux under estimates over a grassland. **Agriculture for Meteorology**, 103: 279-300.

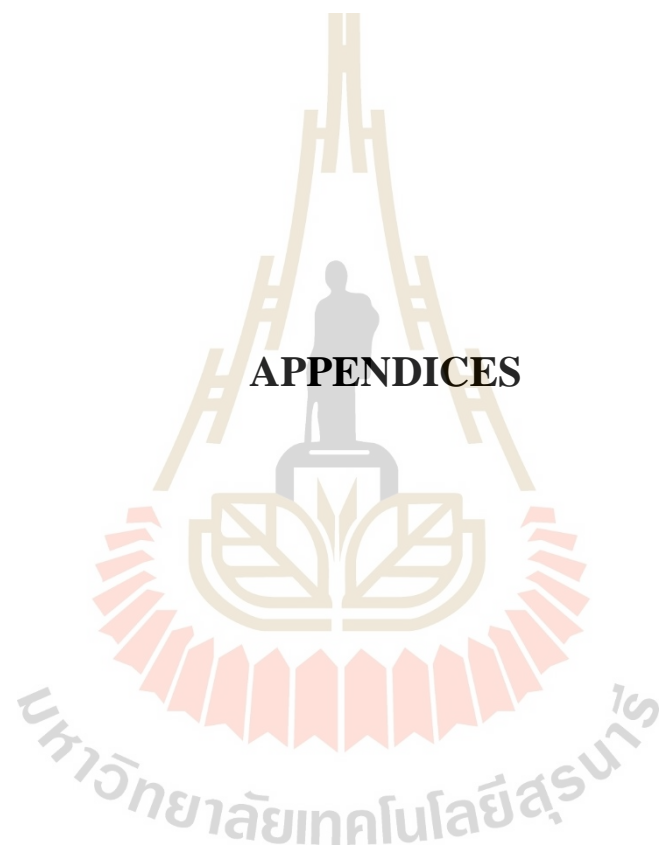
- Tyndall, J. (1862). On the absorption and radiation of heat by gaseous matter. Second Memoir. **The Royal Society Publishing, London, Philosophical Transactions**, 152: 59–98.
- United State Environmental Protection Agency (US EPA). (2020). Overview of greenhouse gases. **Online**. Available at: <https://www.epa.gov/ghgemissions/overview-greenhouse-gases>. (accessed 4 December 2020).
- Dlugokencky, E. and NOAA/ESRL. (2019). Carbon cycle greenhouse gases. **Online**. Available at: [https://esrl.noaa.gov/gmd/ccgg/trends\\_ch4/](https://esrl.noaa.gov/gmd/ccgg/trends_ch4/) (accessed 14 June 2019).
- Valentine, D. (2004). Thermodynamic ecology of hydrogen-based syntrophy, in Cellular Origin, Life in Extreme Habitats and Astrobiology. **Springer Nature, COLE Book series**, (4): 149–161.
- van den Pol-van Dasselaar, A., and Oenema, O. (1999). Methane production and carbon mineralisation of size and density fractions of peat soils. **Soil Biology and Biochemistry**, 31 (6): 877–886.
- Wagner, D., Pfeiffer, E.M., and Bock, E. (1999). Methane production in aerated marshland and model soils: Effects of microflora and soil texture. **Soil Biology and Biochemistry**, 31(7): 999–1006.
- Wang, F., and Bettany, J. (1995). Short Communication : Methane emission from a usually well-drained prairie soil after snowmelt and precipitation. **Canadian Journal of Soil Science**, 75: 239–241.

- Wang, Z., Delaune, R., Patrick Jr., H.W., and Masscheleyn, H.P. (2009). Soil redox and pH effects on methane production in a flooded rice soil. **Soil Science Society of America Journal, Soil Microbiology and Biochemistry**, 57 (2): 382–385.
- Wassmann, R., Neue, H.U., Lantin, R.S., Aduna, J.B., Alberto, M.C.R., J. Andales, M.J. Tan, M.J, Denier van der Gon, H.A.C., Hoffmann, H., Papen, H., Rennenberg, H., and Seiler, W. (1994). Temporal Patterns of Methane Emissions from Wetland Rice Fields Treated Different Modes of N Application. **American Geophysical Union (AGU), Journal of Geophysical Research: Atmosphere**, 99 (D8), 16457–16462.
- Welte, C. and Deppenmeier, U. (2014). Bioenergetics and anaerobic respiratory chains of acetoclastic methanogens. **Biochimica et Biophysica Acta (BBA) - Bioenergetics**, 1837 (7): 1130–1147.
- Westermann, P. (1993). Wetland and swamp microbiology, in Aquatic Microbiology, Ford, T.E. (ed). **Blackwell Scientific Publications, Oxford**.
- Whiting, G.J., and Chanton, J.P. (1992). Plant-dependent CH<sub>4</sub> emission in a subarctic Canadian fen. **American Geophysical Union (AGU), Global Biogeochemical Cycles**, 6 (3): 225–231.
- Williams, R.T., and Crawford, R.L. (1984). Methane production in Minnesota peatlands. **American Society for Microbiology, Applied and Environmental Microbiology**, 47 (6): 1266–1271.
- Wilson, J.D., Catchpoole, V.R., Denmead, O.T., and Thurtell, G.W. (1983). Verification of a simple micrometeorological method for estimating the rate of gaseous mass transfer from the ground to the atmosphere. **Agricultural Meteorology**, 29 (3): 183–189.

- Yagi, K., Chairaj, P., Tsuruta, H., Cholitkul, W., and Minami, K. (1994). Methane emission from rice paddy fields in the central plain of Thailand. **Soil Science and Plant Nutrition**, 40 (1): 29–37.
- Yao, H., and Conrad, R. (1999). Thermodynamics of methane production in different rice paddy soils from China, the Philippines and Italy. **Soil Biology and Biochemistry**, 31 (3): 463–473.
- Yao, H., Conrad, R., Wassmann, R., and Neue, H.U. (1999). Effect of soil characteristics on sequential reduction and methane production in sixteen rice paddy soils from China, the Philippines, and Italy. **Kluwer Academic Press, Biogeochemistry**, 47: 269–295.
- Yavitt, J., Lang, G., and Sexstone, J.A. (1991). Methane fluxes in wetland and forest soils, beaver ponds, and low-order streams of a temperate forest ecosystem. **American Geophysical Union (AGO), Journal of Geophysical Research: Atmosphere**, 95 (D13): 22463-22474
- Yavitt, J.B., and Knapp, A.K. (1995). Methane emission to the atmosphere through emergent cattail (*Typha latifolia* L.) plants. **Taylor & Francis Online, Tellus B: Chemical and Physical Meteorology**, 47 (5): 521–534.
- Yu, K., Hiscox, A., Delaune, R., and DeLaune, R.D. (2013). Greenhouse gas emission by static chamber and eddy flux methods, DeLaune, R.D., Reddy, K., Richardson, C., and Megonigal, J.P. (eds). **SSSA Books Series, Methods in Biogeochemistry of Wetlands**, (10): 427-437.
- Yue, X.L., and Gao, Q.X. (2018). Contributions of natural systems and human activity to greenhouse gas emissions. **Advances in Climate Change Research**, 9 (4): 243–252.

- Zeikus, J.G., Ben-Bassat, A., and Hegge, P.W. (1980). Microbiology of methanogenesis in thermal, volcanic environments. **American Society for Microbiology, Journal of Bacteriology**, 143 (1): 432–440.
- Zeikus, J.G., and Winfrey, M.R. (1976). Temperature limitation of methanogenesis in aquatic sediments. **American Society for Microbiology, Applied and Environmental Microbiology**, 31 (1) 99–107.
- Zeikus, J.G., and Wolfe, R.S. (1972). *Methanobacterium thermoautotrophicus* sp. n., an anaerobic, autotrophic, extreme thermophile. **American Society for Microbiology, Journal of Bacteriology**, 109 (2): 707–715.
- Zhao, L., et al. (2018). Effects of different electron acceptors on the methanogenesis of hydrolyzed polyacrylamide biodegradation in anaerobic activated sludge system. **Bioresource Technology**, 247: 759–768.
- Zinder, S.H., 1993. Physiological Ecology of Methanogens, in Methanogenesis Ferry, J.G. (ed.), **Springer US, Chapman & Hall Microbiology Series**, pp: 128–206.

**APPENDICES**



## APPENDIX A

### METHANE CONCENTRATIONS

**Table A1.** Methane concentration, chamber's temperature recorded, and graph for methane emissions in December 2018, where  $C_n$  = chamber number,  $T_i$  = time intervals of sampling, avg. = average,  $C$  = methane concentration,  $X$  = emission rate of methane, and n.a. = unaccountable

$C_n$	$T_i$ (min)	$T_c$ (°C)	$C$ (ppmv)	Graph of emissions	$X$
1	2	27.0	2.9		0.0049
	22	27.0	3.1		
	42	27.5	3.2		
	62	31.0	3.2		
	82	34.5	3.3		
	102	35.5	3.3		
	122	35.0	3.6		
	avg	31.1	3.2		
2	2	27.5	n.a.		0.0006
	22	27.0	2.5		
	42	27.5	2.4		
	62	31.0	2.3		
	82	35.0	2.2		
	102	36.0	3.0		
	122	35.0	2.2		
	avg	31.3	2.4		
3	2	26.5	n.a.		0.0027
	22	26.0	2.2		
	42	26.5	2.1		
	62	29.0	2.3		
	82	33.0	n.a.		
	102	33.5	n.a.		
	122	32.0	2.4		
	avg	29.5	2.3		

**Table A1.** Methane concentration, chamber's temperature recorded, and graph for methane emissions in December 2018, where  $C_n$  = chamber number,  $T_i$  = time intervals of sampling, avg. = average, C = methane concentration, X = emission rate of methane, and n.a. = unaccountable (cont'd.)

$C_n$	$T_i$ (min)	$T_c$ (°C)	C (ppmv)	Graph of emissions	X
4	2	26.5	n.a.		0.0043
	22	26.0	n.a.		
	42	26.5	n.a.		
	62	29.0	1.7		
	82	33.0	1.8		
	102	33.5	1.9		
	122	32.0	2.0		
<b>avg</b>		29.5	1.8		
5	2	27.5	2.3		0.0059
	22	27.0	2.3		
	42	27.5	2.5		
	62	31.0	2.5		
	82	35.0	2.6		
	102	36.0	2.7		
	122	35.0	3.1		
<b>avg</b>		31.9	2.6		



**Table A2.** Methane concentration, chamber's temperature recorded, and graph for methane emissions in January 2019, where  $C_n$  = chamber number,  $T_i$  = time intervals of sampling, avg. = average, C = methane concentration, X = emission rate of methane, and n.a. = unaccountable

$C_n$	$T_i$ (min)	$T_c$ (°C)	C (ppmv)	Graph of emissions	X
1	2	28	2.17		0.0070
	32	29	2.22		
	62	30	2.48		
	92	31	2.73		
	122	32	2.96		
	avg	30	2.5		
2	2	27	n.a.		0.0031
	32	28	2.07		
	62	29	2.30		
	92	30	2.57		
	122	31	2.29		
	avg	29	2.3		
3	2	27	n.a.		0.0036
	32	28	2.45		
	62	29	2.46		
	92	30	2.46		
	122	31	2.80		
	avg	29	2.5		

**Table A2.** Methane concentration, chamber's temperature recorded, and graph for methane emissions in January 2019, where  $C_n$  = chamber number,  $T_i$  = time intervals of sampling, avg. = average, C = methane concentration, X = emission rate of methane, and n.a. = unaccountable (cont'd)

$C_n$	$T_i$ (min)	$T_c$ (°C)	C (ppmv)	Graph of emissions	X
4	2	27	2.47		0.0006
	32	28	2.52		
	62	29	2.52		
	92	30	n.a.		
	122	31	2.55		
<b>avg.</b>		29	2.5		
5	2	27	8.6		0.4475
	32	28	11.0		
	62	29	39.0		
	92	30	54.4		
	122	31	54.0		
<b>avg.</b>		29	33.4		
6	2	27	2.47		0.0041
	32	28	2.47		
	62	29	2.61		
	92	30	2.90		
	122	31	2.87		
<b>avg.</b>		29	2.7		

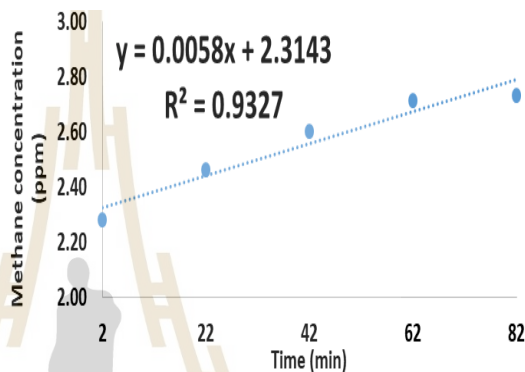
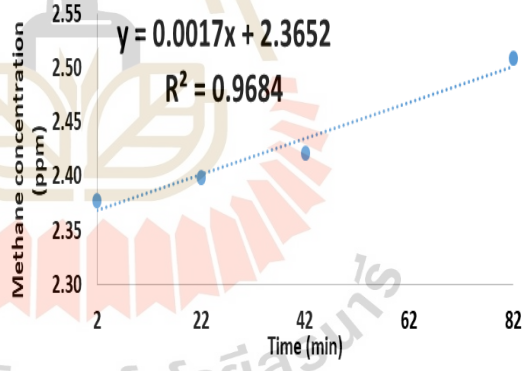
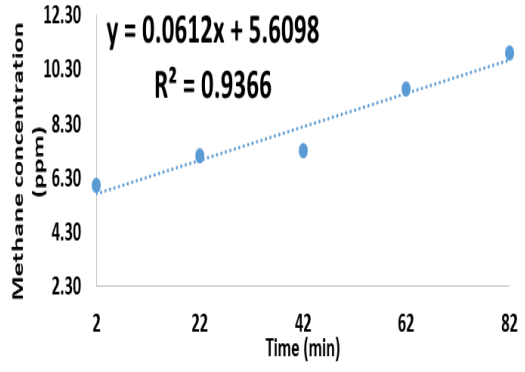
**Table A3.** Methane concentration, chamber's temperature recorded, and graph for methane emissions in February 2019, where  $C_n$  = chamber number,  $T_i$  = time intervals of sampling, avg. = average, C = methane concentration, X = emission rate of methane, and n.a. = unaccountable

$C_n$	$T_i$ (min)	$T_c$ (°C)	C (ppmv)	Graph of emissions	X
1	2	28.0	n.a.		0.0098
	22	28.0	2.48		
	42	29.0	2.86		
	62	30.0	2.92		
	82	28.8	3.11		
	avg		28.0		
2	2	n.a.	n.a.		0.0031
	22	27.5	n.a.		
	42	27.5	2.74		
	62	28.1	2.71		
	82	30.0	2.86		
	avg		28.3		
3	2	n.a.	n.a.		0.0017
	22	27.0	2.78		
	42	27.5	2.80		
	62	28.0	2.81		
	82	31.5	2.89		
	avg		28.5		

**Table A3.** Methane concentration, chamber's temperature recorded, and graph for methane emissions in February 2019, where  $C_n$  = chamber number,  $T_i$  = time intervals of sampling, avg. = average, C = methane concentration, X = emission rate of methane, and n.a. = unaccountable (cont'd)

$C_n$	$T_i$ (min)	$T_c$ (°C)	C (ppmv)	Graph of emissions	X
4	2	n.a.	n.a.		0.0593
	22	27.0	25.72		
	42	27.5	27.14		
	62	26.5	28.09		
	82	29.0	n.a.		
	avg	27.5	26.98		
5	2	n.a.	n.a.		0.0138
	22	27.0	4.15		
	42	27.0	n.a.		
	62	27.0	4.59		
	82	29.1	5.00		
	avg	27.5	4.58		

**Table A4.** Methane concentration, chamber's temperature recorded, and graph for methane emissions in March 2019, where  $C_n$  = chamber number,  $T_i$  = time intervals of sampling, avg. = average, C = methane concentration, X = emission rate of methane, and n.a. = unaccountable

$C_n$	$T_i$ (min)	$T_c$ (°C)	C (ppmv)	Graph of emissions	X
1	2	29.0	2.28		0.0058
	22	31.0	2.46		
	42	31.0	2.60		
	62	32.1	2.72		
	82	33.2	2.73		
	avg		31.3		
2	2	27.5	2.38		0.0017
	22	29.0	2.40		
	42	31.0	2.42		
	62	31.5	2.55		
	82	33.2	2.51		
	avg		30.4		
3	2	28.0	6.03		0.0612
	22	32.5	7.10		
	42	34.8	7.29		
	62	34.0	9.56		
	82	35.0	10.92		
	avg		32.9		

**Table A4.** Methane concentration, chamber's temperature recorded, and graph for methane emissions in March 2019, where  $C_n$  = chamber number,  $T_i$  = time intervals of sampling, avg. = average, C = methane concentration, X = emission rate of methane, and n.a. = unaccountable (cont'd)

$C_n$	$T_i$ (min)	$T_c$ (°C)	C (ppmv)	Graph of emissions	X
4	2	27.0	2.23		0.0081
	22	32.0	2.44		
	42	31.5	2.60		
	62	34.0	2.66		
	82	34.5	2.93		
	avg		31.8		
5	2	27.5	2.33		0.0033
	22	30.5	2.34		
	42	32.0	2.36		
	62	32.5	2.72		
	82	33.5	2.59		
	avg		31.2		
6	2	28.0	2.34		0.0463
	22	31.5	4.31		
	42	32.5	5.53		
	62	33.5	5.91		
	82	34.0	6.17		
	avg		31.9		

**Table A5.** Methane concentration, chamber’s temperature recorded, and graph for methane emissions in April 2019, where  $C_n$  = chamber number,  $T_i$  = time intervals of sampling, avg. = average, C = methane concentration, X = emission rate of methane, and n.a. = unaccountable

$C_n$	$T_i$ (min)	$T_c$ (°C)	C (ppmv)	Graph of emissions	X
1	2	28.0	2.23		0.0090
	22	29.0	2.34		
	42	33.0	2.59		
	62	34.6	2.67		
	82	34.5	2.97		
	avg		31.8		
2	2	29.5	3.48		0.0140
	22	30.0	3.67		
	42	34.8	3.85		
	62	35.2	4.36		
	82	35.5	n.a.		
	avg		33.0		
3	2	29.5	n.a.		0.0151
	22	30.5	2.40		
	42	n.a.	2.96		
	62	35.0	3.17		
	82	35.0	3.34		
	avg		32.5		

**Table A5.** Methane concentration, chamber's temperature recorded, and graph for methane emissions in April 2019, where  $C_n$  = chamber number,  $T_i$  = time intervals of sampling, avg. = average, C = methane concentration, X = emission rate of methane, and n.a. = unaccountable (cont'd)

$C_n$	$T_i$ (min)	$T_c$ (°C)	C (ppmv)	Graph of emissions	X
4	2	28.5	2.62		0.0112
	22	30.0	3.07		
	42	34.0	3.24		
	62	34.0	3.31		
	82	n.a.	n.a.		
<b>avg</b>		31.6	3.06		
5	2	29.8	2.54		0.0134
	22	32.0	2.82		
	42	33.5	3.05		
	62	34.0	3.35		
	82	35.5	n.a.		
<b>avg</b>		33.0	2.94		



**Table A6.** Methane concentration, chamber's temperature recorded, and graph for methane emissions in May 2019, where  $C_n$  = chamber number,  $T_i$  = time intervals of sampling, avg. = average, C = methane concentration, X = emission rate of methane, and n.a. = unaccountable

$C_n$	$T_i$ (min)	$T_c$ (°C)	C (ppmv)	Graph of emissions	X
1	2	31.0	2.26		0.0199
	22	34.5	2.42		
	42	34.0	2.75		
	62	34.0	3.25		
	82	34.0	3.84		
	avg		33.5		
2	2	33.0	5.70		0.0133
	22	35.0	6.18		
	42	36.0	6.28		
	62	37.0	6.38		
	82	36.0	6.93		
	avg		35.4		
3	2	32.5	2.34		0.0113
	22	34.0	2.49		
	42	36.0	2.64		
	62	35.5	2.74		
	82	35.5	3.34		
	avg		34.7		

**Table A6.** Methane concentration, chamber's temperature recorded, and graph for methane emissions in May 2019, where  $C_n$  = chamber number,  $T_i$  = time intervals of sampling, avg. = average, C = methane concentration, X = emission rate of methane, and n.a. = unaccountable (cont'd)

$C_n$	$T_i$ (min)	$T_c$ (°C)	C (ppmv)	Graph of emissions	X
4	2	30.2	5.14		0.1269
	22	34.0	6.88		
	42	34.0	9.93		
	62	34.0	13.80		
	82	34.0	14.37		
	avg		33.2		
5	2	31.5	2.31		0.0062
	22	35.0	2.26		
	42	35.0	2.48		
	62	35.0	n.a.		
	82	34.5	2.76		
	avg		34.2		

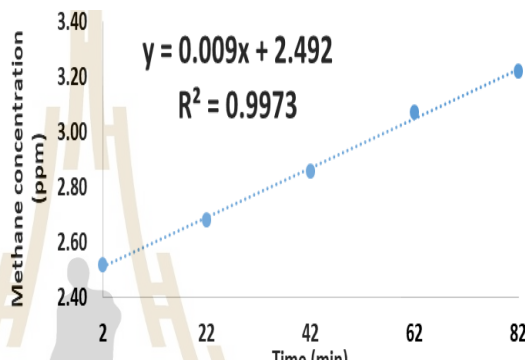
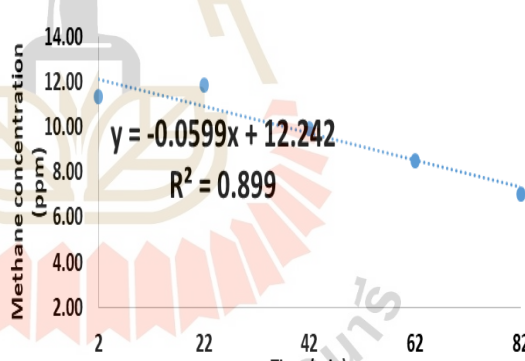
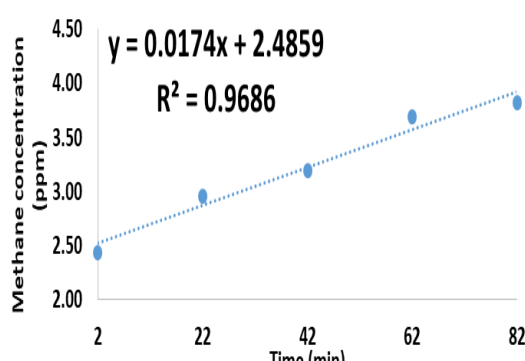
**Table A7.** Methane concentration, chamber's temperature recorded, and graph for methane emissions in June 2019, where  $C_n$  = chamber number,  $T_i$  = time intervals of sampling, avg. = average, C = methane concentration, X = emission rate of methane, and n.a. = unaccountable

$C_n$	$T_i$ (min)	$T_c$ (°C)	C (ppmv)	Graph of emissions	X
1	2	29.5	2.19		0.0079
	22	29.5	2.50		
	42	29.5	2.52		
	62	30.9	2.77		
	82	31.5	2.84		
	avg		30.2		
2	2	29.0	2.42		0.0144
	22	29.0	2.54		
	42	29.0	2.96		
	62	30.0	3.33		
	82	30.5	3.46		
	avg		29.5		
3	2	27.5	2.24		0.0087
	22	28.0	2.51		
	42	28.5	2.71		
	62	30.0	2.76		
	82	n.a.	n.a.		
	avg		28.5		

**Table A7.** Methane concentration, chamber's temperature recorded, and graph for methane emissions in June 2019, where  $C_n$  = chamber number,  $T_i$  = time intervals of sampling, avg. = average, C = methane concentration, X = emission rate of methane, and n.a. = unaccountable (cont'd)

$C_n$	$T_i$ (min)	$T_c$ (°C)	C (ppmv)	Graph of emissions	X
4	2	29.0	2.26		0.0593
	22	29.5	2.43		
	42	30.0	2.37		
	62	31.1	n.a.		
	82	31.2	2.65		
<b>avg</b>		30.2	2.43		
5	2	28.5	2.26		0.0138
	22	29.0	2.35		
	42	30.0	2.54		
	62	30.1	2.56		
	82	31.2	2.62		
<b>avg</b>		29.8	2.47		

**Table A8.** Methane concentration, chamber's temperature recorded, and graph for methane emissions in July 2019, where  $C_n$  = chamber number,  $T_i$  = time intervals of sampling, avg. = average, C = methane concentration, X = emission rate of methane, and n.a. = unaccountable

$C_n$	$T_i$ (min)	$T_c$ (°C)	C (ppmv)	Graph of emissions	X
1	2	27.0	2.52		0.0090
	22	28.0	2.68		
	42	29.0	2.86		
	62	29.2	3.07		
	82	30.1	3.22		
	avg		28.7		
2	2	26.0	11.33		-0.0599
	22	27.0	11.84		
	42	27.5	9.94		
	62	28.0	8.50		
	82	28.8	7.01		
	avg		27.5		
3	2	27.0	2.44		0.0174
	22	28.1	2.96		
	42	29.0	3.19		
	62	29.6	3.69		
	82	30.0	3.82		
	avg		28.7		

**Table A8.** Methane concentration, chamber's temperature recorded, and graph for methane emissions in July 2019, where  $C_n$  = chamber number,  $T_i$  = time intervals of sampling, avg. = average, C = methane concentration, X = emission rate of methane, and n.a. = unaccountable (cont'd)

$C_n$	$T_i$ (min)	$T_c$ (°C)	C (ppmv)	Graph of emissions	X
4	2	27.5	1.94		0.0149
	22	29.0	2.28		
	42	29.5	2.52		
	62	30.0	2.90		
	82	30.2	3.13		
	avg	29.2	2.55		
5	2	27.0	2.53		0.0203
	22	28.0	3.16		
	42	28.5	3.60		
	62	29.0	3.86		
	82	29.5	4.21		
	avg	28.4	3.47		

**Table A9.** Methane concentration, chamber's temperature recorded, and graph for methane emissions in August 2019, where  $C_n$  = chamber number,  $T_i$  = time intervals of sampling, avg. = average, C = methane concentration, X = emission rate of methane, and n.a. = unaccountable

$C_n$	$T_i$ (min)	$T_c$ (°C)	C (ppmv)	Graph of emissions	X
1	2	27.5	2.33		0.0052
	22	28.5	2.36		
	42	29.0	2.48		
	62	29.0	2.69		
	82	29.5	2.69		
	avg		28.7		
2	2	28.5	2.30		0.0047
	22	30.0	2.41		
	42	30.5	2.63		
	62	30.0	2.57		
	82	30.5	2.69		
	avg		29.9		
3	2	27.7	2.09		0.0144
	22	29.5	2.50		
	42	29.5	2.73		
	62	29.0	3.07		
	82	29.2	3.25		
	avg		29.0		

**Table A9.** Methane concentration, chamber's temperature recorded, and graph for methane emissions in August 2019, where  $C_n$  = chamber number,  $T_i$  = time intervals of sampling, avg. = average, C = methane concentration, X = emission rate of methane, and n.a. = unaccountable (cont'd)

$C_n$	$T_i$ (min)	$T_c$ (°C)	C (ppmv)	Graph of emissions	X
4	2	29.5	2.15		0.0106
	22	32.0	2.21		
	42	31.0	2.42		
	62	30.2	2.74		
	82	29.8	2.95		
	avg		30.5		
5	2	27.0	2.17		0.0133
	22	30.0	2.50		
	42	30.0	2.63		
	62	29.5	2.87		
	82	29.9	3.31		
	avg		29.3		



**Table A10.** Methane concentration, chamber's temperature recorded, and graph for methane emissions in September 2019, where  $C_n$  = chamber number,  $T_i$  = time intervals of sampling, avg. = average,  $C$  = methane concentration,  $X$  = emission rate of methane, and n.a. = unaccountable

$C_n$	$T_i$ (min)	$T_c$ (°C)	$C$ (ppmv)	Graph of emissions	$X$
1	2	27.0	2.49		0.0123
	22	23.0	2.80		
	42	23.0	3.04		
	62	22.8	3.21		
	82	23.0	3.52		
	avg		23.8		
2	2	27.0	2.66		0.0061
	22	23.5	2.67		
	42	23.0	2.92		
	62	22.9	3.07		
	82	23.0	3.06		
	avg		23.9		
3	2	26.5	2.57		0.0128
	22	23.8	2.70		
	42	22.2	3.04		
	62	22.2	3.28		
	82	22.5	3.56		
	avg		23.4		

**Table A10.** Methane concentration, chamber's temperature recorded, and graph for methane emissions in September 2019, where  $C_n$  = chamber number,  $T_i$  = time intervals of sampling, avg. = average, C = methane concentration, X = emission rate of methane, and n.a. = unaccountable (cont'd)

$C_n$	$T_i$ (min)	$T_c$ (°C)	C (ppmv)	Graph of emissions	X
4	2	27.0	2.62		0.0105
	22	23.0	2.96		
	42	22.9	3.24		
	62	22.8	3.33		
	82	23.1	3.48		
	avg	23.8	3.12		
5	2	29.0	2.61		0.0126
	22	24.0	2.75		
	42	23.5	3.02		
	62	23.5	3.27		
	82	24.0	3.60		
	avg	24.8	3.05		

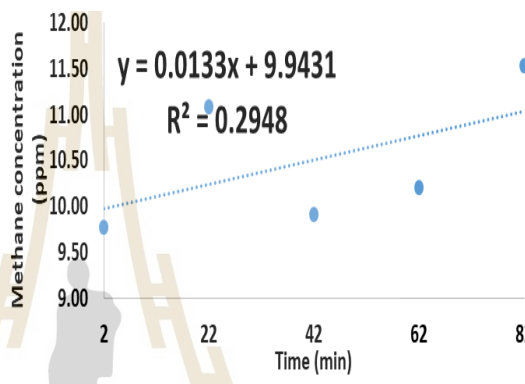
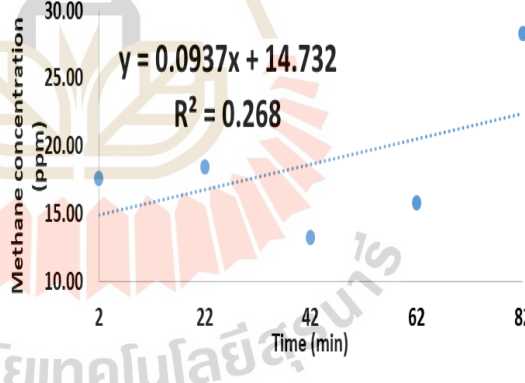
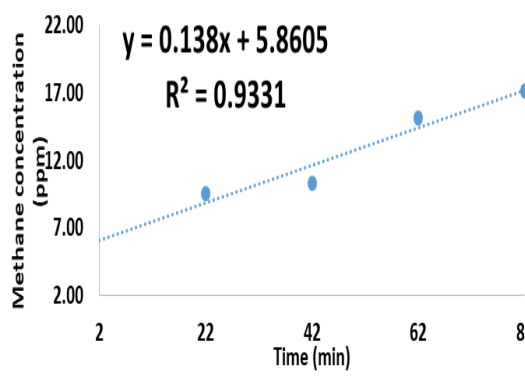
**Table A11.** Methane concentration, chamber's temperature recorded, and graph for methane emissions in October 2019, where  $C_n$  = chamber number,  $T_i$  = time intervals of sampling, avg. = average, C = methane concentration, X = emission rate of methane, and n.a. = unaccountable

$C_n$	$T_i$ (min)	$T_c$ (°C)	C (ppmv)	Graph of emissions	X
1	2	28.0	259.19		7.7701
	22	30.0	640.63		
	42	31.0	780.90		
	62	31.2	861.23		
	82	33.0	925.90		
	avg		30.6		
2	2	27.5	62.86		4.9766
	22	29.0	147.83		
	42	31.0	216.16		
	62	31.0	299.99		
	82	32.5	484.44		
	avg		30.2		
3	2	26.9	142.45		2.7076
	22	27.0	203.14		
	42	30.5	246.65		
	62	31.1	293.04		
	82	31.0	368.26		
	avg		29.3		

**Table A11.** Methane concentration, chamber's temperature recorded, and graph for methane emissions in October 2019, where  $C_n$  = chamber number,  $T_i$  = time intervals of sampling, avg. = average, C = methane concentration, X = emission rate of methane, and n.a. = unaccountable (cont'd)

$C_n$	$T_i$ (min)	$T_c$ (°C)	C (ppmv)	Graph of emissions	X
4	2	29.0	212.48		2.9737
	22	31.0	353.80		
	42	31.5	372.69		
	62	33.1	430.30		
	82	34.0	471.60		
	avg		31.7		
5	2	30.0	157.12		1.5199
	22	30.0	192.29		
	42	30.0	230.64		
	62	30.5	256.74		
	82	31.0	276.88		
	avg		30.3		

**Table A12.** Methane concentration, chamber's temperature recorded, and graph for methane emissions in November 2019, where  $C_n$  = chamber number,  $T_i$  = time intervals of sampling, avg. = average, C = methane concentration, X = emission rate of methane, and n.a. = unaccountable

$C_n$	$T_i$ (min)	$T_c$ (°C)	C (ppmv)	Graph of emissions	X
1	2	28.0	9.77		0.0133
	22	30.0	11.09		
	42	31.0	9.91		
	62	31.2	10.21		
	82	33.0	11.54		
	avg	30.6	10.50		
2	2	35.0	17.56		0.0937
	22	40.0	18.47		
	42	39.0	13.23		
	62	40.0	15.81		
	82	39.0	28.26		
	avg	38.6	18.67		
3	2	28.0	9.54		0.1380
	22	32.5	10.32		
	42	33.5	15.14		
	62	35.0	17.14		
	82	35.5	17.14		
	avg	32.9	13.03		

**Table A12.** Methane concentration, chamber's temperature recorded, and graph for methane emissions in November 2019, where  $C_n$  = chamber number,  $T_i$  = time intervals of sampling, avg. = average,  $C$  = methane concentration,  $X$  = emission rate of methane, and n.a. = unaccountable (cont'd)

$C_n$	$T_i$ (min)	$T_c$ (°C)	$C$ (ppmv)	Graph of emissions	$X$
4	2	31.0	n.a.		
	22	36.0	7.28		
	42	36.0	5.96		
	62	36.0	5.89		
	82	37.0	6.39		
	<b>avg</b>	35.2	6.38		

$$\begin{aligned}
 \text{Methane flux rate, } E_{\text{day}} \text{ (mg/m}^2\text{/day)} &= 1440X \frac{(1.20 \text{ m})(16.04 \text{ g/mol})}{(0.0821)\text{K}} \\
 &= 1440(0.0049) \frac{(1.20 \text{ m})(16.04 \text{ g/mol})}{(0.0821)(31.1)} \\
 &= 53.19 \text{ mg/m}^2\text{/day}
 \end{aligned}$$

**Figure A1.** Example of calculating methane fluxes. The data derived from methane concentration of chamber 1 in December 2018

**Table A13.** Monthly methane flux rates a day

Month	Chamber	X (ppmv/min)	T	E (mg/m <sup>2</sup> /day)
December, 2018	1	0.0049	30.1	5.46
	2	n.a.	31.3	n.a.
	3	n.a.	n.a.	n.a.
	4	0.0027	29.5	3.01
	5	0.0043	31.9	4.76
	6	0.0059	31.9	6.53
January, 2019	1	0.0070	30.0	7.80
	2	n.a.	29.0	n.a.
	3	n.a.	29.0	n.a.
	4	n.a.	29.0	n.a.
	5	0.4475	29.0	500.01
	6	0.0041	29.0	4.58
February	1	0.0098	28.8	10.96
	2	n.a.	28.3	n.a.
	3	0.0017	28.5	1.90
	4	0.0593	27.5	66.59
	5	0.0138	27.5	15.49
March	1	0.0058	31.3	6.43
	2	0.0017	30.4	1.89
	3	0.0612	32.9	67.52
	4	0.0081	31.8	8.97
	5	0.0033	31.2	3.66
	6	0.0463	31.9	51.24

**Table A13.** Monthly methane flux rates a day (cont'd)

Month	Chamber	X (ppmv/min)	T	E(mg/m <sup>2</sup> /day)
April	1	0.0090	31.8	9.96
	2	0.0140	33.0	15.44
	3	0.0151	32.5	16.68
	4	0.0112	31.6	12.41
	5	0.0134	33.0	14.78
May	1	0.0199	33.5	21.91
	2	0.0133	35.4	14.55
	3	0.0113	34.7	12.39
	4	0.1269	33.2	139.83
	5	0.0062	34.2	6.81
June	1	0.0079	31.2	8.76
	2	0.0144	29.5	16.06
	3	0.0087	28.5	9.74
	4	0.0045	30.2	5.01
	5	0.0047	29.8	5.24
July	1	0.0090	28.7	10.07
	2	n.a.	27.5	n.a.
	3	0.0174	28.7	19.46
	4	0.0149	29.2	16.64
	5	0.0203	28.4	22.73
August	1	0.0052	28.7	5.82
	2	0.0047	29.9	5.24
	3	0.0144	29.0	16.09
	4	0.0106	30.5	11.79
	5	0.0133	29.3	14.85
September	1	0.0123	23.8	13.99
	2	0.0061	23.9	6.93
	3	0.0128	23.4	14.57
	4	0.0105	23.8	11.94
	5	0.0126	24.8	14.28
October	1	7.7701	30.6	8634.92
	2	4.9766	30.2	5538.52
	3	2.9737	29.3	3319.32
	4	3.3293	31.7	3686.75
	5	1.5199	30.3	1690.96
November	1	n.a.	n.a.	n.a.
	2	n.a.	30.6	n.a.
	3	n.a.	38.6	n.a.
	4	0.1380	32.9	152.23
	5	n.a.	35.2	n.a.



## APPENDIX B

### DATA OF INFLUENCING FACTORS

**Table B1.** Air and water temperature during sampling periods

Month	Average air temperature (°C)	Average water temperature (°C)
Year 2018		
December	25.0	n.d.
Year 2019		
January	26.5	n.d.
February	29.0	n.d.
March	28.8	n.d.
April	28.8	30.0
May	30.5	30.8
June	28.9	28.0
July	28.0	25.5
August	25.5	28.0
September	22.3	26.0
October	27.2	29.5
November	25.9	28.7

**Table B2.** Soil temperature at each depth during sampling periods

Month	N	Chamber	Soil temperature (°C) at depth (cm)			
			2.5	7.5	12.5	17.5
Year 2018 December	1	1	n.d.	n.d.	n.d.	n.d.
	2	5	n.d.	n.d.	n.d.	n.d.
	3	6	n.d.	n.d.	n.d.	n.d.
Year 2019 January	4	1	25.0	25.0	24.5	25.0
	5	2	26.0	25.0	24.9	25.0
	6	3	27.5	25.5	25.0	25.0
	7	4	27.0	25.5	25.0	25.0
	8	5	26.0	25.0	25.0	25.0
	9	6	28.0	26.5	26.0	26.0
February	10	1	26.5	26.0	25.2	25.5
	11	2	25.0	24.9	24.9	25.0
	12	3	27.0	26.9	25.9	25.5
	13	4	27.5	26.2	25.5	26.2
	14	5	n.d.	25.0	24.5	25.0
March	15	1	28.0	27.5	27.2	27.2
	16	2	28.0	27.8	27.5	27.0
	17	3	28.5	28.0	27.0	27.0
	18	4	29.0	28.5	27.2	26.5
	19	5	30.0	30.0	29.5	28.5
	20	6	31.0	30.0	29.0	28.0
April	21	2	28.0	28.0	27.8	28.0
	22	3	28.0	28.0	28.0	28.0
	23	4	29.0	28.5	28.5	28.5
	24	5	30.0	29.0	32.1	28.5
	25	6	34.5	29.5	29.0	29.0
May	26	2	31.0	30.5	29.5	29.0
	27	3	31.5	31.0	30.0	29.0
	28	4	31.5	31.0	30.0	29.5
	29	5	31.8	31.5	29.5	29.5
	30	6	32.0	31.5	30.5	30.0

**Table B2.** Soil temperature at each depth during sampling period (cont'd.)

Month	N	Chamber	Soil temperature (°C) at depth (cm)			
			2.5	7.5	12.5	17.5
Year 2019 June	31	2	27.0	26.9	26.5	27.0
	32	3	28.0	28.0	28.0	28.0
	33	4	29.0	28.0	28.0	28.0
	34	5	28.0	28.0	28.0	28.0
	35	6	28.0	28.0	27.5	27.1
July	36	2	27.0	26.9	26.5	27.0
	37	4	29.0	28.0	28.0	28.0
	38	5	28.0	28.0	28.0	28.0
	39	6	28.0	28.0	27.5	27.1
August	40	1	26.5	26.0	25.6	25.4
	41	2	26.0	25.8	25.5	25.2
	42	3	26.5	26.2	25.9	25.6
	43	4	26.9	26.5	26.2	25.9
September	44	2	24.0	23.5	23.0	23.0
	45	3	23.0	22.8	22.7	22.5
	46	4	23.5	23.3	23.0	22.8
	47	5	23.5	23.3	23.1	22.9
	48	6	23.7	23.5	23.1	23.1
October	49	2	29.1	28.2	27.9	27.1
	50	3	29.5	28.9	27.9	27.1
	51	4	28.1	29.0	28.3	27.5
	52	5	28.8	28.0	27.5	27.0
	53	6	28.3	28.2	27.9	27.0
November	54	3	28.5	27.9	27.1	26.9
	55	4	30.0	27.5	26.0	25.3
	56	5	27.5	26.8	26.3	25.5
	57	6	28.1	27.5	27.5	25.8

**Table B3.** Soil pH, ORP, and carbon content at each depth during sampling periods

Month	N	Soil pH at depth (cm)			Soil ORP at depth (cm)			Soil % carbon at depth (cm)		
		2.5	7.5	12.5	2.5	7.5	12.5	2.5	7.5	12.5
Year 2018 December	1	5.5	5.3	5.3	237	248	239	0.34	1.62	1.60
	2	6.0	5.0	5.1	232	273	281	0.36	0.33	0.19
	3	6.1	5.3	5.3	234	227	247	0.43	0.47	0.72
Year 2019 January	4	5.5	5.3	n.d.	203	214	n.d.	0.23	0.27	n.d.
	5	4.8	5.2	n.d.	229	231	n.d.	0.50	0.56	n.d.
	6	6.4	6.4	6.8	203	203	183	0.15	0.18	0.07
February	7	6.2	6.5	6.2	221	224	231	0.09	0.06	0.05
	8	6.0	6.0	5.3	216	238	241	0.30	0.07	0.20
	9	5.2	4.8	5.1	241	272	255	0.61	1.48	0.35
March	10	n.d.	n.d.	5.5	n.d.	n.d.	231	0.28	0.57	0.06
	11	6.0	5.8	6.1	232	213	208	n.d.	n.d.	0.17
	12	6.2	5.3	5.4	201	221	225	0.25	0.26	0.72
April	13	6.0	5.2	5.1	205	283	275	0.29	0.26	0.35
	14	6.7	5.8	5.2	213	238	254	0.28	0.39	0.24
	15	6.6	5.5	5.2	202	227	264	0.22	0.49	0.40
May	16	5.1	6.0	5.2	269	230	256	0.29	0.25	0.31
	17	5.2	6.8	5.1	263	204	280	0.19	0.22	0.42
	18	5.0	5.2	4.9	277	273	265	0.20	0.18	0.18
June	19	5.2	4.5	5.7	275	315	267	0.27	0.38	0.09
	20	5.2	5.6	4.7	294	259	326	0.23	0.17	0.08
	21	5.4	4.9	5.3	291	311	271	0.10	0.23	0.09
July	22	6.2	5.1	5.1	211	248	245	0.14	0.24	0.24
	23	7.3	7.3	5.9	174	176	206	0.15	0.09	0.10
	24	7.3	6.9	5.4	152	174	213	0.11	0.06	0.06
August	25	5.2	5.1	5.9	230	254	216	0.08	0.08	0.06
	26	5.0	4.7	4.6	246	260	309	0.07	0.07	0.05
	27	5.4	5.8	5.9	252	252	249	0.04	0.08	0.06

**Table B3.** Soil pH, ORP, and carbon content at each depth during sampling periods

(cont'd.)

Month	N	Soil pH at depth (cm)			Soil ORP at depth (cm)			Soil % carbon at depth (cm)		
		2.5	7.5	12.5	2.5	7.5	12.5	2.5	7.5	12.5
September	28	6.4	6.9	7.3	180	168	157	1.32	0.96	0.62
	29	6.5	7.3	7.2	170	150	173	2.17	1.27	0.80
	30	7.0	7.2	7.4	185	174	164	1.77	1.30	0.78
October	31	6.8	6.7	6.1	183	182	175	0.96	0.70	0.63
	32	7.0	6.8	6.6	204	177	179	1.81	0.70	0.66
	33	6.8	7.1	6.7	189	167	190	1.87	0.91	0.37
November	34	5.5	5.8	5.4	224	219	305	1.51	0.73	0.80
	35	5.4	5.1	5.7	287	288	184	1.89	1.24	0.97
	36	5.6	5.3	5.1	195	211	211	2.97	1.23	0.75





## Seasonal Estimates of Methane Emissions from Natural Wetlands in Nakhon Ratchasima, Thailand \*\*

Preecha Panmoon \* and Nares Chuersuwan\*.<sup>1</sup>

[www.ericjournal.ait.ac.th](http://www.ericjournal.ait.ac.th)

### ARTICLE INFO

#### Article history:

Received 29 June 2020

Received in revised form

28 September 2020

Accepted 29 October 2020

#### Keywords:

Greenhouse gas

Methane emission

Nakhon Ratchasima, Thailand

Natural wetland

### ABSTRACT

Seasonal methane emissions from natural wetlands in Nakhon Ratchasima province were estimated based on 12-month field works obtained from the actual methane flux measurements at a natural wetland. Methane gas was measured monthly with a static closed chamber technique and later analyzed by a gas chromatography equipped with a flame ionization detector (GC-FID). Results showed that methane fluxes varied widely in the range of 1.9–22.7 mg m<sup>2</sup>day<sup>-1</sup> with the median ± SD of 10.1 ± 5.4 mg m<sup>2</sup>day<sup>-1</sup>. Seasonally, the methane fluxes during wet season ranged from 5.2 to 22.7 mg m<sup>2</sup>day<sup>-1</sup> with the median ± SD of 14.1 ± 5.0 mg m<sup>2</sup>day<sup>-1</sup> while the methane fluxes during dry season were between 1.9 and 21.9 mg m<sup>2</sup>day<sup>-1</sup> with the median ± SD of 8.8 ± 5.2 mg m<sup>2</sup>day<sup>-1</sup>. The estimate methane fluxes of the wetland in wet and dry seasons were 1.5–3.1 kg m<sup>2</sup> and 0.7–2.9 kg m<sup>2</sup>, respectively. The estimated methane emission factor from the natural wetland in the province was 1.7 to 5.7 kg m<sup>2</sup>year<sup>-1</sup> compared to the default methane emission factor from IPCC, 0.0136 kg m<sup>2</sup>year<sup>-1</sup>. When considering global warming potential (GWP) of methane based on 100-year time horizon, the natural wetlands in the province may emit about 15.48 to 52.16 million ton CO<sub>2</sub>equivalent a year based on the emission factor derived locally. With the IPCC default emission factor, the methane emission was as low as 0.03 to 0.22 million ton CO<sub>2</sub>equivalent a year.

## 1. INTRODUCTION

Greenhouse gases (GHGs) in the atmosphere play key roles on the Earth's climatic systems—without them the Earth's surface temperature could be -18°C [1]–[3]. Three main GHGs are of concern; carbon dioxide, methane, and nitrous oxide, which are emitted in different proportion from various sources.

Methane emissions from natural wetlands have an important role as source and sink of carbon [4]. Regardless of carbon dioxide, methane gas is very important for enhancing the greenhouse effects because it has the global warming potential (GWP) of 28 times with 100-year time horizon [5]. This gas is biologically produced from methanogenesis by methanogenic bacteria in anaerobic [6] or even aerobic environment [7].

Methane emissions from wetlands vary temporally and spatially. Many factors influence the variations, such as, pH (Wang *et al.*, 2009), temperature [9], water table level [10], soil texture [11], salinity [12], [13],

organic carbon content [14], and climatic conditions [15]. Several studies showed inconsistent relationship of these factors with methane emissions. Recent report indicated the rising of methane in the atmosphere by 150 percent, from 722 ppb in 1750 to 1,874 ppb in 2020 [16].

To reasonably estimate local methane emission, data on the methane emission factor in the area are essential. The locally specific emission factor undoubtedly gives better emission estimation than some value taken from literatures elsewhere. Lack of site-specific methane emission factor is often substitute by the default emission factor from literatures or international organizations, such as Intergovernmental Panel on Climate Change (IPCC)[17]. In Thailand, previous studies focused on methane emission from rice cultivation [18] and constructed wetlands [19], [20]; only two studies focused on natural wetlands [18], [21]. The latest “Thailand's 2nd National Communication” excluded the GHGs emissions from natural sources [22], possibly from limited data on methane emissions from the natural wetlands in Thailand. Thus, this paper aims to examine the methane emissions based on field measurements in Nakhon Ratchasima province and compare the annual methane emissions calculating from recently developed emissions factor and the default emission factor compiled by IPCC.

\*\* This paper was presented at the ICUE 2020 International Conference on Energy, Environment, and Climate Change held at the Asian Institute of Technology, Pathumthani, Thailand from 20-22 October 2020.

\*School of Environmental Health, Suranaree University of Technology, Nakhon Ratchasima, Thailand.

<sup>1</sup>Corresponding author:  
Email: [nares@sut.ac.th](mailto:nares@sut.ac.th).

## 2. METHODS

### 2.1 Study Area

A natural wetland, named Baan San Kumphaeng reservoir, is located downhill from the Phanom Dong Rak's mountain range in Wang Numkheaw district, Nakhon Ratchasima province (14°23'18" N 101°42'30" E), shown in Figure 1. The small dike had been built, creating a reservoir to ease drought in the area. Soil texture is sandy and contains small pebbles. Lam Prapleng stream discharges water into the reservoir year-round. The stream flow is almost stagnant during dry season with no natural discharge. Average annual rainfall is 1,136 mm. The area of the wetland is about 1.6 km<sup>2</sup>. Biologically, the dominant plant species includes water lettuce (*Pistia stratiotes*), cattail (*Typha latifolia*), common frogbit (*Hydrocharis morsus-ranae*), swamp cabbage (*Ipomoea aquatica*), sunrose willow (*Ludwigia adscendens*), and water chestnut (*Eleocharis dulcis*). In wet season, the wetland's edge is dominated by wedelia (*Sphagneticola trilobata*), grass (*Phalaris arundinacea*), and weeds (e.g. *Heliopsis helianthoides*).



Fig. 1. Study area and appearance during wet and dry seasons.

### 2.2 Methane Flux Measurements

A static closed rectangular chamber was used for collecting evolved methane gas [23]. The chamber was made from clear acrylics with a dimension of 0.25 m x 0.25 m x 1.20 m (width x length x height). A thermometer was attached inside the chamber to determine the temperature and a small fan was installed

to provide uniform mixing of gases in the chamber [24]. A rectangular base was made of aluminum with groove to allow the acrylic chamber fitting inside. A chamber base was firmly inserted in the soil at 0.05 m depth. After two hours, the acrylic chamber was placed in the groove of the aluminum base and water was filled in the groove to prevent any leak. Five replicated chambers were used for methane gas sampling. The gas sampling intervals began at 2, 22, 42, 62, and 82 minutes between 8.30 and 11.00 AM. Gas collection was carried out once a month during December 2018 and November 2019.

Plastic syringes were used to draw the gas from the chambers and transferred into the evacuated glass vials. The vials contained gas samples were kept and stored under 4°C until they were analyzed in our laboratory.

A gas chromatography (Agilent®, Model 7890A, USA), equipped with a flame ionization detector and a stainless steel packed column, was used for quantifying the methane concentrations against the certified 19.5 ppmv standard methane gas (Air Liquid Co. Ltd., Thailand) under the optimum conditions of the GC-FID.

### 2.3 Methane Flux Determinations

Methane emission rates were calculated based on a linear change of gas concentrations over time, converted to flux rate (mg m<sup>-2</sup>day<sup>-1</sup>), and corrected for the chamber temperatures [25]. Gas flux rate (mg m<sup>-2</sup>day<sup>-1</sup>) was calculated by the following Equation (1) at standard temperature and pressure (STP) conditions [19].

$$E = XhM(1440)/RT \quad (1)$$

Where E = emission on the aerial basis (mg m<sup>-2</sup>day<sup>-1</sup>), X = rate of change in gas concentration (ppmv/min), h = chamber height (m), M = molecular weight of the methane gas (g/mol), 1441 = conversion factor for emission per day, R = universal gas constant (0.0821 atm.L.K<sup>-1</sup>mol<sup>-1</sup>), and T = absolute temperature (K).

### 2.4 The Annual Methane Emissions from Natural Wetlands in Nakhon Ratchasima

The methane emissions from natural wetlands in the province were estimated based on Equation (2) [5]:

$$Em = \sum A_w \times EF_w \quad (2)$$

Where Em = annual methane emission, Aw = total area of wetland, and EFw = emission factor of wetland.

### 2.5 Statistical Analysis

Statistical analysis was performed using R with packs "base" and "ggplot2" and Microsoft Excel® for Windows®. Data were tested for normal distribution by Shapiro-Wilk's Test. If the data were normally distributed, one samples t-test was carried out. Otherwise non-parametric Mann-Whitney test was applied. All results were considered statistically significant with 95% confident interval.

## 3. FINDINGS

### 3.1 Methane Fluxes

Three hundred and fifteen gas samples were quantified for methane concentrations and the fifty-two fluxes were

calculated. Methane fluxes varied from 1.9 to 8,634.9  $\text{mg m}^{-2} \text{day}^{-1}$ , with the mean  $\pm$  SD of  $467.0 \pm 1,544.6 \text{ mg m}^{-2} \text{day}^{-1}$  and the median of  $13.2 \text{ mg m}^{-2} \text{day}^{-1}$  (n=52). A

histogram showed distribution of methane fluxes (Figure 2).

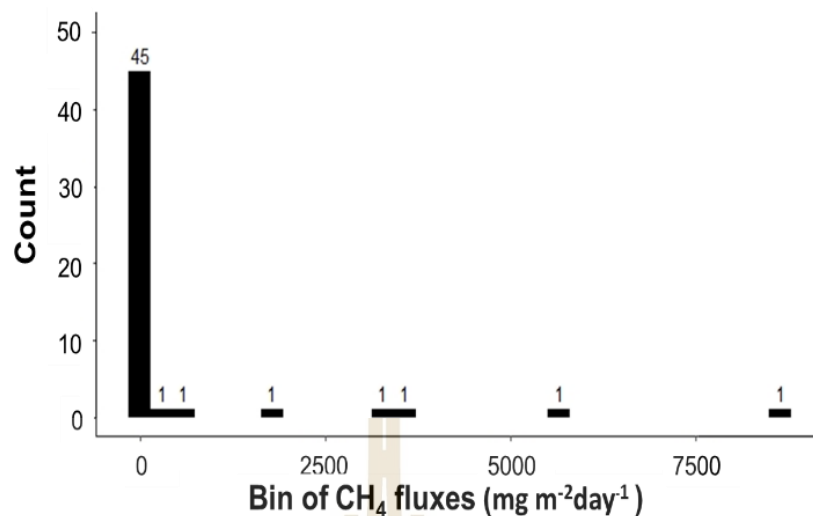


Fig. 2. Histogram of methane fluxes (n=52).

About 87% of methane fluxes grouped between 0 and  $150 \text{ mg m}^{-2} \text{day}^{-1}$ . It was important to note that methane fluxes over the upper fence of  $40.7 \text{ mg m}^{-2} \text{day}^{-1}$  were considered as outliers and thus excluded from statistical analysis.

The total number of monthly gas samples was 41 (n). Wet and dry seasons were classified by the water levels in the wetland and meteorological conditions, observed during the sampling period. Wet season started from mid-June to mid-September (3 months), while dry season started from mid-December to mid-June (7 months). The water levels in the wetland reached the maximum capacity in wet season and the water levels gradually decreased during dry season. The methane fluxes varied in the range of  $1.9\text{--}22.7 \text{ mg m}^{-2} \text{day}^{-1}$  with the mean  $\pm$  SD of  $10.6 \pm 5.4 \text{ mg m}^{-2} \text{day}^{-1}$  and the median of  $10.1 \text{ mg m}^{-2} \text{day}^{-1}$ . The lowest methane flux was found in December 2018 while the highest methane flux was in July 2019 (Figure 3).

The methane fluxes during wet season ranged from  $5.2$  to  $22.7 \text{ mg m}^{-2} \text{day}^{-1}$  with the median  $\pm$  SD of  $14.1 \pm 5.0 \text{ mg m}^{-2} \text{day}^{-1}$  (n=14) while methane fluxes during dry season were between  $1.9$  and  $21.9 \text{ mg m}^{-2} \text{day}^{-1}$  with the median  $\pm$  SD of  $8.8 \pm 5.2 \text{ mg m}^{-2} \text{day}^{-1}$  (n=31). The methane fluxes from the natural wetland seemed to increase from the beginning of dry season in 2018 to February 2019. From mid-December 2018 to February 2019, increasing in temperature from  $25.0$  to  $29.0^\circ\text{C}$  may cause the methane producing microbes at the lower soil layers to become active leading to more methane production [26], [27]. The decreasing of methane fluxes in March 2019 may attribute by the lower water levels

causing more oxic conditions in the lower soil layers, less favorable conditions for active microbial activity [28], [29]. These conditions may cause the lower rate of methane fluxes. After February, the methane fluxes increased continuously and peaked in April 2019. This dry period had slightly higher temperatures, in the range of  $29.0\text{--}31.0^\circ\text{C}$ , than the previous period with the lower water level. The methane fluxes decreased about 1.7 times from April when entered the wet season in mid-June 2019. During this period, the level of water in wetland remained near the lowest capacity of water storage. The gradually increase in methane fluxes potentially resulted from more available substrates with higher water level that methane producing microbes consume while they degrade organic matters. During wet season, the water from the stream continuously discharged into the wetland. The water level of the wetland increased and reached the maximum storage capacity in July 2019. Additionally, the rainstorm from July to August 2019 led more water input into the wetland. The wetland, during this period, had high median methane fluxes with the number of  $14.1 \text{ mg m}^{-2} \text{day}^{-1}$ . The flooded conditions of the wetland provided the ideal conditions for methanogenesis. The organic matters increased as a result of decomposed grass, thus more substrate for methanogenesis [4], [30].

Many studies indicated that methane fluxes varied temporally and spatially. When comparing the results to those of previous studies, shown in Table 1, it can point out that large difference of methane fluxes potentially originated from spatiotemporal variation.



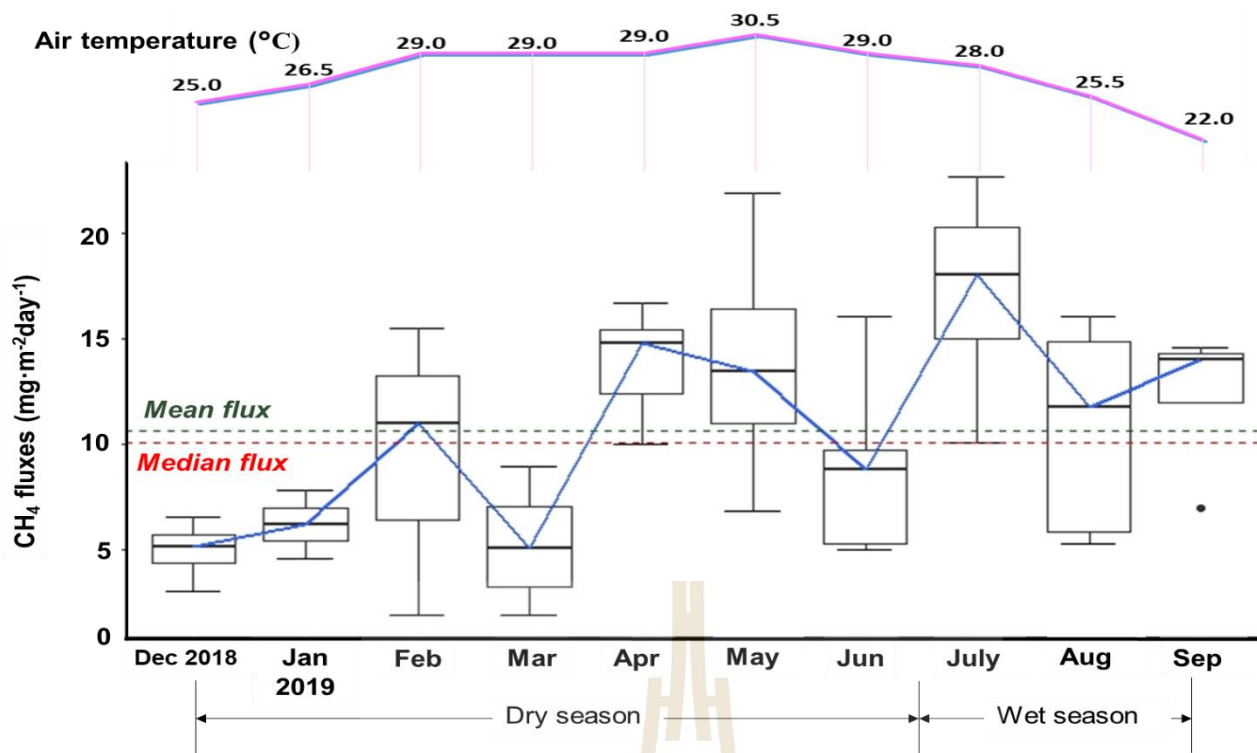


Fig. 3. Time-series Box-Winkler plot of seasonal methane fluxes from the natural wetland (n=41).

Table 1. Methane emissions from some wetland.

Country	Climate	Wetland type	Flux (mg/m <sup>2</sup> /day)	Authors	Year
Thailand	Tropical	Natural reservoir	10.6 ± 5.4 (mean ± SD)	This study	2019
Thailand	Tropical	Mangrove area	0.19 (cold), 0.27 (summer), 0.52 (rainy); (mean)	[21]	2005
Thailand	Tropical	Freshwater marsh	7.1-29.7 (mean ± SD)	[18]	2001
Brazil	Tropical	Lake/reservoir	13.8 (mean)	[31]	2006
France	Tropical	reservoir	44.8 (mean)	[32]	2006
India	Tropical	reservoir	116.6 (mean)	[33]	2015
U.K.	Temperate	Natural pond	1.0-22.5 (range)	[34]	2000
U.S.	Temperate	reservoir	4.4 (mean)	[35]	2004
Finland	Boreal	reservoir	33.6 (mean)	[36]	2003
Canada	Boreal	reservoir	27.36 (mean)	[37], [38]	2005
China	Subtropical	Lake	0.06-5.5 (range)	[39]	2005
China	Subtropical	Meadow	270.5 ± 271.0 (mean ± SD)* 71.8 ± 40.1 (mean ± SD)**	[40]	2018
Australia	Subtropical	reservoir	93.5 (mean)	[41]	2013
China	Subtropical	reservoir	5.12 (mean)	[38]	2013
Taiwan	Subtropical	reservoir	4.8 (mean)	[42]	2013

Note: \* = wetland was dominated by *Carex cinerascens*

\*\* = wetland was dominated by *Artemisia selengensis*

Data from Thailand in Table 1 showed range of the methane flux. Khemjaroen (2001) used the measurement for 4 months, February to May, while this study and Lekphet *et al.* (2005) were observed throughout the year. Discrepancies on the methane fluxes may come from various factors such as different area, time, and even specific properties of the wetlands. On the other

hand, the results from Lekphet *et al.* (2005) may indicate that the methane fluxes fluctuated seasonally [21].

In China, the methane fluxes were largely different between two different plants dominated in a wetland [40].

Similarly, spatial dynamics of methane fluxes can be observed from various wetlands in China [38]-[40].

Additionally, methane flux variation could be attributed to the difference in climate zone of a wetland (Table 1) that affected the balance between methane production and methane reduction, thus spatiotemporal of methane emissions.

### 3.2 Seasonal Estimates of Methane Emissions

According to the official records for season classification, the time span of the dry season was 204 days and 161 days for the wet season. Seasonal estimates of methane emissions from the natural wetland were shown in Table 2. Despite dry season covered more months (Figure 2), the methane emissions during dry season were lower compared to the wet season due to high methane fluxes during wet season.

**Table 2. Seasonal estimates of methane emissions.**

Period	Day	Methane emissions (kg m <sup>2</sup> period <sup>-1</sup> )		
		lower	upper	median
Wet season	161	1.5	3.1	2.3
Dry season	204	0.7	2.9	1.8
Annual	365	1.7	5.7	3.7

### 3.3 Estimating the Methane Emissions from the Natural Wetlands in Nakhon Ratchasima

The approximate area of natural wetlands was calculated from a geospatial database. The area of natural wetlands in Nakhon Ratchasima province was about 298.7 km<sup>2</sup>. The methane emission factor of the natural wetland in this study was 1.7 to 5.7 kg m<sup>-2</sup>year<sup>-1</sup> (Table 2) while the methane emission factor of the natural wetland from IPCC (mean ± SD) was 0.0037-0.0235 kg m<sup>-2</sup>year<sup>-1</sup>. When considering 100-year time horizon, the natural wetlands in the province emitted about 15.48 to 52.16 million ton CO<sub>2</sub>equivalent year<sup>-1</sup> based on our locally derived emission factor while estimation using the IPCC default emission factor yielded 0.03 to 0.22 million ton CO<sub>2</sub>equivalent year<sup>-1</sup> (Figure 4).

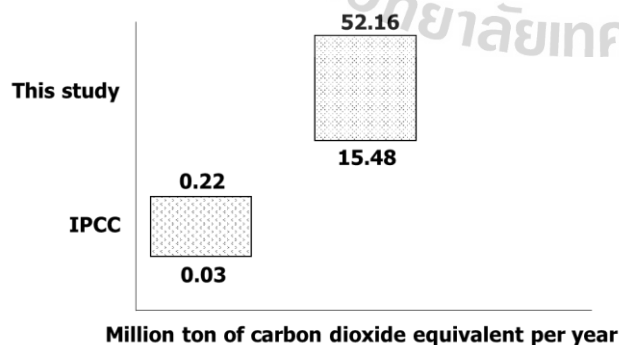


**Fig. 4. Estimated methane emissions in Nakhon Ratchasima by two different emission factors.**

The difference of the estimated methane emissions showed that locally derived emission factor gave 241-454 times higher estimate than the IPCC emission factor. It was possible that the default emission factor

was a global average (IPCC, 2014) and methane emissions vary temporally and spatially [43]–[45].

## 4. CONCLUSION AND RECOMMENDATION

The methane fluxes from a natural wetland in Nakhon Ratchasima varied widely, 1.9–22.7 mg m<sup>-2</sup>day<sup>-1</sup> with the mean ± SD of 10.6 ± 5.4 mg m<sup>-2</sup>day<sup>-1</sup>. The methane fluxes during wet season had the mean ± SD of 13.2 ± 5.0 mg m<sup>-2</sup> day<sup>-1</sup> and 10.3 ± 5.8 mg m<sup>-2</sup>day<sup>-1</sup> in dry season. Annual methane emission rate from a natural wetland in Nakhon Ratchasima during December 2018 to November 2019 ranged between 2,015 and 6,169 mg m<sup>-2</sup>year<sup>-1</sup> with the mean of 4,092 mg m<sup>-2</sup>year<sup>-1</sup>. Estimate of methane emissions from the natural wetlands in Nakhon Ratchasima was 601,880,500 to 1,842,680,300 kg year<sup>-1</sup>. Estimate of methane emissions from the natural wetlands with the IPCC emission factor led to much lower emissions.

## ACKNOWLEDGEMENT

This study was supported by Suranaree University of Technology, Thailand. The authors gratefully acknowledge the support including the contribution from the Environmental Pollution and Safety Program, School of Environmental Health, Institute of Public Health.

## REFERENCES

- [1] Fourier J.B.J., 1824. General Remarks on the Temperature of the Terrestrial Globe and the Planetary Spaces, Translation from the French by Burgess, E., 1837, American Journal of Science, Vol 32, pp. 1-20. Paris - Crochard, vol. 27, *Annals of Chemistry and Physics* 27: 136–167.
- [2] Stephens G.L and S. A Tjemkes, 1993. Water Vapour and Its Role in the Earth's Greenhouse. *Aust. J. Phys.* 46(1): 149. doi: 10.1071/PH930149.
- [3] Tyndall J., 1862. On the Absorption and Radiation of Heat by Gaseous Matter. Second Memoir. *Philosophical Transactions of the Royal Society of London* 152: 59–98.
- [4] Laanbroek, 2010. Methane emission from natural wetlands: interplay between emergent macrophytes and soil microbial processes. A mini-review. *Ann Bot* 105(1): 141–153. doi: 10.1093/aob/mcp201.
- [5] Myhre G. et al., 2013. Anthropogenic and Natural Radiative Forcing. In *Climate Change 2013: The Physical Science Basis. Contribution of Working Group I to the Fifth Assessment Report of the Intergovernmental Panel on Climate Change*, Stocker, T.F., D. Qin, G.K. Plattner, M. Tignor, S.K. Allen, J. Boschung, A. Nauels, Y. Xia, V. Bex and P.M. Midgley (eds.) Cambridge University Press, Cambridge, United Kingdom and New York, NY, USA.
- [6] Fenchel T., Blackburn T.H., and King G.M., 2012. *Bacterial Biogeochemistry*. Third edition. Academic Press, Elsevier Ltd

- [7] Repeta D.J., Ferrón S., Sosa O.A., and Johansson C.G., 2016. Marine methane paradox explained by bacterial degradation of dissolved organic matter. *Nature Geoscience* 9: 884–887.
- [8] Wang Z., Delaune R., Patrick Jr. W.H., and Masscheleyn P.H., 2009. Soil Redox and pH effects on methane production in a flooded rice soil. *Soil Science Society of America Journal - SSSAJ* 57: 382–385. doi:10.2136/sssaj1993.03615995005700020016x.
- [9] Butterbach-Bahl K., Baggs E.M., Dannenmann M., Kiese R., and Zechmeister-Boltenstern S., 2013. Nitrous oxide emissions from soils: how well do we understand the processes and their controls?. *Royal Society Publishing, Soil Science* : 1–13. doi: <https://doi.org/10.1098/rstb.2013.0122>.
- [10] Bubier J., Moore T., and Roulet N. 1993. Methane emissions from wetlands in the Midboreal region of Northern Ontario, Canada. *Ecology* 74: 2240–2254. doi: 10.2307/1939577.
- [11] Brye K.R., Roger C.W., Smartt A.D., and Norman R.J., 2013. Soil texture on methane emissions from direct-seeded, delayed-flood rice production in Arkansas. *Lippincott Williams & Wilkins* 178(10): 519–529. doi: 10.1097/SS.0000000000000020.
- [12] B. Kaesler and P. Schönheit, “The role of sodium ions in methanogenesis. Formaldehyde oxidation to CO<sub>2</sub> and 2H<sub>2</sub> in methanogenic bacteria is coupled with primary electrogenic Na<sup>+</sup> translocation at a stoichiometry of 2-3 Na<sup>+</sup>/CO<sub>2</sub>,” *European journal of biochemistry / FEBS*, vol. 184, pp. 223–32, Oct. 1989, doi: 10.1111/j.1432-1033.1989.tb15010.x.
- [13] Müller V., Blaut M., and Gottschalk G., 1987. Generation of a transmembrane gradient of Na<sup>+</sup> in *Methanosarcina barkeri*. *European journal of biochemistry / FEBS* 162: 461. doi: 10.1111/j.1432-1033.1987.tb10624.x.
- [14] Annisa W., Maas A., Purwanto B.P., and Widada J., 2014. Effect of organic matter level on methane emission in acid sulfate soil from Belandean, South Kalimantan. *Asian Research Publishing Network (ARPN)* 9(4): 146–151.
- [15] Boon P.I. and A. Mitchell. 1995. Methanogenesis in the sediments of an Australian freshwater wetland: Comparison with aerobic decay, and factors controlling methanogenesis. *FEMS Microbiology Ecology* 18(3): 175–190. doi: 10.1016/0168-6496(95)00053-5.
- [16] Dlugokencky E., NOAA/GML. Carbon cycle greenhouse gases, Trends in CH<sub>4</sub>. Retrieved from the World Wide Web: [www.esrl.noaa.gov/gmd/ccgg/trends\\_ch4/](http://www.esrl.noaa.gov/gmd/ccgg/trends_ch4/).
- [17] IPCC, 2013. Supplement to the 2006 IPCC Guidelines for National Greenhouse Gas Inventories: Wetland. Hiraishi, T., Krug, T., Tanabe, K., Srivastava, N., Baasansuren, J., Fukuda, M. and Troxler, T.G. (eds). IPCC, Switzerland, 2014.
- [18] Khemjaroen K., 2001. Methane emissions from natural and man-made wetlands: A comparative study on freshwater marsh, paddy field, and shrimp farm in Bansang district. *Master Thesis of Environmental Management*, Mahidol University, Bangkok, Thailand, 2001.
- [19] Chuersuwat S., Suwanwaree P., and Chuersuwat N., 2014. Estimating greenhouse gas fluxes from constructed wetlands used for water quality improvement. *Songklanakarin Journal of Science and Technology* 36: 367–373.
- [20] Kaewgamtong N., 2002. Methane Emission from Constructed Wetland. *Master Thesis*. King Mongkut's University of Technology Thonburi, Bangkok, Thailand.
- [21] Lekphet S., Adsavakulchai S., and Nitorisavut S., 2005. Estimating methane emissions from mangrove area in Ranong province, Thailand. *Songklanakarin Journal of Science and Technology* 27(1): 153–163.
- [22] Office of Natural Resources and Environmental Policy and Planning, 2017. Thailand's Second National Communication under the United Nations Framework Convention on Climate Change - OD Mekong Datahub. *Open Development Mekong*. Retrieved from the World Wide Web: <https://data.opendevlopmentmekong.net/dataset/9817b4f-380c-4bed-83bb-bf22c809496b>.
- [23] Hutchinson G.L. and A.R. Mosier. 1981. Improved soil cover method for field measurement of nitrous oxide fluxes. *Soil Science Society of America Journal* 45(2): 311–316. doi: 10.2136/sssaj1981.03615995004500020017x.
- [24] Collier S.M., Ruark M.D., Oates L.G., Jokela W.E., and Dell C.J., 2014. Measurement of greenhouse gas flux from agricultural soils using static chambers. *J Vis Exp* (90). doi: 10.3791/52110.
- [25] Healy M.G., Devine C.M., and Murphy R. 1996. Microbial production of biosurfactants. *Resources, Conservation and Recycling* 18(1–4): 41–57. doi: 10.1016/S0921-3449(96)01167-6.
- [26] Dise N.B., 1992. Winter fluxes of methane from Minnesota peatlands. *Biogeochemistry* 17(2): 71–83. doi: 10.1007/BF00002641.
- [27] King G.M. and A.P.S. Adamsen. 1992. Effects of temperature on methane consumption in a forest Soil and in pure cultures of the Methanotroph *Methylomonas rubra*. *Appl Environ Microbiol* 58(9): 2758–2763.
- [28] Castro M.S., Steudler P.A., Melillo J.M., Aber J.D., and Bowden R.D., 1995. Factors controlling atmospheric methane consumption by temperate forest soils. *Global Biogeochemical Cycles* 9(1): 1–10. doi: 10.1029/94GB02651.
- [29] Moore T.R. and M. Dalva. 1993. The influence of temperature and water table position on carbon dioxide and methane emissions from laboratory columns of peatland soils. *Journal of Soil Science* 44(4):651–664. doi: 10.1111/j.1365-2389.1993.tb02330.x.
- [30] Macdonald J.A., Fowler D., Hargreaves K.J., Skiba U., Leith I.D., and Murray M.B. 1998. Methane emission rates from a northern wetland; response to temperature, water table and transport.

- Atmospheric Environment* 32(19): 3219–3227. doi: 10.1016/S1352-2310(97)00464-0.
- [31] dos Santos M.A., Rosa L.P., Sikar B., Sikar E., and dos Santos E.O., 2006. Gross greenhouse gas fluxes from hydro-power reservoir compared to thermo-power plants. *Energy Policy* 34(4): 481–488.
- [32] Guérin F. *et al.*, 2006. Methane and carbon dioxide emissions from tropical reservoirs: Significance of downstream rivers. *Geophysical Research Letters* 33(21). doi: 10.1029/2006GL027929.
- [33] Bansal S., Chakraborty M., Katyal D., and Garg J., 2015. Methane flux from a subtropical reservoir located in the floodplains of river Yamuna, India. *Applied Ecology and Environmental Research* 13. doi: 10.15666/aeer/1302\_597613.
- [34] Casper P., Maberly S.C., Hall G.H., and Finlay B.J., 2000. Fluxes of methane and carbon dioxide from a small productive lake to the atmosphere. *Biogeochemistry* 49(1): 1–19. doi: 10.1023/A:1006269900174.
- [35] Soumis N., Duchemin É., Canuel R., and Lucotte M., 2004. Greenhouse gas emissions from reservoirs of the western United States. *Global Biogeochemical Cycles* 18(3) 2004. doi: 10.1029/2003GB002197.
- [36] Huttunen J.T. *et al.*, 2003. Fluxes of methane, carbon dioxide and nitrous oxide in boreal lakes and potential anthropogenic effects on the aquatic greenhouse gas emissions. *Chemosphere* 52(3): 609–621. doi: 10.1016/S0045-6535(03)00243-1.
- [37] Tremblay A., Therrien J., Hamlin B., Wichmann E., and LeDrew L.J., 2005. GHG Emissions from Boreal Reservoirs and Natural Aquatic Ecosystems. In *Greenhouse Gas Emissions — Fluxes and Processes: Hydroelectric Reservoirs and Natural Environments*, A. Tremblay, L. Varfalvy, C. Roehm, and M. Garneau, Eds. Berlin, Heidelberg: Springer: 209–232.
- [38] Zhao Y., Wu B.F., and Zeng Y., 2013. Spatial and temporal patterns of greenhouse gas emissions from Three Gorges Reservoir of China. *Biogeosciences* 10(2): 1219–1230. doi: <https://doi.org/10.5194/bg-10-1219-2013>.
- [39] Xing Y., Xie P., Yang H., Ni L., Wang Y., and Rong K., 2005. Methane and carbon dioxide fluxes from a shallow hypereutrophic subtropical Lake in China. *Atmospheric Environment* 39(30): 5532–5540. doi: 10.1016/j.atmosenv.2005.06.010.
- [40] Liu S., Chen Y., and Liu J., 2019. Methane emissions from the littoral zone of Poyang lake during drawdown periods. *Journal of Freshwater Ecology* 34(1): 37–48. doi: 10.1080/02705060.2018.1537941.
- [41] Sturm K., Yuan Z., Gibbes B., Werner U., and Grinham A., 2014. Methane and nitrous oxide sources and emissions in a subtropical freshwater reservoir, South East Queensland, Australia. *Biogeosciences* 11(18):5245–5258. doi: <https://doi.org/10.5194/bg-11-5245-2014>.
- [42] Wang Y.-H., Huang H.-H., Chu C.-P., and Chuag Y.-J., 2013. A preliminary survey of greenhouse gas emission from three reservoirs in Taiwan. *Sustainable Environment Research* 23: 215–225.
- [43] Singh S.N., Kulshreshtha K., and Agnihotri S., 2000. Seasonal dynamics of methane emission from wetlands. *Chemosphere - Global Change Science* 2: 39–46. doi: 10.1016/S1465-9972(99)00046-X.
- [44] Wassmann R. *et al.*, 1994. Temporal Patterns of Methane Emissions from Wetland Rice Fields Treated Different Modes of N Application. *Journal of Geophysical Research* 991: 16457–16462. doi: 10.1029/94JD00017.
- [45] Wilson J.O., Crill P.M., Bartlett K.B., Sebacher D.I., Harriss R.C., and Sass R.L., 1989. Seasonal variation of methane emissions from a temperate swamp. *Biogeochemistry* 8(1): 55–71. doi: 10.1007/BF02180167.

# **CURRICULUM VITAE**

**PREECHA PANMOON**

**Email: xiuryo@gmail.com**

## **EDUCATION**

- 2017 - present* Master of Science in Environmental Pollution and Safety at Suranaree University of Technology. Thesis title: “Seasonal methane fluxes from a natural wetland in Nakhon Ratchasima”.
- 2014 - 2017* Bachelor of Science in Environmental Health at Suranaree University of Technology, First Class Honors.

## **ACADEMIC AND RESEARCH EXPERIENCES**

- 2017 - present* Research Assistant to Assoc.Prof. Nares Chuersuwan, School of Environmental Health. Responsibilities for laboratory analyst, data analyst, and project planning.
- 2017 - 2021* Graduate Teaching Assistant, School of Environmental Health. Responsibilities for assisting lecturer with preparation and tutoring in undergraduate laboratory courses.

## **PUBLICATIONS AND PRESENTATIONS**

- 2020* Panmoon, P. and Chuersuwan, N. Seasonal estimates of methane emissions from natural wetlands in Nakhon Ratchasima. ICUE 2020, at AITCC, 20-22 October 2020, Best student paper award.

## **GRANTS AND FELLOWSHIPS**

- 2017 - 2019* Graduate Merit Scholarships from Suranaree University of Technology